Formation and reactivity of copper(II)-nitrosyl complexes

A dissertation submitted to the
Indian Institute of Technology Guwahati as
partial fulfillment for the degree of
Doctor of Philosophy in Chemistry

Submitted by

Apurba Kalita
(Roll No. 09612202)

Supervisor

Dr. Biplab Mondal

Department of Chemistry
Indian Institute of Technology Guwahati

February, 2013

Dedicated to my

Parents

Statement

I hereby declare that this thesis entitled "**Formation and reactivity of copper(II)-nitrosyl complexes**" is the outcome of research work carried out by me under the supervision of Dr. Biplab Mondal, in the Department of Chemistry, Indian Institute of Technology Guwahati, India.

In keeping with the general practice of reporting scientific observations, due acknowledgement has been made whenever work described here based on the findings of other investigators.

February, 2013 **Apurba Kalita**

Certificate

This is to certify that Mr. Apurba Kalita has been working under my supervision since July, 2009 as a regular Ph. D. student in the Department of Chemistry, Indian Institute of Technology Guwahati. I am forwarding his thesis entitled "**Formation and reactivity of copper(II)-nitrosyl complexes**" being submitted for the Ph. D. degree.

I certify that he has fulfilled all the requirements according to the rules of this institute regarding the investigations embodied in his thesis and this work has not been submitted elsewhere for a degree.

February, 2013 **Biplab Mondal**

Acknowledgements

I would like to thank my supervisor, Dr. Biplab Mondal, who provided me with the opportunity and the resources to be as creative as I like, inspiring me to do my best, and making sure I am progressing along a forward path. It is these things that have given me the most confidence in my scientific abilities.

I would like to acknowledge my sincere gratitude to all my doctoral committee members Dr. Bhisma Kumar Patel, Dr. Gopal Das, Dr. Subhradip Ghosh for their insightful advice and valuable suggestions. I am also grateful to the entire faculty and staff of the Department of Chemistry, Indian Institute of Technology Guwahati for providing a wonderful work atmosphere throughout this period.

My special thanks to Prof. Ramesh C. Deka from Department of Chemical Sciences, Tezpur University for helping me in theoretical calculation part of my thesis.

I would like to thank my labmates Amardeep-da, Moushumi-didi, Rajib-da, Pankaj-da, Aswini, Vikash, Kanhu, Somnath, Hemanta, Kuldeep, Soumen, Sayantani, Neeraj, Satish, Madhav, Soham, Najmul, Narayani, Ivy, Pritam, Tulika, Debabrata, Gorachand and Pokhraj whom I had an opportunity to work with. No words can express my thankfulness for giving me their time and companionship, which made the time spent in the laboratory and outside pleasant and memorable.

The financial support from Council of Scientific and Industrial Research (CSIR), New Delhi for the research fellowship is duly acknowledged.

Finally, I would like to thank my family members, without their love and support this work would not have been completed.

February, 2013 **Apurba Kalita**

Contents

Page No.

Synopsis i

Chapter 1: Introduction

1.1 General aspects of nitric oxide 1

1.2 Copper (II) - nitrosyl 3

1.3 References 10

Chapter 2: Role of ligand to control the mechanism of nitric oxide reduction of copper (II) complexes and ligand nitrosation

Abstract 16

2.1 Introduction 17

2.2 Results and discussion 20

2.3 Nitric oxide reactivity 23

2.4 Conclusion 33

2.5 Experimental section 34

2.6 References 39

Chapter 3: Synthesis of a copper(II)–nitrosyl complex and its reaction with water: Example of copper(I)-(η^2-O, O) nitrite complex derived from copper(II)-nitrosyl

Abstract 47

3.1 Introduction 48

3.2 Results and discussion 49

3.3 Nitric oxide reactivity 51

3.4 Conclusion 58

3.5 Experimental section 58

3.6 References 61

Chapter 4: Reaction of a copper(II)–nitrosyl complex with hydrogen peroxide: putative formation of a copper(I)–peroxynitrite intermediate

Abstract 66

4.1 Introduction 67
4.2 Results and discussion 68
4.3 Conclusion 73
4.4 Experimental section 73
4.5 References 76

Chapter 5: Reaction of a copper (II)–nitrosyl complex with hydrogen peroxide: Mimicking of tyrosine nitration
Abstract 79
5.1 Introduction 80
5.2 Results and discussion 81
5.3 Nitric oxide reactivity 83
5.4 Conclusion 89
5.5 Experimental section 89
5.6 References 93

Appendix I 97
Appendix II 112
Appendix III 122
Appendix IV 128
List of publications 136

Synopsis

The thesis entitled, "**Formation and reactivity of copper(II)-nitrosyl complexes**" is divided into five chapters.

Chapter 1: Introduction

Nitric oxide (NO) plays various fundamental roles in biochemical processes.[1] Physiological activities of NO are known to include roles in blood pressure control, neurotransmission, and immune response. Most of the roles played by NO in biology are attributed to the formation of nitrosyl complexes of the metallo-proteins, mostly iron or copper. Subsequent reports have identified a number of disease states involving NO imbalances.[2] For instance, in bioregulatory purposes, less than 1 μM concentration of NO has been reported to be generated in endothelium cells for blood pressure control; however, the NO concentrations produced during immune response to pathogen invasion are much higher and under these conditions, reactive nitrogen species such as peroxynitrite anion ($^{-}$OONO) and N_2O_3 may form which have immense physiological importance.[3] Such observations have stimulated extensive research activity into the chemistry, biology, and pharmacology of NO.

Several theoretical and matrix-isolation studies on copper nitrosyls have been reported.[4] These investigations have found that N-bound nitrosyls are more stable than O-bound nitrosyls and that the ground-state geometry for [Cu^{II}-NO] is bent while that for [Cu^{I}-NO] is linear.

It has been well documented in literature that NO induces reduction of copper(II) centre in various copper(II)-complexes. This reduction in some cases proceeds through a deprotonation mechanism as reported by the Ford's group or through the [Cu^{II}-NO] complex formation in others as it happens in case of ferriheme systems.[5-9]

This thesis has been focused on the formation, stabilization of copper(II)-nitrosyls and their reactivity towards water, hydrogen peroxide etc. Second chapter of this thesis describes a comparative study to show the roles of ligand frameworks to control the mechanistic pathway for the reduction of copper(II) centre by NO. Subsequent chapters describe the stable [Cu^{II}-NO] complex and their reactivity studies.

Chapter 2: Role of ligand to control the mechanism of nitric oxide reduction of copper(II) complexes and ligand nitrosation

The NO reactivity of two copper(II) complexes, **2.1** and **2.2** with ligands $\mathbf{L_1}$ and $\mathbf{L_2}$ [$\mathbf{L_1}$ = 5,5,7,12,12,14-hexamethyl-1,4,8,11 tetraazacyclotetradecane, $\mathbf{L_2}$ = 5,5,7-trimethyl-[1,4]-diazepane], respectively, have been studied. The complexes were characterized by various analytical techniques. The single crystal structures of complexes **2.1** and **2.2** were determined and the perspective ORTEP views are shown in figure 1.

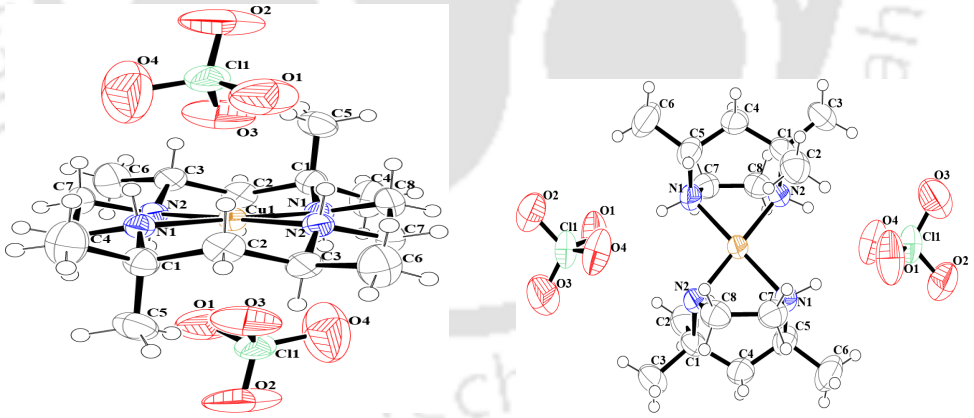

(a) **(b)**

Figure 1 ORTEP diagrams of complexes (a) **2.1** and (b) **2.2** (50% thermal ellipsoid plot).

It should be noted that these two ligands have been chosen as they afford analogous complexes except one is macrocyclic and the other is cyclic amine ligand. The crystal structures indicate that complexes **2.1** and **2.2** have similar structural parameters. NO

reactivity of the complexes was studied in acetonitrile and methanol media. Complex **2.1**, in dry and degassed acetonitrile, did not react with NO. Even after purging NO gas into the acetonitrile solution of complex **2.1** for 2 minutes, no spectral change was observed. However, in methanol solution, complex **2.1** was found to react with NO in presence of sodium methoxide to result in a colorless solution indicating the reduction of copper(II) to copper(I). The reduction was monitored by UV-visible and EPR spectroscopic studies (Figure 2).

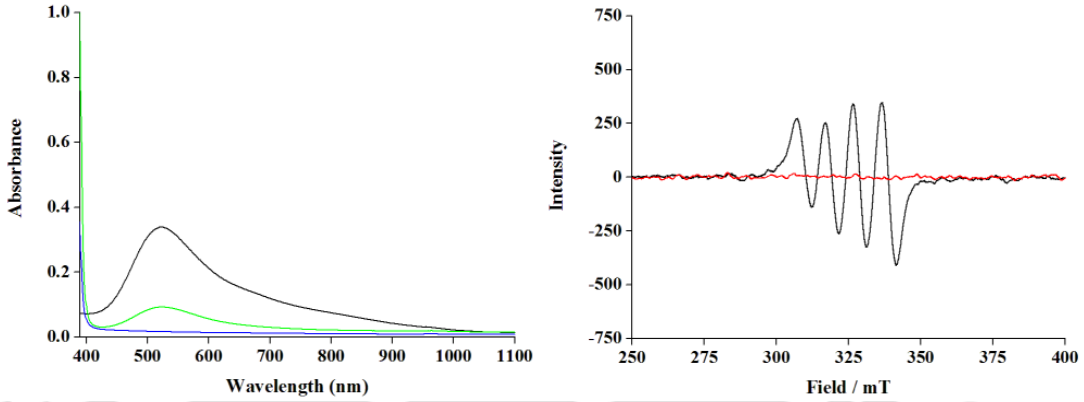

(a) (b)

Figure 2 (a) UV-visible spectra of the reaction of complex **2.1** (black) with NO in presence of sodium methoxide in methanol solvent at room temperature. Green and blue traces represent the spectral changes at an intermediate stage and after complete reduction, respectively. (b) X-band EPR spectra of the complex **2.1** (black) and after its reaction with NO (red) in presence of sodium methoxide in methanol solvent at room temperature.

Mechanistic studies revealed that in this case the reduction of copper(II) centre proceeds through a deprotonation pathway as reported earlier by Ford et al (Scheme 1).

To a dry and degassed acetonitrile solution of complex **2.2** exposure of NO gas resulted in the formation of a thermally unstable intermediate. In UV-visible spectrum, the intermediate shows a *d-d* band centred with λ_{max} at 600 nm. The intensity of this band was found to decay gradually with time indicating the decomposition of the intermediate to a

colorless solution (Figure 3a) following first order kinetics. The observed rate constant at 298 K is 8.45×10^{-3} s^{-1}. The intermediate was found to be EPR silent.

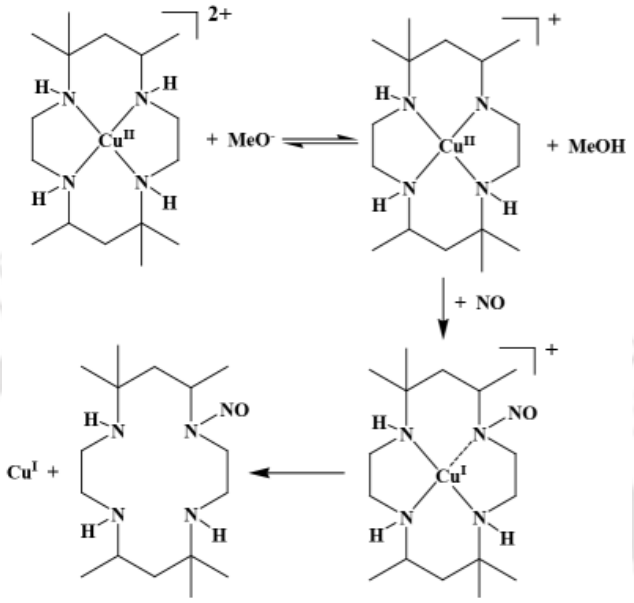

Scheme 1

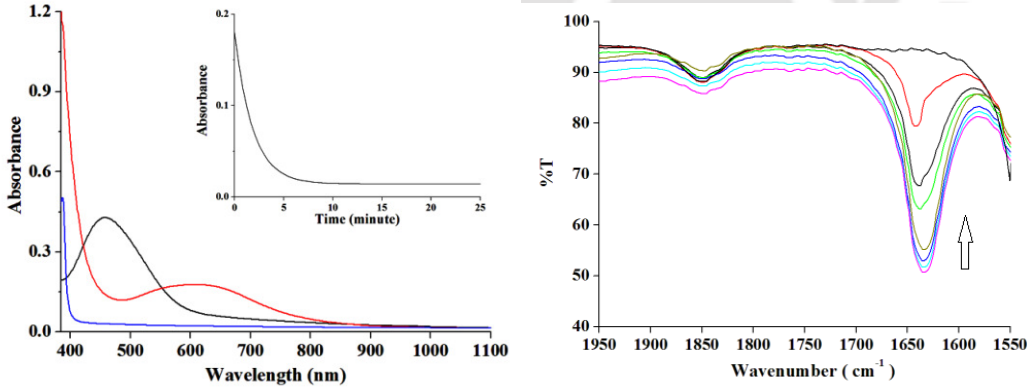

(a) (b)

Figure 3 (a) UV-visible spectra of complex **2.2** (black); [Cu^{II}–NO] intermediate (red) and its decomposition to copper (I) species (blue) in acetonitrile solution. Inset: first order kinetic trace (λ = 600 nm) of decay of [Cu^{II}–NO] intermediate to copper(I) species in acetonitrile solution. (b) FT-IR spectrum of complex **2.2** and after reaction with NO in acetonitrile solution at room temperature. Arrow head indicates the gradual decrease of the band intensity with time.

In FT-IR spectrum of acetonitrile solution of **2.2** after addition of NO, a new intense and sharp band was found to appear at ~1635 cm^{-1} corresponding to the vibration of NO coordinated to the copper(II) centre. This band was found to decrease in intensity with time (Figure 3b). Thus, the spectral studies support the formation of the [Cu^{II}–NO] intermediate prior to the reduction of the copper(II) centre in the case of complex **2.2**. Theoretical studies also suggested the feasibility of formation of [Cu^{II}-NO] intermediate in case of **2.2**. In both the cases, the reduction of copper(II) centre by NO was found to result in concomitant N-nitrosation of the ligands.

Thus, in case of complex **2.1**, the reduction of copper(II) to copper(I) takes place in methanol medium in presence of base; whereas, the same in case of **2.2** was observed to be very facile in dry acetonitrile through the formation of a [Cu^{II}–NO] intermediate. From the present study, it has been observed that though the macrocyclic ligands prefer deprotonation pathway, the nonmacrocyclic one prefers the [Cu^{II}–NO] intermediate pathway.

Chapter 3: Synthesis of a copper (II)–nitrosyl complex and its reaction with water: Example of copper (I)-(η^2-O, O) nitrite complex derived from copper (II)-nitrosyl

Copper(II) complex, **3.1**, was synthesized with the bidentate ligand, $\mathbf{L_3}$ [$\mathbf{L_3}$ = *bis* (2-ethyl-4-methyl-imidazol-5yl) methane], as its perchlorate salt. The single crystal structure of complex **3.1** was determined. The perspective ORTEP view for **3.1** is shown in figure 4.

Complex **3.1** in acetonitrile solution exhibits a broad *d–d* band having λ_{max} (ε/M^{-1} cm^{-1}), 685 nm (120), along with relatively strong intra-ligand absorptions in the UV region. Addition of NO to a degassed acetonitrile solution of complex **3.1** resulted in the corresponding [Cu^{II}–NO] complex, **3.2**. Micro-analytical data and ESI-mass spectrum also

supports the formulation (Figure 5). It absorbs at λ_{max} (ε/M^{-1} cm^{-1}), 704 nm (110) (Figure 6a) in acetonitrile solvent. It was found to be EPR silent (Figure 6b).

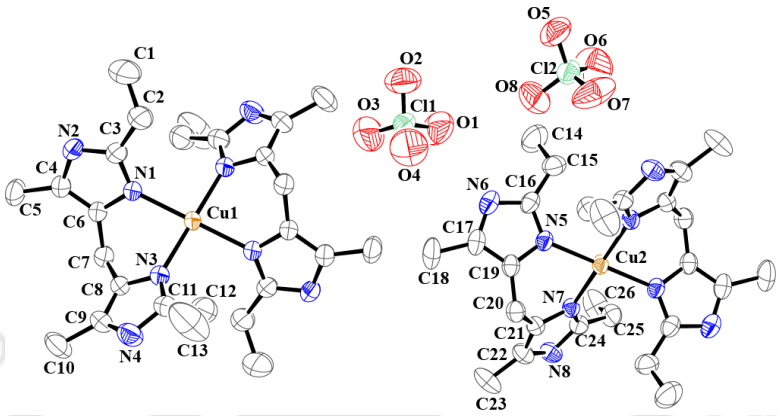

Figure 4 ORTEP diagram of complex **3.1** (50% thermal ellipsoid plot). Hydrogen atoms and solvent molecules are not shown for clarity.

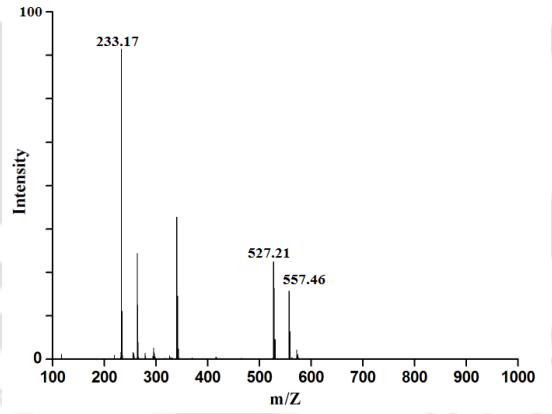

Figure 5 ESI-Mass spectrum of complex **3.2** in methanol.

In the FT-IR spectrum, it exhibits a vibration at 1662 cm^{-1}, which is attributed to the coordinated nitrosyl stretching frequency.[10] The frequency of this vibration was found to shift to 1631 cm^{-1} on ^{15}NO labelling experiment which further confirms its assignment as ν_{NO}. Complex **3.2** is stable at room temperature in the absence of moisture.

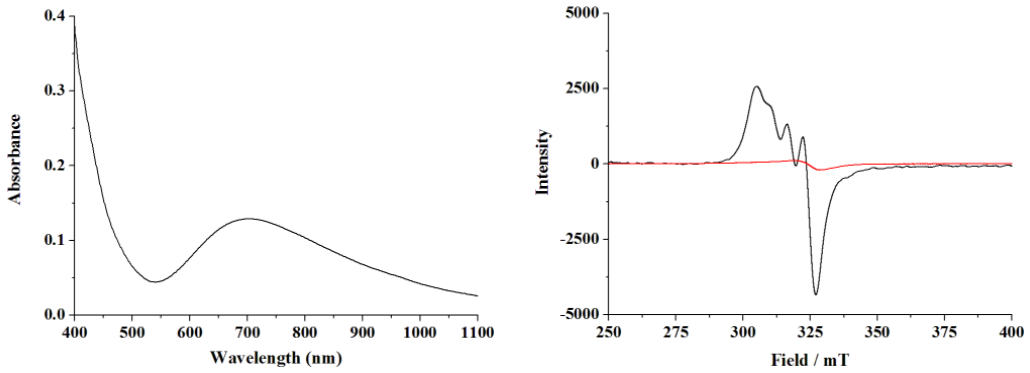

(a) (b)

Figure 6 (a) UV-visible spectrum of complex **3.2** in acetonitrile solution at room temperature. (b) X-band EPR spectra of the complexes **3.1** (black) and **3.2** (red) in acetonitrile solution at room temperature.

Complex **3.2** was found to react with water to result into the reduction of the copper (II) centre to copper(I) with a concomitant oxidation of coordinated NO to nitrite yielding a copper(I)–nitrite complex, **3.3** (Scheme 2).

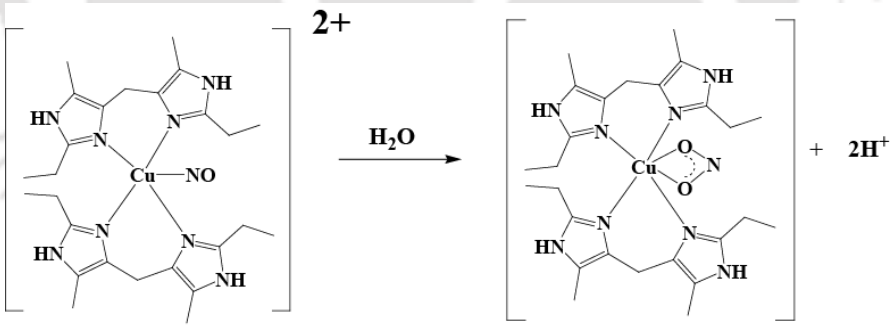

3. 2 **3. 3**

Scheme 2

The reduction of copper(II) to copper(I) has been monitored by the UV-visible spectroscopic studies (Figure 7a). The reaction mixture after the complete reduction was found to be EPR silent. In solution FT-IR study in acetonitrile solvent, the stretching frequency at 1662 cm^{-1} was found to disappear on addition of water (Figure 7b). The

formation of complex **3.3** was further authenticated by its single crystal X-ray structure determination. The ORTEP view of complex **3.3** is shown in figure 8.

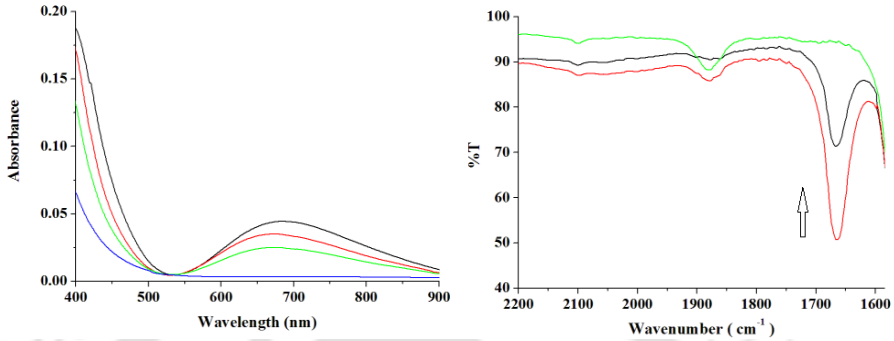

(a) (b)

Figure 7 (a) UV-visible spectroscopic monitoring of the reaction of complex **3.2** with water in acetonitrile. Black and blue traces represent complexes **3.2** and **3.3**, respectively; whereas, red and green ones represent the intermediate steps for the gradual decomposition of complex **3.2** to **3.3**. (b) Solution FT-IR spectroscopic monitoring of the reaction of complex **3.2** with water in acetonitrile. Only the gradual decay of ν_{NO} at 1662 cm^{-1} in presence of water is shown for clarity.

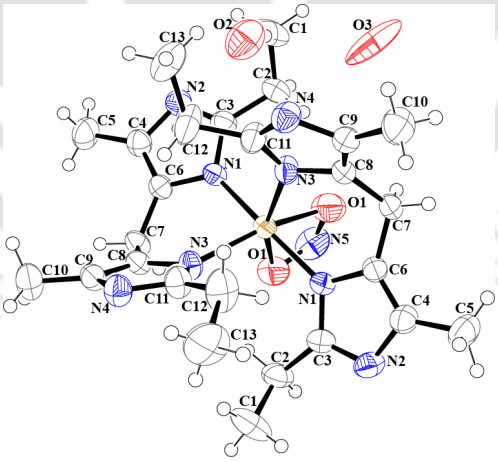

Figure 8 ORTEP diagram of complex **3.3** (50% thermal ellipsoid plot).

Thus the present chapter demonstrates an example of formation of stable copper(II)–nitrosyl from the reaction of copper(II) complex and NO gas. The copper(II)–nitrosyl

complex, in acetonitrile solvent, in the presence of water affords the corresponding copper(I)–nitrite (O-bound) complex. The sequence of the formation of these complexes, essentially, is just the reverse of the key steps of the postulated nitrite reduction cycle by copper containing nitrite reductases.

Chapter 4: Reaction of a copper (II)–nitrosyl complex with hydrogen peroxide: putative formation of a copper (I)–peroxynitrite intermediate

Stoichiometric addition of pre-cooled hydrogen peroxide to a cold (-20 °C) solution of complex **3.2** resulted in the formation of a colorless solution. The *d–d* transition band of complex **3.2** having λ_{max} at 704 nm was found to decrease in intensity with time upon addition of H_2O_2 suggesting the formation of copper(I) from copper(II) (Figure 9a). This has been formulated as a copper(I)–peroxynitrite complex. The putative formation of copper(I)-peroxynitrite was confirmed by its characteristic phenol ring nitration reaction.

In solution FT-IR studies at room temperature, the intensity of the ν_{NO} band at ~1662 cm^{-1} was found to be diminished upon addition of H_2O_2 with the appearance of NO_3^- stretching at ~1384 cm^{-1} (Figure 9b).

The reduction of the copper(II) centre to copper(I), in this case, was further authenticated by isolation and X-ray single crystal structure determination of the final copper(I) product, $[(L_3)_2Cu(NO_3)]$, **4.1**. The perspective ORTEP view for **4.1** is shown in figure 10a. The colorless solution on exposure to air resulted in the corresponding copper(II) complex, $[(L_3)_2Cu(NO_3)](ClO_4)$, **4.2**. The formation of complex **4.2** was confirmed by various spectroscopic analyses as well as its X-ray single crystal structure determination. The ORTEP view of complex **4.2** is shown in figure 10b.

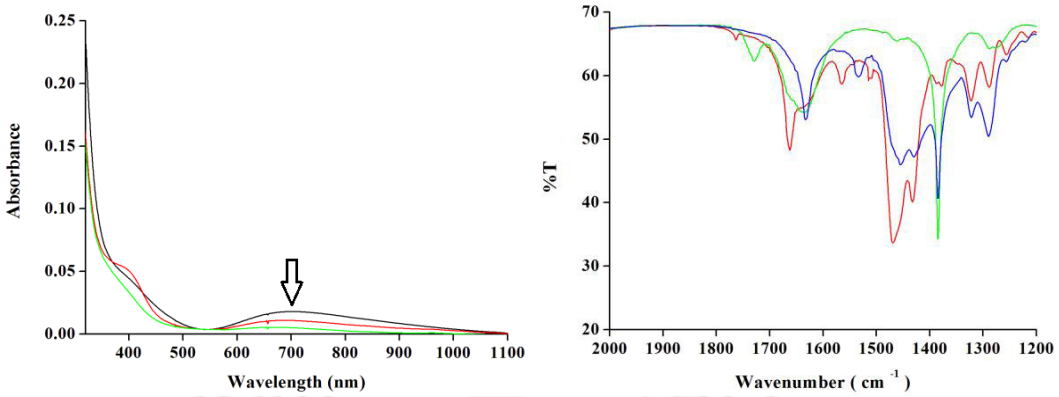

(a) (b)

Figure 9 (a) UV-visible monitoring of the reaction of complex **3.2** with H_2O_2 in acetonitrile at -20°C (black trace represents the spectrum of complex **3.2** and green represents that of the colorless intermediate). (b) FT-IR spectra of complexes **3.2**(red), **4.1** (green), **4.2** (blue) in KBr.

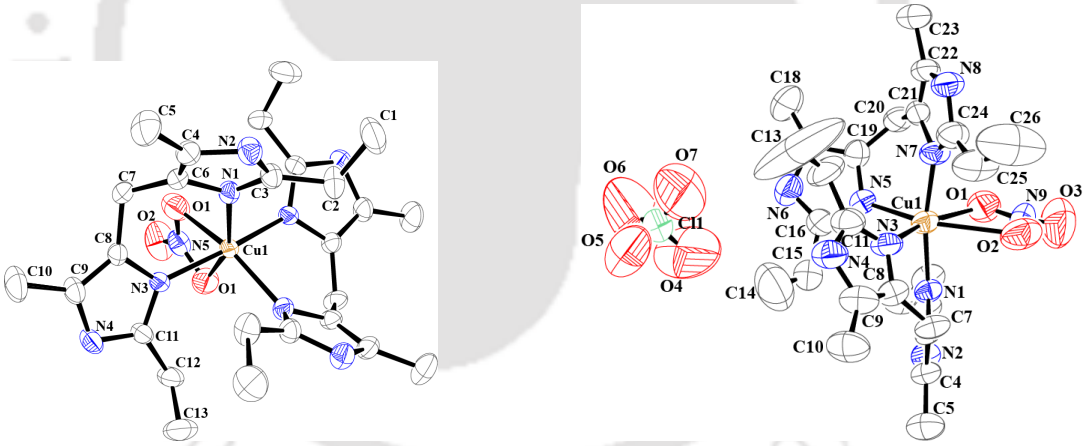

(a) (b)

Figure 10 ORTEP diagrams of complexes (a) **4.1** and (b) **4.2**. (Solvent molecules and hydrogen atoms are removed for clarity; 50% thermal ellipsoid plot).

The formation of complex **4.1** essentially supports the formation of a peroxynitrite intermediate in the course of the reaction (Scheme 3) as nitrate is the common decomposition / isomerisation product of peroxynitrite.[11]

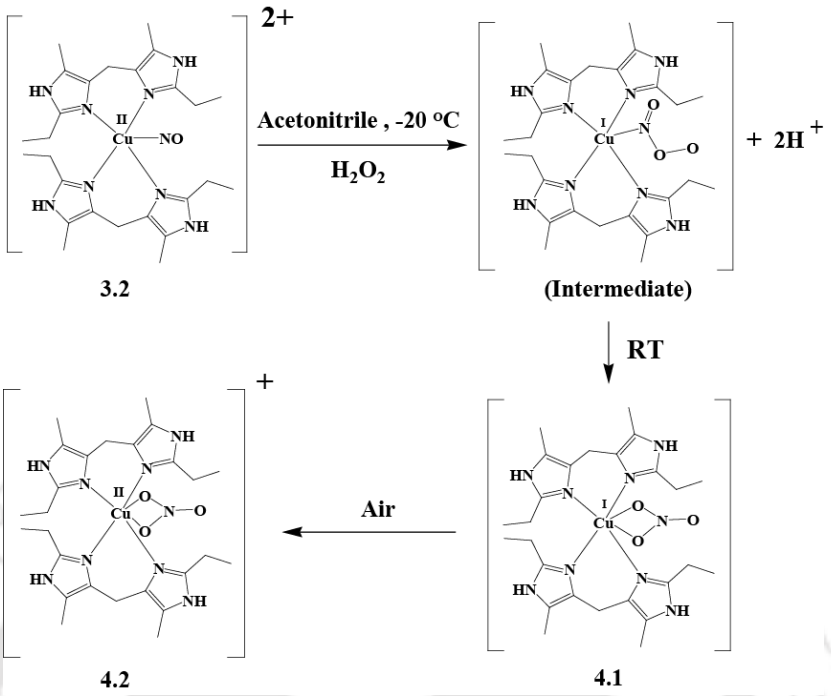

Scheme 3

The present chapter describes a possible decomposition pathway of both H_2O_2 as well as NO formed in biological systems.

Chapter 5: Reaction of a copper(II)–nitrosyl complex with hydrogen peroxide: Mimicking of tyrosine nitration

Copper(II) complex, **5.1**, was synthesized with the tetradentate ligand, $\mathbf{L_4}$ [$\mathbf{L_4}$ = methyl 2-(2-hydroxybenzylamino)-3-(1H-imidazol-5-yl)propanoate], as its perchlorate salt. Ligand $\mathbf{L_4}$ was synthesised purposefully to have a phenol ring in the ligand framework itself. In solid state, complex **5.1** crystallized as a phenoxo bridging dimer. The single crystal structure of complex **5.1** was determined. The perspective ORTEP view for **5.1** is shown in figure 11.

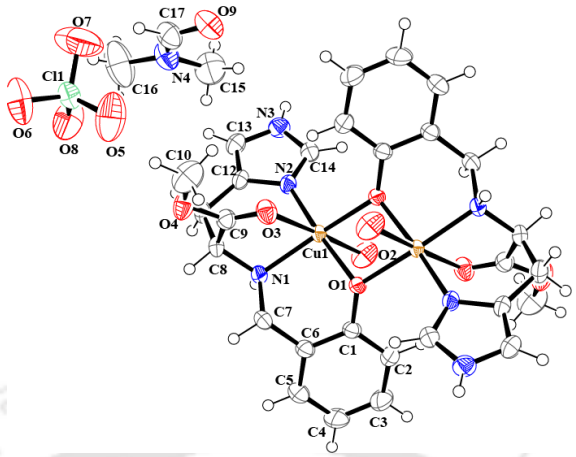

Figure 11 ORTEP diagram of complex **5.1** (50% thermal ellipsoid plot).

Complex **5.1** in acetonitrile solution exhibits a broad *d–d* band at λ_{max} (ε/M^{-1} cm^{-1}), 660 nm (244), along with relatively strong intra-ligand absorptions in the UV region. Addition of NO to a degassed acetonitrile solution of complex **5.1** resulted in the corresponding [Cu^{II}–NO] complex, **5.2**. ESI-mass spectrum also supports the formulation (Figure 12).

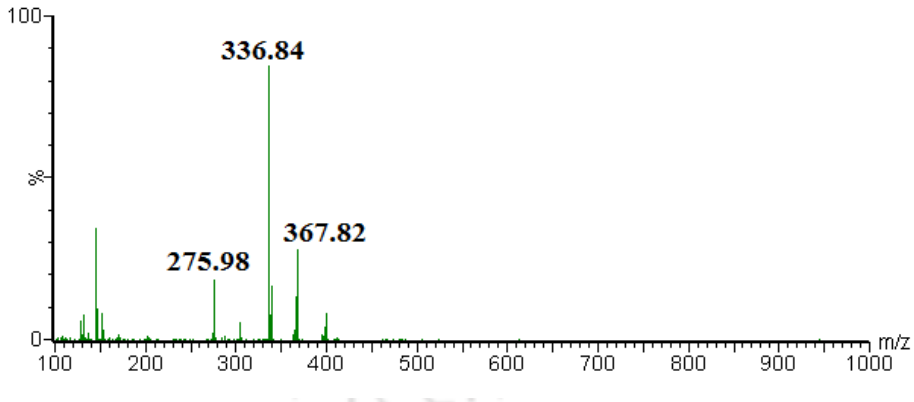

Figure 12 ESI-mass spectrum of complex **5.2** in acetonitrile.

In the FT-IR spectrum, it exhibits a vibration at 1846 cm^{-1}, which is attributed to the coordinated nitrosyl stretching frequency. The frequency of this vibration was found to shift to 1815 cm^{-1} on ^{15}NO labelling experiment which further confirms its assignment as ν_{NO}.

Stoichiometric addition of pre-cooled H_2O_2 to a cold (- 20 °C) solution of complex **5.2** resulted in the formation of a colorless solution as observed earlier in case of complex **3.2**. The *d–d* band of complex **5.2** centred at 645 nm was found to decay with time upon addition of H_2O_2 suggesting the formation of copper(I) from copper(II) (Figure 13a). The reduction of copper(II) centre in complex **5.2**, was accompanied with a simultaneous nitration of the ligand $\mathbf{L_4}$ and release of the modified phenol ring nitration product; $\mathbf{L_4'}$ was isolated and characterized (Scheme 4). This is attributed to the formation of an unstable copper(I)-peroxynitrite intermediate. Solution FT-IR studies at room temperature, also shows the decay of ν_{NO} band at ~1846 cm^{-1} upon addition of H_2O_2 (Figure 13b).

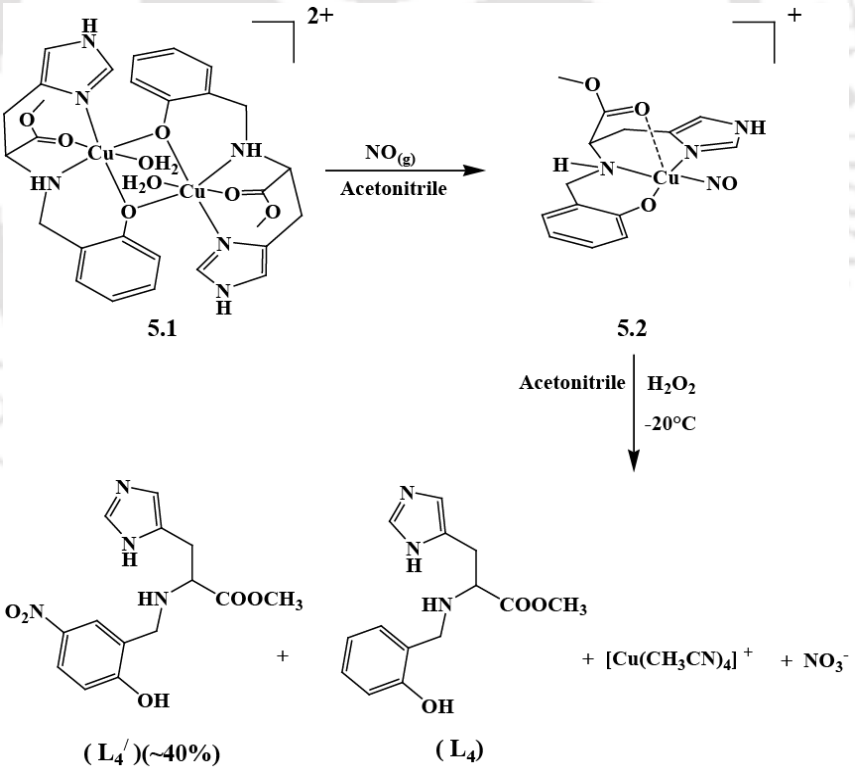

Scheme 4

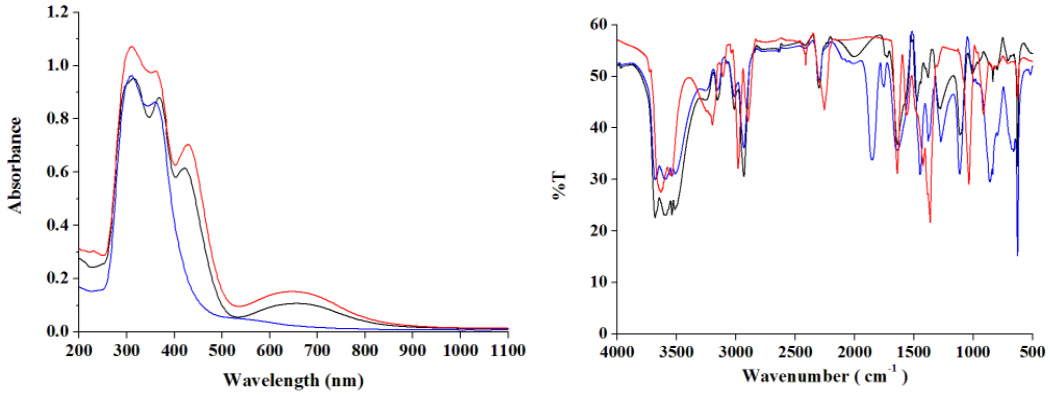

(a) (b)

Figure 13 (a) UV-visible spectra of complex **5.1** (black), complex **5.2** (red) and after reaction of complex **5.2** with H_2O_2 (blue) in acetonitrile solvent at room temperature. (b) Solution FT-IR spectra of complex **5.1** (black), complex **5.2** (blue) and after reaction of complex **5.2** with H_2O_2 (red) in acetonitrile solvent.

This chapter discusses the formation of stable [Cu^{II}-NO] complex from the reaction of copper(II) complex of a tetradentate ligand, $\mathbf{L_4}$. The [Cu^{II}-NO] complex, in presence of H_2O_2 resulted in corresponding copper(I)-peroxynitrite intermediate which induced the nitration of the phenol ring present in the ligand framework.

References

1. Moncada, S.; Palmer, R. M. J.; Higgs, E. A. *Pharmacol. Rev.* **1991**, *43*, 109.

2. Ignarro, L. J., Ed. *Nitric Oxide: Biology and Pathobiology* Academic Press: San Diego, 2000.

3. Ghosh, S.; Dey, A.; Usov, O. M.; Sun, Y.; Grigoryants, V. M.; Scholes, C. P.; Solomon, E. I. *J. Am. Chem. Soc*. **2007**, *129*, 10310.

4. Zhou, M. F.; Andrews, L. *J. Phys. Chem. A* **2000**, *104*, 2618.

5. Tran, D.; Ford, P. C. *Inorg. Chem*. **1996**, *35*, 2411.

6. (a) Tsuge, K.; DeRosa, F.; Lim, M. D.; Ford, P. C. *J. Am. Chem. Soc.* **2004**, *126*, 6564. (b) Khin, C.; Lim, M. D.; Tsuge, K.; Iretskii, A.; Wu, G.; Ford, P. C. *Inorg. Chem.* **2007**, *46*, 9323.

7. Sarma, M.; Kalita, A.; Kumar, P.; Singh, A.; Mondal, B. *J. Am. Chem. Soc.* **2010**, *132*, 7846.

8. Sarma, M.; Singh, A.; Mondal, B. *Inorg. Chim. Acta* **2010**, *363*, 63.

9. Sarma, M.; Mondal, B. *Inorg. Chem.* **2011**, *50*, 3206.

10. Tsumore, N.; Xu, Q. *Bull. Chem. Soc. Jpn.* **2002**, *75*, 1861. (b) Diaz, A.; Ortiz, M.; Sanchez, I.; Cao, R.; Mederos, A.; Sanchiz, J.; Brito, F. *J. Inorg. Biochem.* **2003**, *95*, 283. (c) Wright, A. M.; Wu, G.; Hayton, T. W. *J. Am. Chem. Soc.* **2010**, *132*, 14336.

11. Herold, S.; Koppenol, W. H. *Coord. Chem. Rev.* **2005**, *249*, 499. (b) Ford, P. C.; Lorkovic, I. M. *Chem. Rev.* **2002**, *102*, 993.

Chapter 1

Introduction

1.1 General aspects of nitric oxide

Nitric oxide (NO) plays fundamental roles in biochemical processes.[1] Natural physiological activities of NO are now known to include roles in blood pressure control, neurotransmission and immune response. Subsequent reports have identified a number of disease states involving NO imbalances and such observations have stimulated extensive research activity into the chemistry, biology, and pharmacology of NO.[2,3] Most of the role played by NO in biology is attributed to the formation of nitrosyl complexes of the metallo-proteins, mostly iron or copper. The best characterized example is the ferro-heme enzyme soluble guanylyl cyclise (sGC).[4] Formation of a nitrosyl complex with Fe(II) leads to labilization of a *trans* axial (proximal) histidine ligand in the protein backbone, and the resulting change in the protein conformation is believed to activate the enzyme for catalytic formation of the secondary messenger cyclic-guanylyl monophosphate (cGMP) from guanylyl triphosphate (GTP). The enzymatic formation of cGMP leads to relaxation of smooth muscle tissue of blood vessels, hence lowering blood pressure. For bioregulatory purposes, NO concentrations generated are low and less than 1 μM have been reported to be generated in endothelium cells for blood pressure control.[5]

Another example includes the catalytic cycle of bacterial copper containing nitrite reductase (Cu-NiRs) where a [Cu^{I}-NO^{+} ↔ Cu^{II}-NO] intermediate is known to involve in the conversion of NO_2^- to NO or, in some cases to N_2O (Scheme 1.1).[6-10]

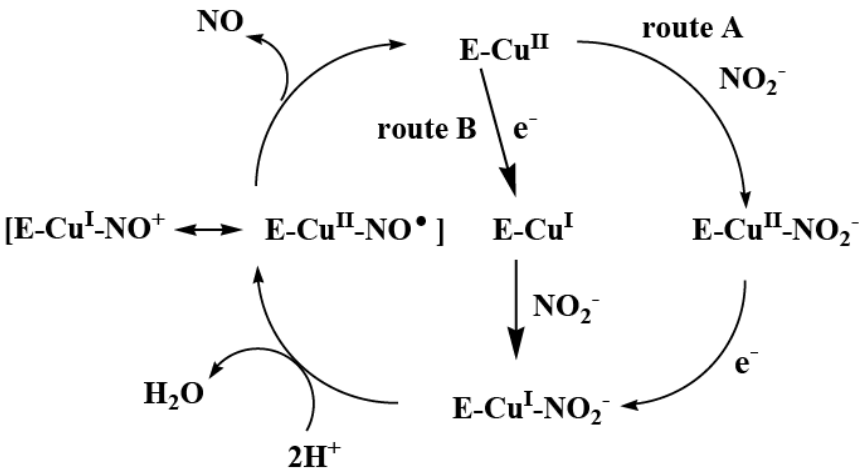

Scheme 1.1

In a complex with a metal centre, the character of the NO ligand can range from that of a nitrosyl cation (NO^+), which binds to the metal with an M-NO angle of ~180°, to that of a nitroxyl anion (NO^-), for which a bond angle of ~120° might be anticipated. The ability to form a stable NO complex and the structure of that species depend strongly on the oxidation state of the metal. In this direction, the iron-nitrosyls, both in protein and synthetic model systems have been studied extensively. In this regard, NO has been found to interact reversibly with many metal complexes to form stable Fe-NO complexes.[11] The binding in these complexes is similar to the coordination of dioxygen to such metal centres, although the nitrosyl products are far more stable and easy to characterize than are their superoxo analogues. The nitroprusside anion, $[Fe(CN)_5(NO)]^{2-}$ is perhaps the earliest discovered nitrosyl complex, and it remains the subject of intense research efforts.[12-15]

$\{Fe\text{-}NO\}^7$ coordination complexes such as [Fe(NO)(EDTA)] and $[Fe(L)(NO)(N_3)_2]$ (L= triazacyclononane and derivatives) have been studied in great detail by Solomon and co workers using diverse spectroscopic and analytical techniques. These studies have shown the $\{Fe\text{-}NO\}^7$ complexes to be best described as a high-spin ferric ion (S = 5/2)

antiferromagnetically coupled to NO^- ($S = 1$).[16-20] Mossbauer spectroscopic studies on these complexes also found to be in agreement with this description.[21,22] A series of trigonal bipyramidal $\{Fe\text{-}NO\}^7$ complexes has been reported by Borovik and co-workers. These complexes were synthesized with tripodal ligands derived from *tris*(carbamoylmethyl) amine by reaction of $[Fe(OAc)_2]$ with the tripotassium salt of the ligand. Magnetic moment, Mossbauer and ESR data are all consistent with an electronic configuration of $[Fe^{III}\text{-}NO^-]$.[23,24] Lippard and co-workers have described the diiron dinitrosyl complex $[Fe_2(\mu\text{-Et-HPTB})(\mu\text{-}O_2CPh)(NO)_2][BF_4]_2.3MeCN$ (Et-HPTB = N,N,N′,N′-*tetrakis*(N-ethyl-2 benzimidazolylmethyl)-2-hydroxy-1,3,diaminopropane) as a model for the binding of O_2 to non-heme iron proteins.[25] The iron nitrosyl complexes $[Fe(NO)X(CH_2CH_2SC_6H_4\text{-}o\text{-}S)_2]$ (X = NR, S) have also been cited as models for the active sites in nitrogenase enzymes.[26-28]

1.2 Copper(II)-nitrosyl

Several theoretical and matrix-isolation studies on copper(II)–nitrosyl complexes have been reported.[29,30] These investigations have found that N-bound nitrosyls are more stable than O-bound nitrosyls. Copper-containing zeolites have been found to form mono- and dinitrosyl species when exposed to NO.[31,32] Alcoholic solutions of CuX_2 (X = Cl, Br, F) have been reported to absorb NO, generating deeply colored solutions that exhibit strong ν_{NO} in their solution IR spectra, but the structures of these are not known.[33-35] Another $\{CuNO\}^{10}$ complex reported is $[Cu(NO)(H_2SO_4)_n]^{2+}$, though not properly characterized.[36] The lack of structural data for these complexes highlights the need for new copper(II)-nitrosyls to be isolated and characterized. Cao and coworkers reported the formation of air-stable copper(II)-nitrosyl and dinitrosyl species in the reaction of copper(II)-

dithiocarbamates with NO in aqueous solution.[37] This was, perhaps, the first report of formation of air stable [Cu^{II}-NO] complex (Scheme1.2).

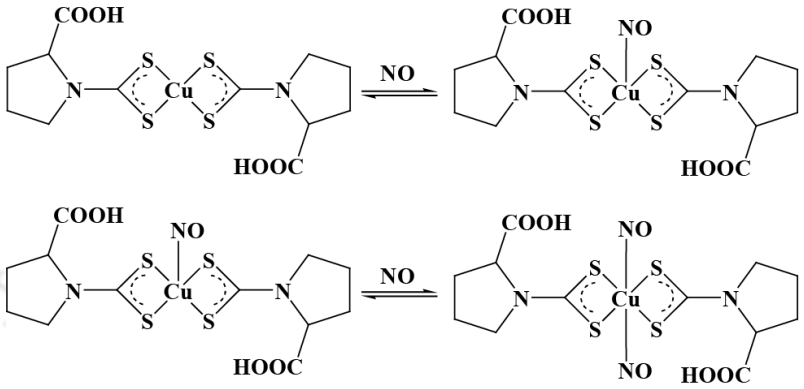

Scheme 1.2

Vagliasindi et al has reported the interaction of NO with a series of copper(II) complexes of small peptides coming from the N-terminal prion protein octa-repeat region. In aqueous solutions of Cu-Ac-HGGG-NH_2 and Cu-Ac-PHGGGWGQ-NH_2 systems at ~ pH 7.5, reduction of copper(II) centres were observed in presence of NO source.[38] Spectral studies suggested that these reductions were probably mediated by the formation of a labile [Cu^{II}-NO] adduct.[38]

Copper(II) has also been known to promote the nitrosation of various thiolates (forming *S*-nitrosothiols) and copper(II) reduction was found to correlate with formation of *S*-nitroso bovine serum albumin (BSA) and *S*-nitroso glutathione. Such observations have been used to fomulate a potential mechanism for the formation of RSNO compounds found in blood.[39,40] However, copper(I) centres are known to participate in side reactions leading to RSNO degradation to reform NO (Equation 1.1).[41] This pathway have received attention as a possible route to β-cys-93 S-nitrosylated hemoglobin which is controversial proposal regarding the NO transport in cardiovascular systems.[42]

$$Cu^{II} + BSA\text{-}SH \underset{+H^+}{\overset{-H^+}{\rightleftharpoons}} [\,Cu^{II} + BSA\text{-}S^-\,]^+ \overset{-NO}{\underset{+NO}{\rightleftharpoons}} BSA\text{-}SNO + Cu^{I} \quad \text{..... (1.1)}$$

With the greatly increased interest in NO reactions under biologically relevant conditions, there has been renewed attention to reductive nitrosylation and its mechanisms involving the reduction of iron(III) and copper(II) centres (Equation 1.2).[43]

$$L_nM^{m+} + NO + X^- \rightleftharpoons L_nM^{(m-1)+} + X\text{-}NO \quad \text{..... (1.2)}$$

X = nucleophile, M = Fe / Cu

It is notable that not only the reduction of the metal centre but also the formation of the nitrosated product X-NO may have significance in mammalian physiology, because such species may have roles in NO transport and in redox sensing and signaling.[44,45]

In this direction, though the interaction of NO with heme protein have been studied in details, only a few literatures are available that deal with the detail kinetic studies of the copper(II) *vs.* NO reactions. Tran et al has reported the reaction of NO with the copper(II) complex, $[Cu(dmp)_2(H_2O)]^{2+}$ (dmp = 2,9-dimethyl-1,10-phenanthroline), in methanol that leads to formation of a tetra-coordinated $[Cu(dmp)_2]^+$ complex along with methyl nitrite and H_2O (Equation 1.3). They have proposed that this reaction proceeds through the formation of $[Cu^{II}\text{-}NO]$ species.[46]

$$[Cu(dmp)_2(H_2O)]^{2+} + NO + CH_3OH \longrightarrow [Cu(dmp)_2]^+ + CH_3ONO + H_2O + H^+ \quad \text{..... (1.3)}$$

Ford et al has reported another interesting reactivity of NO with the copper(II) complex, $[Cu(DAC)]^{2+}$ [DAC is 1,8-bis(9-anthracylmethyl)-derivative of the macrocyclic tetraamine cyclam (1,4,8,11-tetraazacyclotetradecane)].[47] Although the free ligand is fluorescent, the analogous solution of $[Cu(DAC)]^{2+}$ displays no luminescence at room temperature because of its intramolecular quenching by the copper(II) centre. Introduction of NO to the methanolic solution of $[Cu(DAC)]^{2+}$ restores the fluorescence through the reduction of copper(II) to copper(I). The reduction of copper(II) centre was also found to follow by nitrosation of the ligand and subsequent demetalation (Scheme 1.3). The kinetic studies of this reaction showed that there was a first-order dependence on concentration of NO and the reaction was accelerated at higher pH.

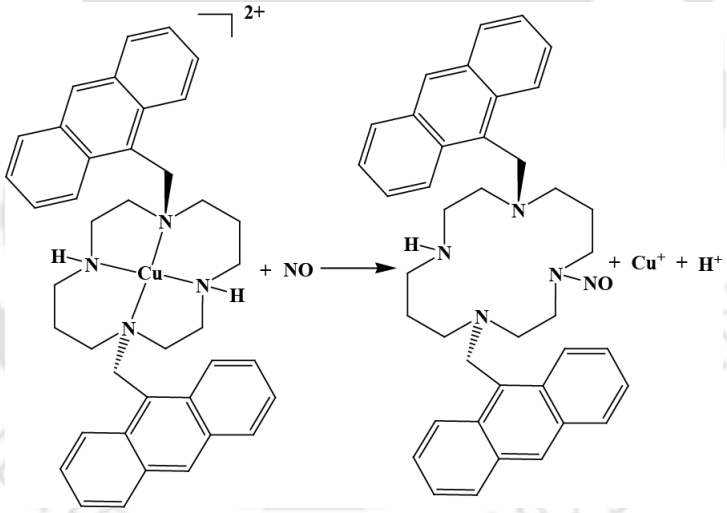

Scheme 1.3

In recent reports of reaction of NO with $[Cu(TEAEA)(CH_3CN)]^{2+}$, **1.1** and $[Cu(TIAEA)(CH_3CN)]^{2+}$, **1.2** {TEAEA = *tris*(2-ethylaminoethyl)amine; TIAEA = *tris*(2-isopropylaminoethyl)amine}complexes , reduction of copper(II) entre has been reported to proceed through the formation of a thermally unstable [Cu^{II}-NO] intermediate (Scheme 1.4).[48]

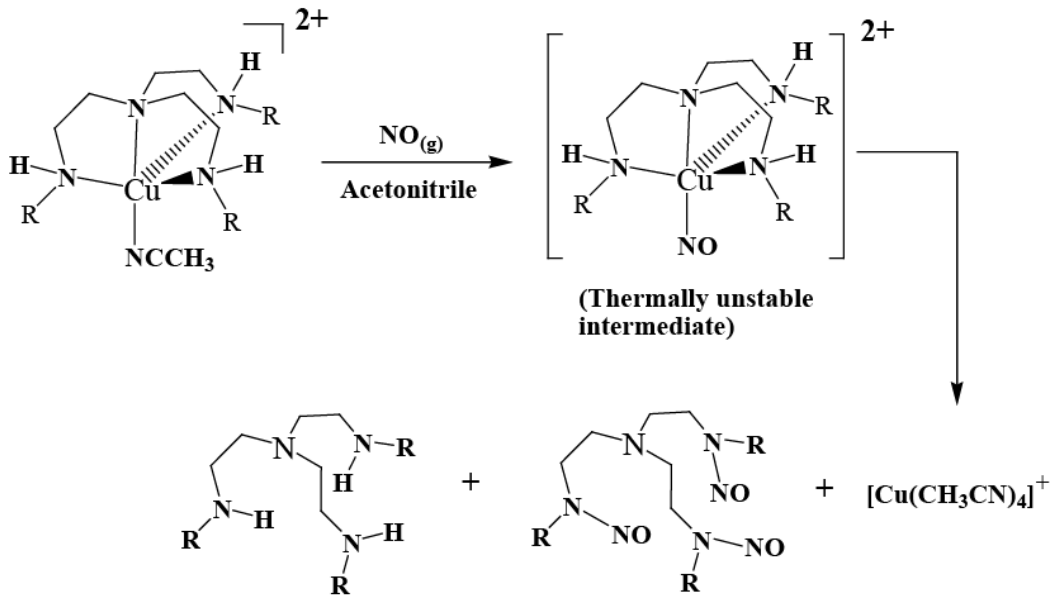

R= -Et, -^{i}Pr

Scheme 1.4

The reaction was monitored by UV-visible, EPR and solution FT-IR spectroscopic studies. Complexes, **1.1** and **1.2** in acetonitrile solvent exhibit broad *d-d* bands at λ_{max} (ε/ M^{-1} cm^{-1}), 826 nm (340) and 615 nm (110) (shoulder) for **1.1;** 620 nm (200) and 820 nm (150) (shoulder) for **1.2,** along with relatively strong intraligand absorptions in the UV region. Upon exposure to NO gas, deep-blue solutions of **1.1** and **1.2** in dry, degassed acetonitrile produced thermally unstable intermediates with shifts of λ_{max} to 640 and 605 nm, respectively (Figure 1.1). EPR studies of the frozen solutions of the intermediates revealed that these are EPR silent. Hence, it is logical to believe that in both the cases, [Cu^{II}-NO] intermediates were formed.

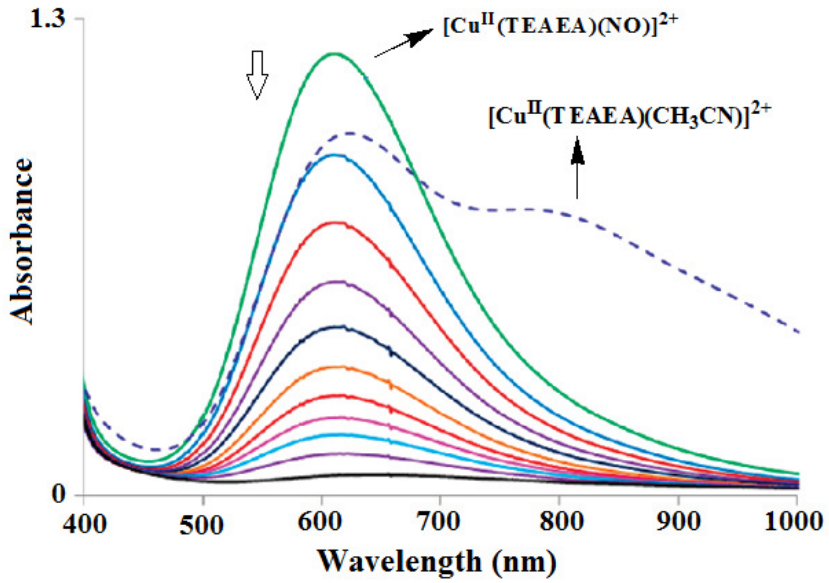

Figure 1.1 UV-visible spectroscopic monitoring of the formation of a [Cu^{II}-NO] intermediate and its gradual decomposition to copper(I) species in the case of complex **1.2**

Spectral evidences for the formation [Cu^{II}-NO] intermediate has been reported in the reaction of NO with $[Cu(TAEA)(CH_3CN)]^{2+}$, **1.3**; $[Cu(PYMEA)_2]^{2+}$, **1.4** and $[Cu(BAEA)(CH_3CN)]^{2+}$, **1.5** {TAEA = *tris*(2- aminoethyl)amine; PYMEA = pyridine-2-methylamine and BAEA = *bis*(2-amino ethyl)amine}complexes.[49,50]

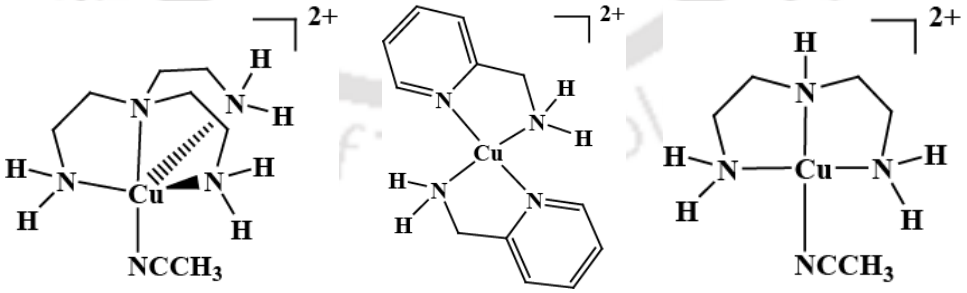

1.3 **1.4** **1.5**

In the FT-IR spectra of the acetonitrile solutions of complexes **1.3**, **1.4** and **1.5** after addition of NO a new intense and sharp band was found to appear at ~1650 , 1642 and

1635 cm^{-1}, respectively. These were assigned as stretching of NO (ν_{NO}) coordinated to the copper(II) centre.[49,50] These were found to disappear with time, indicating the unstable nature of the intermediate (Figure 1.2).

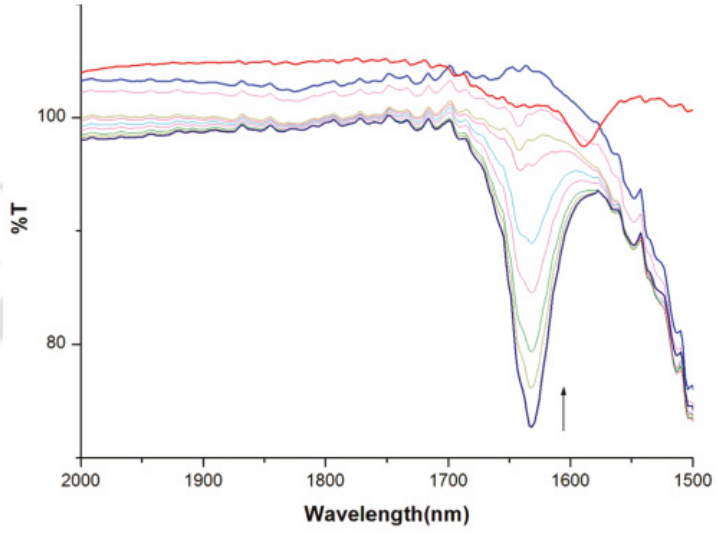

Figure 1.2 The solvent subtracted FT-IR spectra obtained from the reaction of complex **1.5** with NO in acetonitrile at room temperature. The top blue trace represents the spectrum of complex **1.5** in acetonitrile. The bottom dark trace represents the spectrum of the [Cu^{II}-NO] intermediate after the reaction of complex **1.5** with NO, and the red one represents the complete conversion of copper(II) to copper(I) .The gradual decrease of the intensity of the band is represented by the arrow.

Recently, Hayton et al have reported structurally characterized copper(II)-nitrosyl ($\{CuNO\}^{10}$ configuration) complex, [Cu $(CH_3NO_2)_5(NO)][PF_6]_2$, **1.6**.[51] Here, Cu-N-O angle is found to be 121.0(3)°. This complex shows ν_{NO} at 1933 cm^{-1} in FT-IR spectrum in nujol. This complex was reported to react with mesitylene to form [mesitylene, NO][PF_6] and [Cu(η^2-1,3,5-$Me_3C_6H_3)_2$][PF_6] by transfer of NO^+ to the mesitylene ring.[51]

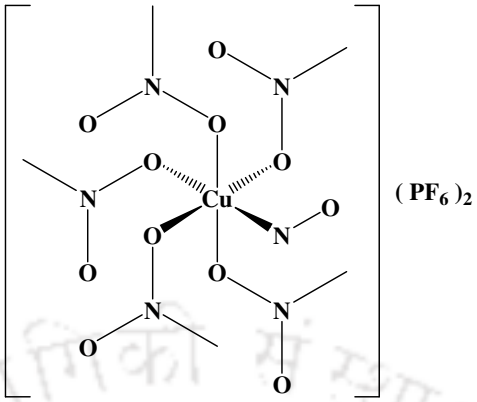

1.6

These results essentially instigate us to study the reactivity of NO with copper(II) complexes with various ligand frameworks with a target to identify, stabilize and characterize the possible [Cu^{II}-NO] intermediate. The works presented in the proceeding chapters of the thesis will preliminary focus on:

- General introduction on [Cu^{II}-NO] intermediate in reduction of copper(II) by NO.
- The study of role of ligands in controlling the mechanism of reduction of copper(II) by NO.
- Stabilization of [Cu^{II}-NO] intermediate complex and its potential role in CuNiR cycle.
- Reaction of [Cu^{II}-NO] with H_2O_2 to form peroxynitrite complex as a possible decomposition pathway for NO and H_2O_2 in biological systems.

1.3 References

1. Moncada, S.; Palmer, R. M. J.; Higgs, E. A. *Pharmacol. Rev.* **1991**, *43*, 109.

2. Ignarro, L. J., Ed. *Nitric Oxide: Biology and Pathobiology* Academic Press: San Diego, 2000.

3. Fang, F. C., Ed. *Nitric Oxide and Infection* Kluwer Academic/ Plenum Publishers: New York, 1999.

4. (a) Kim, S.; Deinum, G.; Gardner, M. T.; Marletta, M. A.; Babcock, G. T. *J. Am. Chem. Soc.* **1996**, *118*, 8769. (b) Burstyn, J. N.; Yu, A. E.; Dierks, E. A.; Hawkins, B. K.; Dawson, J. H. *Biochemistry* **1995**, *34*, 5896.

5. Malinski, T.; Czuchajowski, C. *Methods in Nitric Oxide Research*; Feelisch M., Stamler, J. S., Eds.; John Wiley and Sons: Chichester, England, 1996; Chapter 22.

6. Tolman, W. B. *Adv. Chem. Ser.* **1995**, *246*, 195.

7. Ferguson, S. J. *Curr. Opin. Chem. Biol.* **1998**, *2*, 182.

8. Richardson, D. J.; Watmough, N. J. *Curr. Opin. Chem. Biol.* **1999**, *3*, 207.

9. Moura, I.; Moura, J. J. G. *Curr. Opin. Chem. Biol.* **2001**, *5*, 168.

10. Ghosh, S.; Dey, A.; Usov, O. M.; Sun, Y.; Grigoryants, V. M.; Scholes, C. P.; Solomon, E. I. *J. Am. Chem. Soc*. **2007**, *129*, 10310.

11. Haskin, C. J.; Ravi, N.; Lynch, J. B.; Munck, E.; Que, L., Jr. *Biochemistry* **1995**, *34*, 11090.

12. Estrin, D. A.; Baraldo, L. M.; Slep, L. D.; Barja, B. C.; Olabe, J. A.; Paglieri, L.; Corongiu, G. *Inorg. Chem.* **1996**, *35*, 3897.

13. Nikol'skii, A. B.; Kotov, V. Y.; Vitalii, Y. *Mendeleev Commun.* **1995**, *4*, 139.

14. Gomez, J. A.; Guenzburger, D. *Chem. Phys.* **2000**, *253*, 73.

15. Inoue, H.; Narino, S.; Yoshioka, N.; Fluck, E. *Z. Naturforsch., B: Chem. Sci.* **2000**, *55*, 685.

16. Brown, C. A.; Pavlosky, M. A.; Westre, T. E.; Zhang, Y.; Hedman, B.; Hodgson, K. O.; Solomon, E. I. *J. Am. Chem. Soc.* **1995**, *117*, 715.

17. Westre, T. E.; Dicicco, A.; Filipponi, A.; Natoli, C. R.; Hedman, B.; Solomon, E. I.; Hodgson, K. O. *J. Am. Chem. Soc.* **1994**, *116*, 6757.

18. Westre, T. E.; Di Cicco, A.; Filipponi, A.; Natoli, C. R.; Hedman, B.; Solomon, E. I.; Hodgson, K. O. *Physica B* **1995**, *208/209*, 137.

19. Zhang, Y.; Pavlosky, M. A.; Brown, C. A.; Westre, T. E.; Hedman, B.; Hodgson, K. O.; Solomon, E. I. *J. Am. Chem. Soc.* **1992**, *114*, 9189.

20. Farrar, J. A.; Grinter, R.; Pountney, D. L.; Thomson, A. J. *J. Chem. Soc., Dalton Trans.* **1993**, 2703.

21. Hauser, C.; Glaser, T.; Bill, E.; Weyhermuller, T.; Wieghardt, K. *J. Am. Chem. Soc.* **2000**, *122*, 4352.

22. Marlin, D.; Mascharak, P. *Chemtracts* **2000**, *13*, 539.

23. Hammes, B. S.; Ramos-Maldonado, D.; Yap, G. P. A.; Liable- Sands, L.; Rheingold, A. L.; Young, V. G.; Borovik, A. S. *Inorg. Chem.* **1997**, *36*, 3210.

24. Ray, M.; Golombek, A. P.; Hendrich, M. P.; Yap, G. P. A.; Liable- Sands, L. M.; Rheingold, A. L.; Borovik, A. S. *Inorg. Chem.* **1999**, *38*, 3110.

25. Feig, A. L.; Bautista, M. T.; Lippard, S. J. *Inorg. Chem.* **1996**, *35*, 6892.

26. Sellmann, D.; Becker, T.; Hofmann, T.; Knoch, F.; Moll, M. *Inorg. Chim. Acta* **1994**, *219*, 75.

27. Sellmann, D.; Hohn, K.; Moll, M. *Z. Naturforsch., B: Chem. Sci.* **1991**, *46*, 665.

28. Sellmann, D.; Hohn, K.; Moll, M. *Z. Naturforsch., B: Chem. Sci.* **1991**, *46*, 673.

29. Zhou, M. F.; Andrews, L. *J. Phys. Chem. A* **2000**, *104*, 2618.

30. Dobos, S.; Cesaro, S. N. *High Temp. Mater. Sci.* **1997**, *37*, 81.

31. Spoto, G.; Bordiga, S.; Scarano, D.; Zecchina, A. *Catal. Lett.* **1992**, *13*, 39.

32. Spoto, G.; Zecchina, A.; Bordiga, S.; Ricchiardi, G.; Martra, G.; Leofanti, G.; Petrini, G. *Appl. Catal., B* **1994**, *3*, 151.

33. Kohlschutter, V.; Kutscheroff, M. *Chem. Ber.* **1904**, *37*, 3044.

34. Fraser, R. T. M.; Dasent, W. E. *J. Am. Chem. Soc.* **1960**, *82*, 348.

35. Fraser, R. T. M. *J. Inorg. Nucl. Chem.* **1961**, *17*, 265.

36. Tsumore, N.; Xu, Q. *Bull. Chem. Soc. Jpn.* **2002**, *75*, 1861.

37. Diaz, A.; Ortiz, M.; Sanchez, I.; Cao, R.; Mederos, A.; Sanchiz, J.; Brito, F. *J. Inorg. Biochem.* **2003**, *95*, 283.

38. Bonomo, R. P.; Pappalardo, G.; Rizzarelli, E.; Santoro, A. M.; Tabb`I, G.; Vagliasindi, L. I. *Dalton Trans.* **2007**, 1400.

39. Studbauer, G.; Giuffre, P.; Sarti, P. *J. Biol. Chem.* **1999**, *274*, 28128.

40. (a) Bryan, N. S.; Rassaf, T.; Maloney, R. E.; Rodriguez, C. M.; Saijo, F.; Rodriguez, J. R.; Feelisch, M. *Proc. Natl. Acad. Sci. U.S.A.* **2004**, *101*, 4308. (b) Rassaf, T.; Feelisch, M.; Kelm, M. *Free Radical Biol. Med.* **2004**, *36*, 413. (c) Giustarini, D.; Milzani, A.; Colombo, R.; Dalle-Donne, I.; Rossi, R. *Clin. Chim. Acta* **2003**, *330*, 85.

41. Ford, P. C.; Fernandez, B. O.; Lim, M. D. *Chem. Rev*. **2005**, *105*, 2439.

42. (a) Luchsinger, B. P.; Rich, E. N.; Gow, A. J.; Williams, E. M.; Stamler, J. S.; Singel, D. J. *Proc. Natl. Acad. Sci. U.S.A.* **2003**, *100*, 461. (b) Moriel, P.; Pereira, I. R. O.; Bertolami, M. C.; Abdalla, D. S. P. *Free Radical Biol. Med.* **2001**, *30*, 318. (c) Inoue, K.; Akaike, T.; Miyamoto, Y.; Okamoto, T.; Sawa, T.; Otagiri, M.; Suzuki, S.; Yoshimura, T.; Maeda, H. *J. Biol. Chem.* **1999**, *274*, 27069.

43. Lorkovic, I. M.; Ford, P. C. *Chem. Rev*. **2002**, *102*, 993.

44. (a) McMahon, T. J.; Gow, A. J.; Stamler, J. S. In *Nitric Oxide: Biology and Pathobiology*; Ignarro, L. J., Ed.; Academic Press: San Diego, CA, 2000; Chapter 15. (b) Gow, A. J.; Luchsinger, B. P.; Pawloski, J. R.; Singel, D. J.; Stamler, J. S. *Proc. Natl. Acad. Sci. U.S.A.* **1999**, *96*, 9027. (c) Luchsinger, B. P.; Rich, E. N.; Gow, A. J.; Williams, E. M.; Stamler, J. S.; Singel, D. J. *Proc. Natl. Acad. Sci. U.S.A.* **2003**, *100*, 461. (d) Gladwin, M. T.; Lancaster, J. R., Jr.; Freeman, B. A.; Schechter, A. N. *Nat. Med.* **2003**, *9*, 496. (e) Han, T. H.; Fukuto, J. M.; Liao, J. C. *NO Biol. Chem.* **2004**, *10*, 74.

45. (a) Feelisch, M. S.; Rassaf, T.; Mnaimneh, S.; Singh, N.; Byran, N. S.; Jourd'Heuil, D.; Kelm, M. *FASEB J.* **2002**, *16*, 1775. (b) Bryan, N. S.; Rassaf, T.; Maloney, R.

E.; Rodriguez, C. M.; Saijo, F.; Rodriguez, J. R.; Feelisch, M. *Proc. Natl. Acad. Sci. U.S.A.* **2004**, *101*, 4308.

46. Tran, D.; Ford, P. C. *Inorg. Chem.* **1996**, *35*, 2411.

47. Tsuge, K.; DeRosa, F.; Lim, M. D.; Ford, P. C. *J. Am. Chem. Soc.* **2004**, *126*, 6564.

48. Sarma, M.; Kalita, A.; Kumar, P.; Singh, A.; Mondal, B. *J. Am. Chem. Soc.* **2010**, *132*, 7846.

49. Sarma, M.; Singh, A.; Mondal, B. *Inorg. Chim. Acta* **2010**, *363*, 63.

50. Sarma, M.; Mondal, B. *Inorg. Chem.* **2011**, *50*, 3206.

51. Wright, A. M.; Wu, G.; Hayton, T. W. *J. Am. Chem. Soc.* **2010**, *132*, 14336.

Chapter 2

Role of ligand to control the mechanism of nitric oxide reduction of copper(II) complexes and ligand nitrosation

Abstract

The NO reactivity of two copper(II) complexes, **2.1** and **2.2** with ligands $\mathbf{L_1}$ and $\mathbf{L_2}$, respectively, [$\mathbf{L_1}$ = 5,5,7,12,12,14-hexamethyl-1,4,8,11-tetraazacyclotetradecane, $\mathbf{L_2}$ = 5,5,7-trimethyl-[1,4]-diazepane] have been studied. The copper(II) centre in complex **2.1** was found to be unreactive toward NO in pure acetonitrile; however, it displayed reduction in methanol solvent in presence of base. The copper(II) centre in **2.2**, in acetonitrile solvent, on exposure to NO has been found to be reduced to copper(I). The same reduction was observed in methanol, also, in case of complex **2.2**. In case of complex **2.1**, presumably, the attack of NO on the deprotonated amine is the first step, followed by electron transfer to the copper(II) centre to afford the reduction. Alternatively, first NO coordination to the copper(II) followed by NO^+ migration to the secondary amine is the most probable in case of complex **2.2**. The observation of the transient intermediate in UV-visible and FT-IR spectroscopy prior to reduction in case of complex **2.2** also supports this possibility. In both cases, the reduction resulted into N-nitrosation; in **2.1**, only mononitrosation was observed whereas complex **2.2** afforded dinitrosation as major product along with a minor amount of mononitrosation. Thus, it is evident from the present study that the macrocyclic ligands prefer the deprotonation pathway leading to mononitrosation; whereas nonmacrocyclic ones prefer the [Cu^{II}–NO] intermediate pathway resulting into nitrosation at all the available sites of the ligand as major product.

2.1 Introduction

Activation of NO by transition metal ions have attracted the chemists' attention as various biological and physiological reactivities of NO are attributed to the formation of nitrosyl complexes of metallo-proteins, mostly iron or copper-proteins.[1–3] In this direction, the iron-nitrosyls, both in protein and synthetic model systems have been studied extensively. Ferriheme proteins are known to undergo reduction in aqueous media in the presence of NO following a two-step process: (i) the formation of iron(III)-nitrosyl intermediate; (ii) followed by pH dependent reduction.[4,5] It is believed that in the next step the hydroxide ion attacks the activated nitrosonium group to afford nitrite ion and iron(II).[4] The ferrous protein then reacts with excess of NO to form stable ferro-heme nitrosyl.[6–8]

The reduction of copper(II) centres in some proteins, such as cytochrome *c* oxidase and laccase, to copper(I) on exposure to NO has been known for a long time, though has not been studied as extensively as in iron systems.[9–12] In model systems, this has been exemplified by a number of copper(II) complexes in recent years.[13–23]

The copper(II) centre in $[Cu(dmp)_2(X)]^{2+}$ (dmp = 2,9- dimethyl-1,10-phenanthroline, X = solvent) and in analogous complexes is found to undergo reduction in presence of NO, and the detailed study of the reduction mechanism has been reported by Ford et al.[24,25] It is observed that the reduction was accompanied by the nitrosation of the solvent resulting into methylnitrite or NO_2^- in case of methanol or water, respectively.[24,25]

The copper(II) centre in $[Cu^{II}(DAC)]^{2+}$ {DAC = 1,8-bis(9-anthracylmethyl) derivative of the macrocyclic tetraamine cyclam (1,4,8,11-tetraazacyclotetradecane)} in methanol solution is reported to undergo reduction by NO with a concomitant nitrosation of the ligand.[26] In contrast, copper(I) complexes with electron rich β-diketiminate ligands are found to induce reductive cleavage of the N-nitrosoamine bond leading to the release of

NO and the formation of copper(II)-amide complex.[27] It would be worth mentioning here that $[Cu(DAC)]^{2+}$ is reported as fluorescence sensor for NO.[26] Lippard's group used the same reduction strategy to develop copper complex based NO sensors and reported the examples of copper(II) complexes of anthracenyl and dansyl fluorophore ligands in this regard.[28,29] The quenched fluorescence intensity of the ligand fluorophore was observed to restore in presence of NO in methanol / dichloromethane solutions of the complexes. In addition, $[Cu(Ds\text{-}en)_2]$ and $[Cu(Ds\text{-}AMP)_2]$ [Ds-en and Ds-AMP are the conjugate bases of dansylethylenediamine (Ds-Hen) and dansyl aminomethylpyridine (Ds-HAMP), respectively], have been found to detect NO in aqueous solution, also.[27] Similar observations were reported for the reactions of $[Cu(Fl_n)]$ (Fl_n = a Fluorescine modified with a functionalized 8-aminoquinoline group) with NO which gave N-nitrosation of the Fl_n ligands.[28,29] From detail quantitative and theoretical studies, it has been established that in case of $[Cu(DAC)]^{2+}$, the reaction proceeds through a pathway analogous to the inner-sphere mechanism for electron transfer between two metal centres through a bridging ligand. In this case, NO is the reductant, copper(II), the oxidant, and the coordinated amido anion behaves as the bridging ligand. Owing to the preference of copper(I) for tetrahedral coordination and the decrease in donor ability of the nitrosated ligand, demetalation of the macrocyclic ring was observed after the reduction.

An example of such a mechanism is reported by Armor et al where the reaction of $[Ru(NH_3)_6]^{3+}$ with NO in alkaline solution results into the Ru(II)-dinitrogen complex, $[Ru(NH_3)_5(N_2)]^{2+}$.[30] Since, Ru(III) complexes are substitution inert and the reaction is base catalyzed, the N_2 ligand must be originated from one of the ammines. Nitrosation of a coordinated amide ligand with the concomitant reduction of Ru(III) to Ru(II) leads to the

formation of a coordinated nitroso amine, which on subsequent dehydration results in the coordinated dinitrogen complex.

The alternative mechanism, which is more close to that of ferriheme reduction, for the nitrosation would be the one involving the initial NO coordination to the copper(II) centre to form [Cu^{II}–NO ↔ Cu^{I}–NO^{+}].[31] In the successive steps, amine deprotonation and migration of NO^{+} to the coordinated amide would result into the nitrosoamine. Subsequently, demetalation from the ligand will occur. This, indeed, has been suggested earlier by Wayland and others.[32–36]

In our recent studies, with $[Cu(TAEA)(CH_3CN)]^{2+}$, $[Cu(TEAEA)(CH_3CN)]^{2+}$, $[Cu(TIAEA)(CH_3CN)]^{2+}$, $[Cu(PYMEA)_2]^{2+}$, and $[Cu(BAEA)(CH_3CN)]^{2+}$ [TAEA = *tris*(2-aminoethyl)amine; TEAEA = *tris*(2-ethylaminoethyl)amine; TIAEA = *tris*(2-isopropylaminoethyl)amine; PYMEA = pyridine-2-methylamine and BAEA = *bis*(2-aminoethyl)amine], the reduction was found to proceed through the formation of a thermally unstable [Cu^{II}–NO] intermediate.[37] This difference in mechanistic pathway is, perhaps, because of the difference in ligand environment. Hence, it is logical to believe that the ligand frameworks have a significant role in controlling the mechanistic pathway for the reduction of copper(II).

To study the role of ligand on the reactivity of the complex toward NO, this chapter describes the examples of copper(II) complexes with a cyclam derivative (**L_1**) and cyclic amine (**L_2**) ligands (Figure 2.1). Both the ligands have been known for a long time for their coordination chemistry with various transition metal ions.[38–45] The similar structural feature (Results and discussion section) of the corresponding complexes derived from these ligands essentially prompted to choose them for the present study.

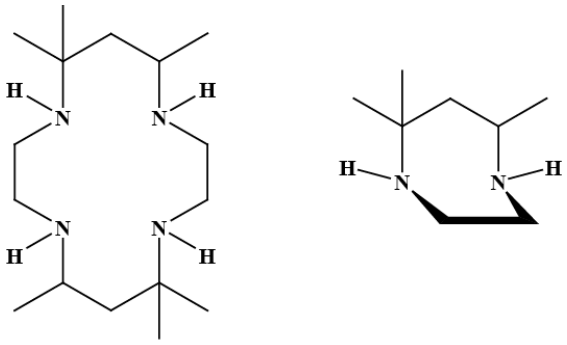

(L_1) **(L_2)**

Figure 2.1 Ligands used for the present study.

2.2 Results and discussion

Two copper(II) complexes, **2.1** and **2.2**, were synthesized with ligands, $\mathbf{L_1}$ and $\mathbf{L_2}$ [$\mathbf{L_1}$ = 5,5,7,12,12,14-hexamethyl-1,4,8,11-tetraazacyclotetradecane, $\mathbf{L_2}$ = 5,5,7-trimethyl-[1,4] diazepane], respectively, as their perchlorate salts. The complexes were characterized by various analytical techniques (Experimental section). Elemental analyses were found to be satisfactory for both the complexes (Experimental section). The single crystal structure of complex **2.1** was reported earlier.[46] The single crystal structures of both complexes were determined. The perspective ORTEP view for **2.2** is shown in figure 2.2. In **2.1**, copper(II) is found to be surrounded by four nitrogen donor atoms from $\mathbf{L_1}$ in a distorted square-planar geometry. In **2.2**, the copper(II) centre is coordinated with two $\mathbf{L_2}$ in square-planar fashion (Figure 2.2). The crystallographic table and important bond lengths and angles are given in appendix I (Tables A1.1, A1.2 and A1.3, respectively).

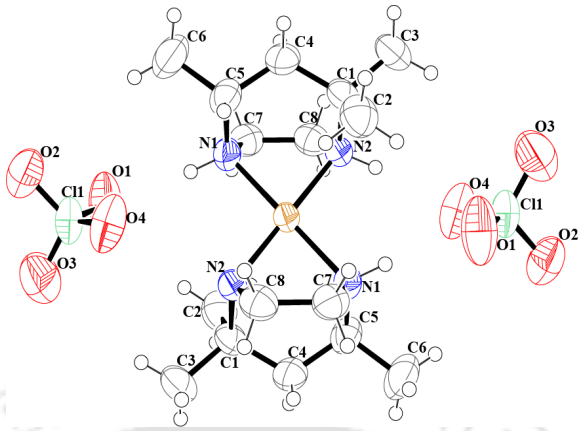

Figure 2.2 ORTEP diagram of complex **2.2** (50% thermal ellipsoid plot).

The Cu(1)–N(1) and Cu(1) –N(2) distances in complexes **2.1** / **2.2** are found to be 2.046(1) / 1.999(2) Å and 2.027(2) / 2.010(3) Å, respectively, which are within comparable ranges. The other bond lengths of the coordinated ligands in both complexes are very similar. For instance, the N(1)–C(1), C(1)–C(4), C(4)–C(5), and C(5)–N(2) distances in **2.1** / **2.2** are 1.504(3) / 1.509(4)Å, 1.536(3) / 1.534(5)Å, 1.515(3) / 1.525(5) Å, and 1.496(2) / 1.518(4) Å, respectively. The N(1)–C(8), N(2)–C(7), and C(7)–C(8) distances in **2.1/2.2** are found to be 1.480(3) / 1.498(4) Å, 1.476(2) / 1.484(5) Å, and 1.516(3) / 1.537(5) Å, respectively. From the structural parameters, it is evident that both complexes have similar ligand environment and geometry around the copper centre. The only difference is in complex **2.1** where the ligand is a tetradentate macrocycle and in complex **2.2** the ligand is a bidentate cyclic amine. The complexes **2.1** and **2.2**, in acetonitrile solvent, exhibit broad *d-d* bands at λ_{max} (ε/M^{-1} cm^{-1}), 523 nm (120) and 454 nm (275), along with relatively strong intraligand absorptions in the UV region (Figure 2.3).

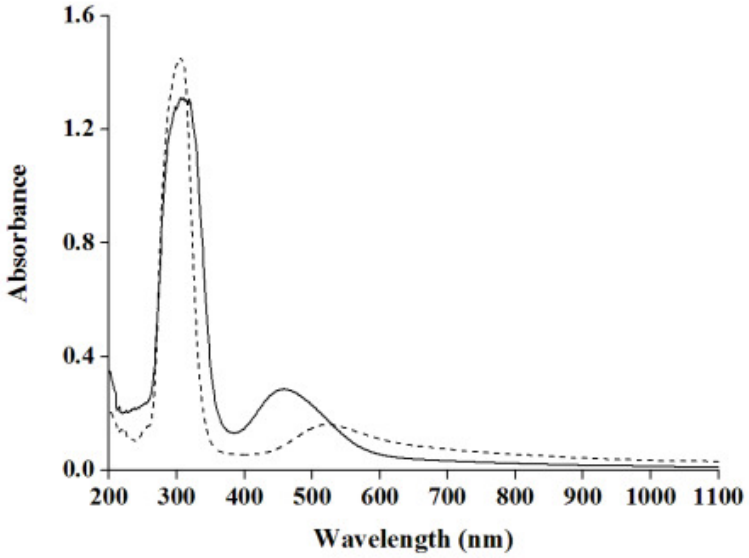

Figure 2.3 UV-visible spectra of complexes **2.1**(dashed line) and **2.2**(solid line) in acetonitrile solution at room temperature.

The acetonitrile solutions of the complexes displayed characteristic four line axial spectra in X-band EPR studies at 77 K (Figure 2.4).[47]

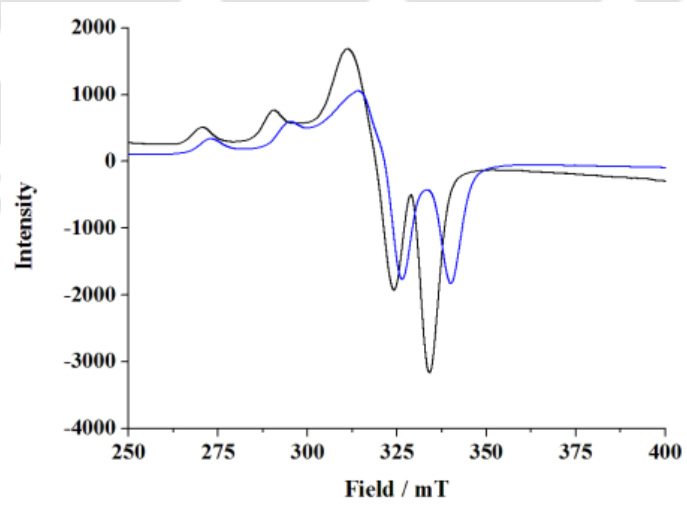

Figure 2.4 X-Band EPR spectra of complexes **2.1** (black) and **2.2** (blue) in acetonitrile at 77 K.

The calculated spectral parameters, $g_{\|}$, $g_{\perp}$, and $A_{\|}$ are 2.152, 2.040, and 192 × 10^{-4} cm^{-1} for complex **2.1** and 2.118, 2.011, and 190 × 10^{-4} cm^{-1} for complex **2.2**, respectively. Both the complexes exhibit one electron paramagnetism at room temperature, as expected.

The cyclic voltammetirc studies of the pure complexes have been carried out in acetonitrile solvent. Complex **2.1** exhibited one irreversible couple at −1.15 V *versus* Ag/Ag^{+}, and this has been attributed to the Cu^{II}/Cu^{I} couple (Appendix I, Figure A1.25). Earlier, Olson et al also reported this couple to appear at −1.161 V *versus* Ag/Ag^{+} electrode.[48] The Cu^{II}/Cu^{I} couple was also observed to appear in this range for analogous reported compounds.[49] On the other hand, for complex **2.2**, irreversible reduction was observed at −0.91 V *versus* Ag/Ag^{+} (Appendix I, Figure A1.26).The difference in reduction potential for the two complexes is attributed to the difference in ligand framework.[50] The cyclic voltammograms of complex **2.1** in presence of sodium methoxide was also recorded (Appendix I, Figure A1.27). However, the voltammogram becomes progressively ill-defined with the increasing amount of sodium methoxide which essentially precluded its further studies.

2.3 Nitric oxide reactivity

NO reactivity of the complexes was studied in acetonitrile and methanol media. Complex **2.1**, in dry and degassed acetonitrile, did not react with NO. Even after purging NO gas into the acetonitrile solution of complex **2.1** for 2 minutes, no spectral change has been observed. However, in methanol solution, complex **2.1** was found to react with NO in presence of base to result in a colorless solution indicating the reduction of copper(II) centre to copper(I) (Scheme 2.1).

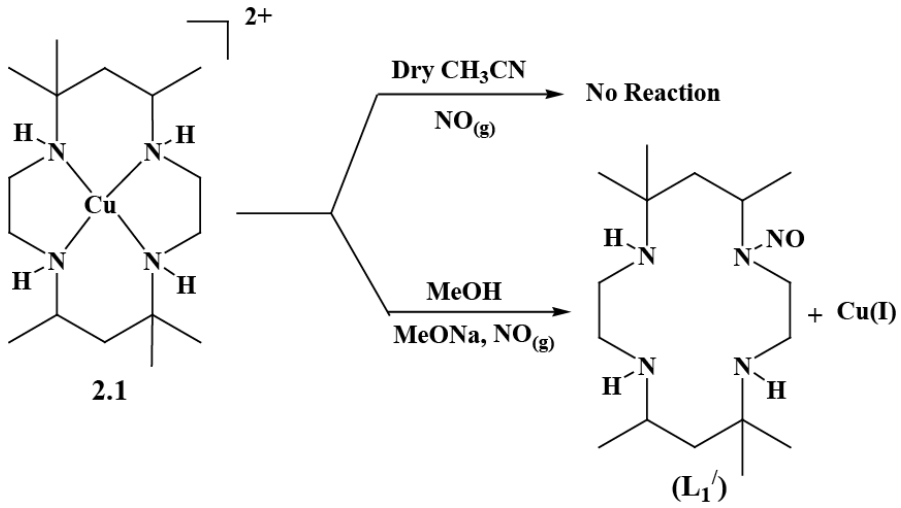

Scheme 2.1

The reduction was monitored by UV-visible spectroscopic studies. The intensity of the *d-d* band was found to decrease with time and finally diminished suggesting the complete reduction of copper(II) centre to copper(I) (Figure 2.5).[51]The reaction was found to be very slow in absence of base. The decrease of intensity of the *d-d* band was found to be retarded considerably upon addition of acids. Similar behaviour was reported for the NO reactivity of $[Cu(DAC)]^{2+}$ complex.[51] In case of $[Cu(DAC)]^{2+}$, the spectral changed were found to be strongly dependent on conditions. In this case, in unbufferred methanol / water mixture, the spectroscopic changes appeared to show an induction period which was no longer apparent in the buffered medium. This is, presumably, because of the shift in effective pH in the course of the reaction. In the present study, we have also observed an induction period in methanol / water (8:2, v/v) medium in unbufferred condition. When the absorbance of a single wavelength (at 523 nm) was plotted versus time, however, there was no indication of the presence of an induction period in neutral medium (Figure 2.6). This plot fits well with the exponential decay curve from which the observed pseudo first order rate constant with 10 equivalent of base has been calculated and found to be 5.49 ×

10^{-4} s^{-1} at 298 K. The rate of the reaction was observed to be dependent on the base concentration (Appendix I, Figure A1.6).

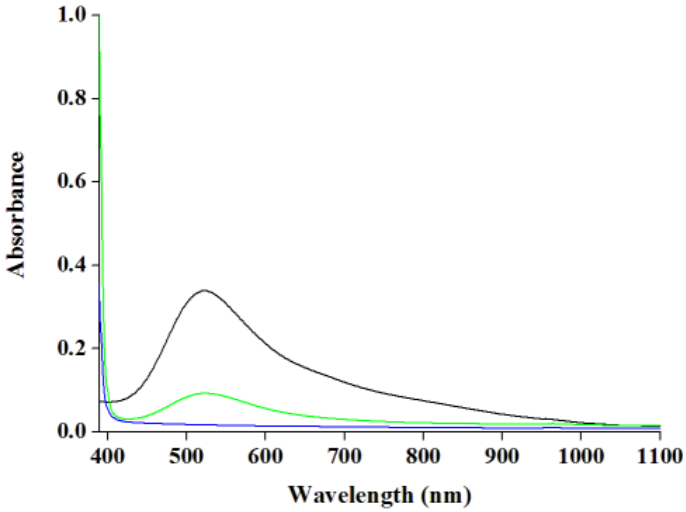

Figure 2.5 UV-visible spectra of the reaction of complex **2.1** (black) with NO in methanol solvent and in presence of sodium methoxide, at room temperature. Green and red traces represent the spectral change at an intermediate stage and after complete reduction of copper(II) to copper(I), respectively.

The reduction of the copper (II) centre by NO further has been authenticated by the X-band EPR spectroscopic studies. The square planar complex **2.1** was found to display a characteristic spectrum in EPR at room temperature. The colorless solution resulting from the reaction of complex **2.1** in presence of base and NO was observed to be EPR inactive. This is attributed to the formation of diamagnetic copper(I) species from the reduction of copper(II) by NO (Figure 2.7). It would be worth mentioning here that the [Cu^{II}–NO] intermediate is also expected to be EPR inactive; however, the bleached color (i.e., the absence of *d-d* transition band after reaction of copper(II) and NO) of the solution clearly ruled out this option.

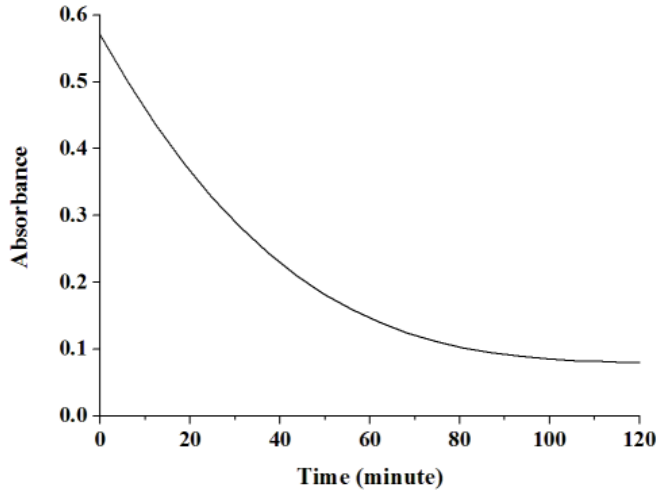

Figure 2.6 Time scan plot of complex **2.1** (λ_{max}, 523 nm) generated after reaction with NO in methanol in presence of base at 298K.

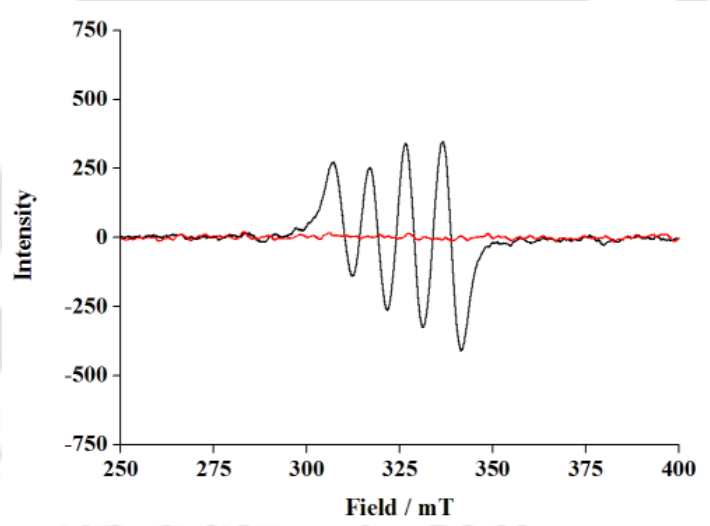

Figure 2.7 X-band EPR spectra of the complex **2.1** (black) and after its reaction with NO (red) in methanol in presence of base at room temperature.

The reduction of copper(II) centre, in case of complex **2.1**, was observed to afford a concomitant nitrosation of $\mathbf{L_1}$ resulting in the formation of $\mathbf{L_1}'$ (Scheme 2.1). The

nitrosation product, $\mathbf{L_1}'$, has been isolated and characterized (Experimental section). In case of the analogous $[Cu(DAC)]^{2+}$ complex, similar results were exemplified by Ford et al.[6] The copper(II) centre in complex **2.2**, on the other hand, was observed to undergo reduction by NO in pure acetonitrile solvent (Scheme 2.2). The reddish solution of **2.2**, in dry and degassed acetonitrile, on exposure to NO gas resulted in a thermally unstable blue

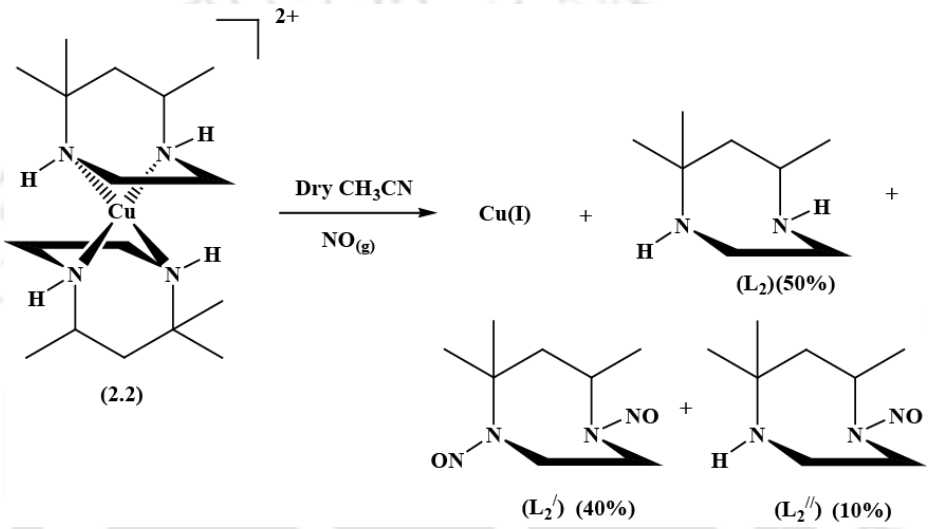

Scheme 2.2

intermediate with a shift of λ_{max} to 600 nm. The intermediate was found to be EPR silent.[37,52] The intermediate was decomposed gradually to afford a colorless solution following first order kinetics, and the spectral changes were monitored by UV-visible spectroscopic studies (Figure 2.8). The observed rate constant at 298 K is 8.45×10^{-3} s^{-1}.

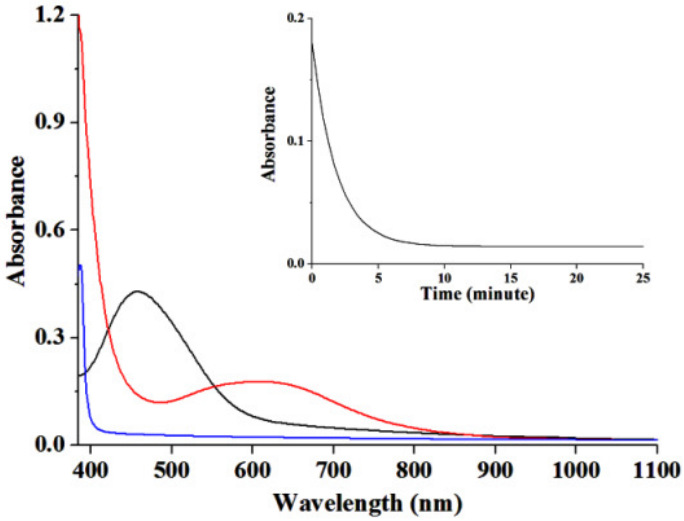

Figure 2.8 UV-visible spectra of complex **2.2** (black); [Cu^{II}–NO] intermediate (red) and its decomposition to copper(I) species (blue) in acetonitrile. Inset: first order kinetic trace (λ = 600 nm) of decay of [Cu^{II}–NO] intermediate to copper(I) species in acetonitrile.

The FT-IR spectra of the acetonitrile solutions of complex **2.2** before and after purging NO were recorded. A new intense and sharp band was found to appear at ~1635 cm^{-1}, corresponding to the vibration of NO coordinated to the copper(II) centre. This band was found to decrease in intensity with time (Figure 2.9).

The appearance of the thermally unstable band at ~1635 cm^{-1} supports the formation of the [Cu^{II}–NO] intermediate prior to the reduction of the copper(II) centre in the cases of complex **2.2**. In case of $[Cu(TAEA)(CH_3CN)]^{2+}$ complex, the ν_{NO} of [Cu^{II}–NO] was found to appear at 1650 cm^{-1}.[37] It would be worth mentioning here that for the air-stable solid copper(II)-nitrosyl of copper(II)-dithiocarbamate, the ν_{NO} for the NO coordinated to copper appears at 1682 cm^{-1}.[53]

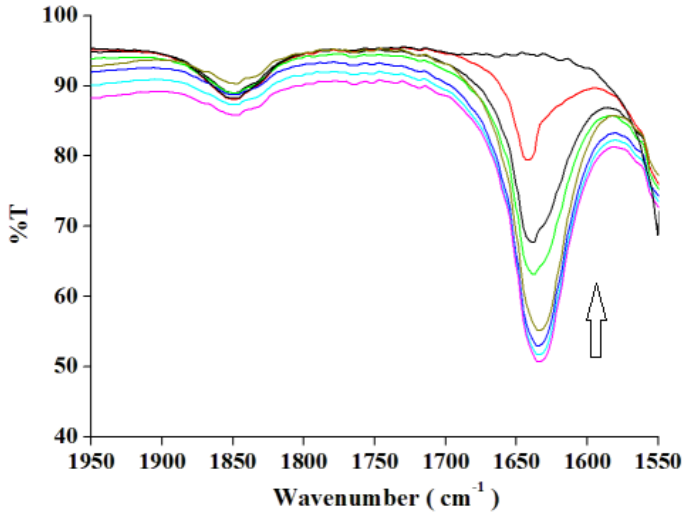

Figure 2.9 Solution FT-IR spectra of complex **2.2** and after reaction with NO in acetonitrile solvent at room temperature. Arrow head indicates the gradual decrease of the band intensity with time. Only ν_{NO} frequency is shown for clarity.

The colorless solution was also observed to be EPR silent (Figure 2.10) which is consistent with the reduction of copper(II) to copper(I).[37,52] Thus, in the case of complex **2.2**, presumably a unstable copper(II)-nitrosyl intermediate was formed, prior to the reduction of copper(II) to copper(I). Since both [Cu^{I}–NO^{+}] and [Cu^{II}–NO] are EPR silent, it is hard to assign the electronic nature of the intermediate precisely. However, in the UV-visible spectrum of the intermediate, the presence of the *d-d* band supports the existence of the copper(II) state rather copper(I). The same result was observed in methanol solution also (Appendix I, Figure A1.14).

With $[Cu(TEAEA)(CH_3CN)]^{2+}$ and $[Cu(TIAEA)(CH_3CN)]^{2+}$, the formation of [Cu^{II}–NO] intermediates were observed earlier.[37] In the reduction of copper(II)- dithiocarbamates with NO in aqueous solution, the formation of air-stable copper-nitrosyl and dinitrosyl species were reported by Cao et al.[53] Detailed kinetics studies of the copper (II) / NO reactions are

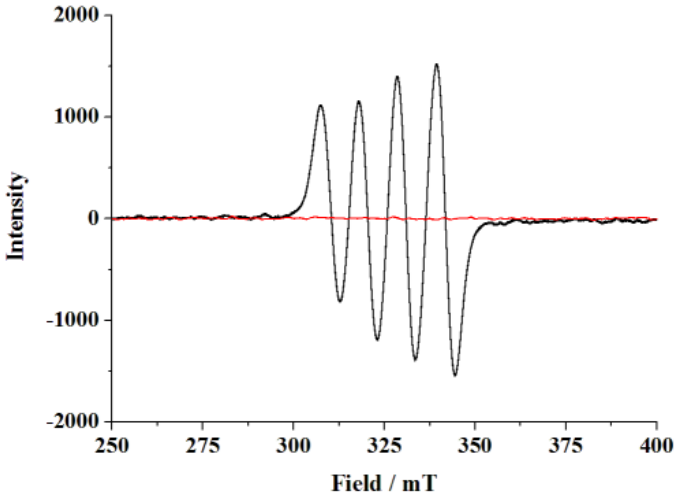

Figure 2.10 X-band EPR spectra of the complex **2.2** (black) and after its reaction with NO (red) in acetonitrile solvent at room temperature.

still limited. It would be worth mentioning here that in the NO reduction of the copper(II) complexes, $[Cu(dmp)_2(H_2O)]^{2+}$ and $[Cu(dpp)_2]^{2+}$ (dmp = 2,9-dimethyl-1,10-phenanthroline; dpp = 2,9-diphenyl-1,10- phenanthroline), in aqueous solution and in various mixed solvents, though a putative inner sphere complex $[Cu(dmp)_2(NO)]^{2+}$ was proposed to form, no spectral evidence was observed.[24a] Even in the early stage of spectral changes when the reactive aqueous solutions were mixed in the stopped-flow kinetics spectrophotometer, there was no obvious indication of the formation of the $[Cu^{II}–NO]$ intermediate, in case of $[Cu(dmp)_2(NO)]^{2+}$.[24a]

The NO reduction of copper(II) centre in complex **2.2**, in acetonitrile, was accompanied with a simultaneous nitrosation of the ligand and release of the modified nitrosoamines; $\mathbf{L_2}'$(~ 40%) and $\mathbf{L_2}''$ (~10%) were isolated and characterized (Scheme 2.2). The single crystal X-ray structure of $\mathbf{L_2}'$ has been determined. The perspective ORTEP view of $\mathbf{L_2}'$ is shown in figure 2.11. The crystallographic table and important bond lengths and angles are given in appendix I (Tables A1.1, A1.2 and A1.3, respectively). The 1440 cm^{-1}, 1478

cm^{-1}, and 1475 cm^{-1} bands in the FT-IR spectra of $\mathbf{L_1}'$, $\mathbf{L_2}'$, and $\mathbf{L_2}''$, respectively, were consistent with the expected ν_{NO} of nitrosoamine.[26] It is important to note that the free ligands do not react with NO at the reaction condition.

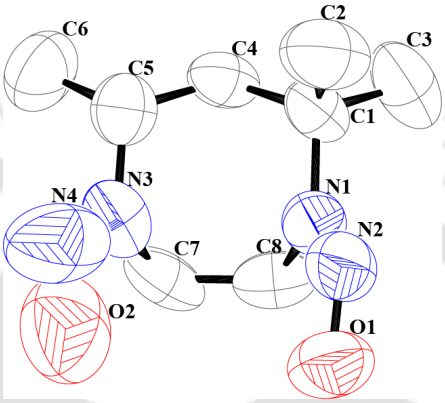

Figure 2.11 ORTEP diagram of $\mathbf{L_2}'$ (Hydrogen atoms are removed for clarity; 50% thermal ellipsoid plot).

The reactivity pathway, thus, depends on the ligand environment which is also playing a key role in controlling the degree of ligand nitrosation. With macrocyclic ligands, both $\mathbf{L_1}$ and DAC, the copper(II) centres were found to react with NO in presence of base through a plausible copper(II)-amide complex formation, whereas in complex **2.2**, it has been found that the copper(II) centre reacts with NO leading to the formation of a $[Cu^{II}–NO]$ intermediate prior to the reduction of copper(II) to coppper(I). The similar observation was reported for $[Cu(TEAEA)(CH_3CN)]^{2+}$, $[Cu(TIAEA)(CH_3CN)]^{2+}$, and $[Cu(TAEA)(CH_3CN)]^{2+}$.[37] Thus, the proposed mechanism of the attack of NO on the deprotonated amine site followed by electron transfer to the copper centre as reported in case of $[Cu(DAC)]^{2+}$ is true for macrocyclic ligands only. Alternatively, first NO coordination to the copper(II) followed by NO^+ migration to the secondary amine is true in

case of other amine ligands. The observation of the transient intermediates in UV-visible and EPR spectroscopy prior to reduction also supports this possibility. This is, perhaps, because of the extra stability of the complex imparted by the macrocycle compared to the others.[50] Since long ago, it is well documented in the literature that the copper(II) complexes of macrocyclic tetraammine ligands are kinetically and electrochemically more inert compared to the nonmacrocyclic analogues.[50] This perhaps prevents the formation of an inner-sphere [Cu^{II}–NO] complex prior to the reduction of the copper(II) centre as observed in case of nonmacrocyclic ligands. It should be noted that though the N-nitrosation was reported in cases of [$Cu(Fl_n)$] complexes (Fl_n = fluorophore ligands), the mechanism was not very clear.[29] It was proposed that N-nitrosation of Fl_n might happen through initial NO coordination to copper(II) followed by internal electron transfer and migration of NO^+ from copper(I) centre to the secondary amine group with loss of proton or through an alternative deprotonation mechanism as observed in case of $[Cu(DAC)]^{2+}$.[29] DFT calculations were performed to have some insight into the likelihood of the formation of the [Cu^{II}–NO] intermediates in the reaction sequences for both the complexes. The calculated structures for the cationic part of complexes **2.1** and **2.2** in gas phase are in good agreement with the crystal structures (Appendix I, Figures A1.30 and A1.31). In the vibrational frequency calculations, no imaginary frequency was found for the complexes suggesting their stable structures (local minima) in the potential energy surface. Similar calculations were performed for complexes **2.1** and **2.2** after NO coordination (i.e., for respective [Cu^{II}–NO] species). It is interesting to note that no negative vibrational frequency (imaginary frequency) was observed for these, also. Thus, on the basis of vibrational frequency calculations, [Cu^{II}–NO] species for both complexes **2.1** and **2.2** are possible. To have more insight on the stability of these [Cu^{II}–NO] species for both the

complexes, the HOMO–LUMO gaps were calculated. The calculated HOMO–LUMO gap of [Cu^{II}–NO] species for complexes **2.1** and **2.2** are 0.206 and 1.020 eV, respectively. This suggests that complex **2.2** is more likely to form [Cu^{II}–NO] upon reaction with NO and the same for complex **2.1** is somewhat unfavorable. The higher chemical hardness value of [Cu^{II}–NO] species for the complex **2.2** (0.510 eV) compared to that for **2.1** (0.103 eV) also supports this.[54] It would be worth mentioning here that for $[Cu(DAC)]^{2+}$ also, the formation of an NO coordinated intermediate was reported to be unfavorable.[51] From the theoretical studies, it has been found that for complex **2.1**, the calculated geometry of the [Cu^{II}–NO] species is square pyramidal with the NO group in the axial position (Appendix I, Figure A1.32), whereas for complex **2.2**, it is trigonal bipyramidal with NO coordinated to the copper at an equatorial site (Appendix I, Figure A1.33). It should be noted that for the structurally characterized copper(II)-nitrosyl complex, $[Cu(CH_3NO_2)_5(NO)][PF_6]_2$, the NO group was reported to be coordinated to the copper centre in a bent geometry [Cu–N–O, 121.0(3)°] at an equatorial site.[52] In the case of complex **2.2**, the calculated geometry of [Cu^{II}–NO] also suggests a bent geometry for NO coordination to the copper centre with an angle of 125.78°. Hence, presumably, the geometry of the [Cu^{II}–NO] species might be crucial in controlling the observed reactivity pathways of the respective complexes. Further, the NBO calculations support the [Cu^{II}–NO] electronic distribution rather than [Cu^{I}–NO^{+}] for the intermediate. This, indeed, is in agreement with the experimentally observed data.

2.4 Conclusion

In conclusion, in case of complex **2.1**, the reduction of copper(II) to copper(I) takes place

in methanol medium in presence of base; whereas, the same in case of **2.2** was observed to be very facile in dry acetonitrile. The copper(II) to copper(I) reduction in **2.2** was found to proceed through a [Cu^{II}–NO] intermediate. In both cases, the reduction resulted into N-nitrosation; in **2.1**, only mono-nitrosation was observed whereas complex **2.2** afforded di-nitrosation as major product along with a minor amount of mono-nitrosation. Hence, in the present study, it has been observed that though the macrocyclic ligands prefer deprotonation pathway, the nonmacrocyclic one prefers the [Cu^{II}–NO] intermediate pathway resulting in nitrosation at all the available sites of the ligand as major product. DFT calculations also suggest the facile formation of [Cu^{II}–NO] intermediate for complex **2.2** which is in good agreement with the experimental observations.

2.5 Experimental section

2.5.1 Materials and methods

All reagents and solvents were purchased from commercial sources and were of reagent grade. Acetonitrile was distilled from calcium hydride. Deoxygenation of the solvent and solutions was effected by repeated vacuum/purge cycles or bubbling with nitrogen for 30 minutes. NO gas was purified by passing through KOH and P_2O_5 column. UV-visible spectra were recorded on a Perkin-Elmer lambda 25 UV-visible spectrophotometer. FT-IR spectra were taken on a Perkin-Elmer spectrophotometer with either sample prepared as KBr pellets or in solution in a potassium bromide cell. Solution electrical conductivity was checked using a Systronic 305 conductivity bridge. ^{1}H- NMR spectra were obtained with a 400 MHz Varian FT-spectrometer. Chemical shifts (ppm) were referenced either with an internal standard (Me_4Si) for organic compounds or to the residual solvent peaks. The X-band Electron Paramagnetic Resonance (EPR) spectra of the complexes and of the reaction

mixtures were recorded on a JES-FA200 ESR spectrometer. Electrochemical measurements were made using a CH Instruments 660A potentiostat. A Pt working electrode, Pt wire auxiliary electrode, and a Ag/Ag^+ reference electrode were used in a three-electrode configuration. All electrochemical measurements were done at 298 K under nitrogen atmosphere in acetonitrile solvent containing *tetra*-butyl ammonium perchlorate (TBAP) as supporting electrolyte. The scan rate used was 50 mV/s. The half-wave potential E^o_{298} was set equal to $0.5(E_{pa} + E_{pc})$, where E_{pa} and E_{pc} are anodic and cathodic cyclic voltammetric peak potentials, respectively. All the electrochemical data are uncorrected for junction potential. Elemental analyses were obtained from a Perkin-Elmer Series II Analyzer. The magnetic moment of complexes were measured on a Cambridge Magnetic Balance. Mass spectra of the compounds in methanol were recorded in a Waters Q-Tof Premier and Aquity instrument.

Single crystals were grown by slow diffusion followed by slow evaporation technique. The intensity data were collected using a Bruker SMART APEX-II CCD diffractometer, equipped with a fine focus 1.75 kW sealed tube MoKα radiation (λ = 0.71073 Å) at 273(3) K, with increasing ω (width of 0.3° per frame) at a scan speed of 3 s/ frame. The SMART software was used for data acquisition. Data integration and reduction were undertaken with the SAINT and XPREP software.[55] Structures were solved by direct methods using SHELXS-97 and refined with full-matrix least-squares on F^2 using SHELXL-97.[56] All non-hydrogen atoms were refined anisotropically. Structural illustrations have been drawn with ORTEP-3 for Windows.[57] The disorder present in the crystal structure has been tried to be minimized by use of SHELXL.

Density functional theory (DFT) calculations were done for complexes **2.1**, **2.2**, and their respective [Cu^{II}–NO] complexes. The complexes **2.1** and **2.2** were generated from their X-

ray crystallographic data. Both the complexes were fully optimized using the BP functional and DNP basis sets as implemented in the program DMol^3.[58] The BP model was chosen as the use of other DFT models like BLYP or B3LYP results in larger error to the bond lengths for copper complexes.[54] The geometry of [Cu^{II}–NO] species obtained from complexes **2.1** and **2.2** were also optimized at the BP/DNP level. Finally to confirm the stability of the complexes the vibrational frequencies calculations were done at the optimized structures. The relative stabilities of the [Cu^{II}–NO] for complexes **2.1** and **2.2** are compared by calculating the value of the gap between their highest occupied molecular orbital (HOMO) and lowest unoccupied molecular orbital (LUMO) and chemical hardness values.

2.5.2 Synthesis of ligand L_1

The macrocyclic ligand (**L_1**) was prepared by using the procedure described by Curtis et al.[59] It is characterized by elemental analyses, FT-IR, ^{1}H-NMR, and ^{13}C-NMR spectroscopy. Elemental analyses: Calcd. (%) for $C_{16}H_{36}N_4$: C, 67.55; H, 12.75; N, 19.69. Found (%): C, 67.53; H, 12.79; N, 19.67. FT-IR (in KBr): 753, 1177, 1372, 1465, 2832, 2923, 2965, 3275 cm^{-1}; ^{1}H-NMR (400 MHz, $CDCl_3$): δ_{ppm}, 2.96(m, 2H), 2.66(t, 8H), 2.24(s, 4H), 1.79(d, 4H), 1.13(s, 12H), 1.09(d, 6H). ^{13}C-NMR (100 MHz, $CDCl_3$): δ_{ppm}, 53.9, 48.3, 46.5, 45.6, 45.2, 29.7, 28.2, 24.5.

2.5.3 Synthesis of ligand L_2

The synthesis of ligand **L_2** was carried out by a method adapted from Curtis.[60] It is characterized by microanalysis, FT-IR, ^{1}H-NMR and ^{13}C-NMR spectroscopy. Elemental analyses: Calcd. (%) for $C_8H_{18}N_2$: C, 67.55; H, 12.75; N, 19.69. Found (%): C, 67.53; H,

12.78; N, 19.68. FT-IR: 1014, 1329, 1397, 1622, 2979 cm^{-1}; ^{1}H-NMR (400 MHz, $CDCl_3$): δ_{ppm}, 3.01(m, 1H), 2.58(t, 4H), 1.56(d, 2H), 1.03(s, 9H). ^{13}C- NMR (100 MHz, $CDCl_3$): δ_{ppm}, 52.7, 49.3, 47.2, 44.5, 44.4, 29.6, 28.2, 22.8.

2.5.4 Synthesis of complex 2.1, [Cu (L_1)](ClO_4)$_2$

The complex was reported earlier.[61] Copper(II) perchlorate hexahydrate (2 g, 5.4 mmol) was dissolved in 20 ml of freshly distilled acetonitrile, and to this blue solution, the ligand **L_1** (1.53 g, 5.4 mmol), was added dropwise. The color of the solution changed to red. The resulting mixture was stirred for 1 h. Then the volume of the solution was reduced to ~5 ml and layered with benzene. It was then kept in a freezer for overnight which resulted in a red crystalline compound. Yield: 2.51 g (~85%). Elemental analyses: Calcd. (%) for $CuC_{16}H_{36}N_4O_8Cl_2$: C, 35.19; H, 6.64; N, 10.26. Found (%): C, 35.23; H, 6.66; N, 10.31. FT-IR (KBr pellet): 1082, 627, 2970, 1448, 2812 cm^{-1}. Molar conductance, 247 S cm^2 mol^{-1}. Magnetic moment, 1.65 BM.

2.5.5 Synthesis of complex 2.2, [Cu (L_2)$_2$](ClO_4)$_2$

Copper(II) perchlorate hexahydrate (2 g, 5.4 mmol), was dissolved in 20 ml of freshly distilled acetonitrile, and to this blue solution, the ligand **L_2** (1.53 g, 10.8 mmol), was added dropwise. The color of the solution changed to red. The resulting mixture was stirred for 1 h. Then the volume of the solution was reduced to ~5 ml and layered with benzene. The mixture was then kept in freezer for overnight which resulted in a red crystalline compound. Yield: 2.55 g (~85%). Elemental analyses: Calcd. (%) for $CuC_{16}H_{36}N_4O_8Cl_2$: C, 35.19; H, 6.64; N, 10.26. Found (%): C, 35.15; H, 6.64; N, 10.21.

FT-IR (KBr pellet): 1082, 627, 2959, 3077, 3178 cm^{-1}.Molar conductance, 224 S cm^2 mol^{-1}. Magnetic moment, 1.60 BM.

2.5.6 Isolation of $L_1^{/}$

To 10 ml of degassed, distilled methanolic solution of complex **2.1** (0.546 g, 1 mmol), NO was bubbled for 1 minute in presence of one equivalent sodium methoxide. The solution turned colorless. The excess NO was removed by vacuum and purging nitrogen gas for several cycles. The colorless solution was then opened to air and stirred at room temperature for 2 h to ensure the complete conversion of copper(I) to copper(II). Then the solvent was removed under reduced pressure using rotavapor. Water (5 ml) was added to the dried mass followed by the addition of 5 ml of saturated Na_2S solution. The black precipitate of CuS was filtered out. The crude organic part was then extracted from the aqueous layer using $CHCl_3$ (25 ml × 4 portions). The crude product, obtained after removal of solvent, was then purified by column chromatography using neutral alumina column and hexane / ethyl acetate solvent mixture to get the pure modified ligand $\mathbf{L_1^{/}}$. Yield: 0.265 g (~85%). Elemental analyses: Calcd. (%) for $C_{16}H_{35}N_5O$: C, 61.30; H, 11.25; N, 22.34. Found (%): C, 61.27; H, 11.26; N, 22.37. FT-IR (KBr pellet): 1440, 1385, 1177, 2925, 2858 cm^{-1}; ^{1}H-NMR (400 MHz, $CDCl_3$): δ_{ppm}, 4.43, 2.79, 2.62, 1.84, 1.43, 1.21. Mass: $(m+H^+)/z$: Calcd. 314.49; Found, 314.42.

2.5.7 Isolation of $L_2^{/}$ and $L_2^{//}$

To 10 ml of degassed, distilled acetonitrile solution of complex **2.2** (0.546 g, 1mmol), NO was bubbled for 1 minute. The red color of the solution became blue and finally colorless. The excess NO was removed by vacuum and purging nitrogen gas for several cycles. The

colorless solution was then opened to air and stirred at room temperature for 2 h to ensure the complete conversion of copper(I) to copper(II). Then the solvent was removed under reduced pressure using rotavapor. Water (5 ml) was added to the dried mass followed by the addition of 5 ml of saturated Na_2S solution. The black precipitate of CuS was filtered out. It would be worth to mention here that direct addition of aqueous saturated Na_2S solution to copper(I) solution affords the precipitation of Cu_2S leading to the same result. The crude organic part was then extracted from the aqueous layer using $CHCl_3$ (25 ml × 4 portions). The crude product, obtained after removal of solvent, was then purified by column chromatography using neutral alumina column and hexane/ethyl acetate solvent mixture to get the pure $\mathbf{L_2'}$ and $\mathbf{L_2''}$. Unreacted $\mathbf{L_2}$ was recovered from the column by using pure methanol solvent. $\mathbf{L_2'}$: Yield: 0.155 g (~ 40%). Characterization of $\mathbf{L_2'}$: Elemental analyses: Calcd.(%) for $C_8H_{16}N_4O_2$: C, 47.99; H, 8.05; N, 27.98. Found (%): C, 47.97; H, 8.06; N, 28.03. FT-IR (KBr pellet): 1475, 1135, 1363, 1138, 2975 cm^{-1}; ^{1}H- NMR (400 MHz, $CDCl_3$): δ_{ppm}, 4.53, 3.85, 2.12, 1.56, 1.31. Mass: $(m+Na^+)/z$: Calcd. 223.24; Found, 223.21. $\mathbf{L_2''}$: Yield: 0.028 g (~ 10%). Characterization of $\mathbf{L_2''}$: Elemental analyses: Calcd.(%) for $C_8H_{17}N_3O$: C, 56.11; H, 10.01; N, 24.54. Found (%): C, 56.08; H, 10.01; N, 24.56. FT-IR (KBr pellet):1478, 1138, 1363, 1361, 2987, 3021 cm^{-1}; ^{1}H- NMR (400 MHz, $CDCl_3$): δ_{ppm}, 4.68, 3.57, 1.97, 1.64, 1.48. Mass: $(m+Na^+)/z$: Calcd. 194.24; Found, 194.26.

2.6 References

1. (a) Ignarro, L. J., Ed. *Nitric Oxide: Biology and Pathobiology* Academic Press: San Diego, CA, 2000. (b) Martin, C. T.; Morse, R. H.; Kanne, R. M.; Gray, H. B.; Malmstrom, B. G.; Chan, S. I. *Biochemistry* **1981**, *20*, 5147.

2. (a) Cooper, C. E.; Torres, J.; Sharpe, M. A.; Wilson, M. T. *FEBS Lett.* **1997**, *414*, 281. (b) Richter-Addo, G. B.; Legzdins, P. *Metal Nitrosyls*; Oxford University Press: New York, 1992.

3. (a) Studbauer, G.; Giuffre, P.; Sarti, P. *J. Biol. Chem.* **1999**, *274*, 28128. (b) McCleverty, J. A. *Chem. Rev.* **2004**, *104*, 403.

4. (a) Chien, J. C. W. *J. Am. Chem. Soc.* **1969**, *91*, 2166. (b) Wayland, B. B.; Olson, L. W. *J. Am. Chem. Soc.* **1974**, *96*, 6037.

5. (a) Hoshino, M.; Maeda, M.; Konishi, R.; Seki, H.; Ford, P. C. *J. Am. Chem. Soc.* **1996**, *118*, 5702. (b) Hoshino, M.; Ozawa, K.; Seki, H.; Ford, P. C. *J. Am. Chem. Soc.* **1993**, *115*, 9568. (c) Lehnert, N.; Praneeth, V. K. K.; Paulat, F. *J. Comput. Chem.* **2006**, *27*, 1338.

6. (a) Fernandez, B. O.; Ford, P. C. *J. Am. Chem. Soc.* **2003**, *125*, 10510. (b) Fernandez, B. O.; Lorkovic, I. M.; Ford, P. C. *Inorg. Chem.* **2004**, *43*, 5393.

7. (a) Ellison, M. K.; Scheidt, W. R. *J. Am. Chem. Soc.* **1999**, *121*, 5210. (b) Linder, D. P.; Rodgers, K. R.; Banister, J.; Wyllie, G. R. A.; Ellison, M. K.; Scheidt, W. R. *J. Am. Chem. Soc.* **2004**, *126*, 14136.

8. (a) Lim, M. D.; Lorkovic, I. M.; Ford, P. C. *J. Inorg. Biochem.* **2005**, *99*, 151. (b) Shamir, D.; Zilbermann, I.; Maimon, E.; Gellerman, G.; Cohen, H.; Meyerstein, D. *Eur. J. Inorg. Chem.* **2007**, 5029.

9. (a) Martin, C. T.; Morse, R. H.; Kanne, R. M.; Gray, H. B.; Malmstrom, B. G.; Chan, S. I. *Biochem.* **1981**, *20*, 5147. (b) Gorren, A. C. F.; de Boer, E.; Wever, R. *Biochem. Biophys. Acta* **1987**, *916*, 38.

10. Torres, J.; Cooper, C. E.; Wilson, M. T. *J. Biol. Chem.* **1998**, *273*, 8756.

11. (a) Torres, J.; Svistunenko, D.; Karlsson, B.; Cooper, C. E.; Wilson, M. T. *J. Am. Chem. Soc.* **2002**, *124*, 963. (b) Brown, G. C. *Biochim. Biophys. Acta* **2001**, *1504*, 46.

12. (a) Torres, J.; Sharpe, M. A.; Rosquist, A.; Cooper, C. E.; Wilson, M. T. *FEBS Lett.* **2000**, *475*, 263. (b) Wijma, H. J.; Canters, G. W.; de Vries, S.; Verbeet, M. P. *Biochemistry* **2004**, *43*, 10467.

13. Miranda, K. M.; Bu, X.; Lorkovic, I. M.; Ford, P. C. *Inorg. Chem.* **1997**, *36*, 4838.

14. (a) Lorkovic, I. M.; Miranda, K. M.; Lee, B.; Bernhard, S.; Schoonover, J. R.; Ford, P. C. *J. Am. Chem. Soc.* **1998**, *120*, 11674. (b) Lorkovic, I. M.; Ford, P. C. *Inorg. Chem.* **1999**, *38*, 1467.

15. (a) Lorkovic, I. M.; Ford, P. C. *J. Am. Chem. Soc.* **2000**, *122*, 6516. (b) Laverman, L. E.; Wanat, A.; Oszajca, J.; Stochel, G.; Ford, P. C.; van Eldik, R. *J. Am. Chem. Soc.* **2001**, *123*, 285.

16. (a) Laverman, L. E.; Ford, P. C. *J. Am. Chem. Soc.* **2001**, *123*, 11614. (b) Kurtikyan, T. S.; Martirosyan, G. G.; Lorkovic, I. M.; Ford, P. C. *J. Am. Chem. Soc.* **2002**, *124*, 10124.

17. (a) Lim, M. D.; Lorkovic, I. M.; Wedeking, K.; Zanella, A. W.; Works, C. F.; Massick, S. M.; Ford, P. C. *J. Am. Chem. Soc.* **2002**, *124*, 9737. (b) Patterson, J. C.; Lorkovic, I. M.; Ford, P. C. *Inorg. Chem.* **2003**, *42*, 4902.

18. (a) Ford, P. C. *Pure Appl. Chem.* **2004**, *76*, 335. (b) Martirosyan, G. G.; Azizyan, A. S.; Kurtikyan, T. S.; Ford, P. C. *Chem. Commun.* **2004**, 1488.

19. (a) Kurtikyan, T. S.; Gulyan, G. M.; Martirosyan, G. G.; Lim, M. D.; Ford, P. C. *J. Am. Chem. Soc.* **2005**, *127*, 6216. (b) Ford, P. C.; Fernandez, B. O.; Lim, M. D. *Chem. Rev.* **2005**, *105*, 2439.

20. (a) Gow, A. J.; Luchsinger, B. P.; Pawloski, J. R.; Singel, D. J.; Stamler, J. S. *Proc. Natl. Acad. Sci. U.S.A.* **1999**, *96*, 9027. (b) Luchsinger, B. P.; Rich, E. N.; Gow, A. J.; Williams, E. M.; Stamler, J. S.; Singel, D. J. *Proc. Natl. Acad. Sci. U.S.A.* **2003**, *100*, 461.

21. (a) Gladwin, M. T.; Lancaster, J. R. Jr.; Freeman, B. A.; Schechter, A. N. *Nat. Med.* **2003**, *9*, 496. (b) Han, T. H.; Fukuto, J. M.; Liao, J. C. *Nitric Oxide, Biol. Chem.* **2004**, *10*, 74.

22. (a) Feelisch, M. S.; Rassaf, T.; Manimneh, S.; Singh, N.; Byran, N. S.; Jourd'Heuil, D.; Kelm, M. *FASEB J.* **2002**, *16*, 1775. (b) Bryan, N. S.; Rassaf, T.; Maloney, R. E.; Rodriguez, C. M.; Saijo, F.; Rodriguez, J. R.; Feelisch, M. *Proc. Natl. Acad. Sci., U.S.A.* **2004**, *101*,4308.

23. (a) Rassaf, T.; Feelisch, M.; Kelm, M. *Free Radical Biol. Med.* **2004**, *36*, 413. (b) Bryan, N. S.; Fernandez, B. O.; Bauer, S. M.; Garcia-Saura, M. F.; Milsom, A. B.; Rassaf, T.; Maloney, R. E.; Bharti, A.; Rodriguez, J.; Feelisch, M. *Nat. Chem. Biol.* **2005**, *1*, 290.

24. (a) Tran, D.; Skelton, B. W.; White, A. H.; Laverman, L. E.; Ford, P. C. *Inorg. Chem.* **1998**, *37*, 2505. (b) Tran, D.; Ford, P. C. *Inorg. Chem.* **1996**, *35*, 2411.

25. Lim, M. D.; Capps, K. B.; Karpishin, T. B.; Ford, P. C. *Nitric Oxide, Biol. Chem.* **2005**, *12*, 244.

26. Tsuge, K.; DeRosa, F.; Lim, M. D.; Ford, P. C. *J. Am. Chem. Soc.* **2004**, *126*, 6564.

27. Melzer, M. M.; Mossin, S.; Dai, X.; Bartell, A. M.; Kapoor, P.; Meyer, K.; Warren, T. H. *Angew. Chem., Int. Ed.* **2010**, *49*, 904.

28. (a) Lim, M. H.; Lippard, S. J. *J. Am. Chem. Soc.* **2005**, *127*, 12170. (b) Lim, M. H.; Xu, D.; Lippard, S. J. *Nat. Chem. Biol.* **2006**, *2*, 375. (c) Lim, M. H.; Kuang, C.; Lippard, S. J. *ChemBioChem* **2006**, *7*, 1571.

29. (a) Lim, M. H.; Wong, B. A.; Pitcock, W. H. Jr.; Mokshagundam, D.; Baik, M.-H.; Lippard, S. J. *J. Am. Chem. Soc.* **2006**, *128*, 14364. (b) Smith, R. C.; Tennyson, A. G.; Won, C.; Lippard, S. *Inorg. Chem.* **2006**, *45*, 9367. (c) Lim, M. H.; Lippard, S. J. *Inorg. Chem.* **2006**, *45*, 8980.

30. Pell, S. D.; Armor, J. N. *J. Am. Chem. Soc.* **1973**, *95*, 7625.

31. Ruggiero, C. E.; Carrier, S. M.; Antholine, W. E.; Whittaker, J. W.; Cramer, C. J.; Tolman, W. B. *J. Am. Chem. Soc.* **1993**, *115*, 11285.

32. (a) Wayland, B. B.; Olson, L. W. *Chem. Commun.* **1973**, 897. (b) Choi, I.-K.; Liu, Y.; Wei, Z.; Ryan, M. D. *Inorg. Chem.* **1997**, *36*, 3113.

33. (a) Bohle, D. S.; Hung, C.-H. *J. Am. Chem. Soc.* **1995**, *117*, 9584. (b) Killday, K. B.; Tempesta, M. S.; Bailey, M. E.; Metral, C. J. *J. Agric. Food Chem.* **1988**, *36*, 909.

34. (a) Trofimova, N. S.; Safronov, A. Y.; Ikeda, O. *Inorg. Chem.* **2003**, *42*, 1945. (b) Vilhena, F. S. D. S.; Louro, S. R. W. *J. Inorg. Biochem.* **2004**, *98*, 459.

35. Nakagawa, S.; Yashiro, T.; Munakata, H.; Imai, H.; Uemori, Y. *Inorg. Chim. Acta* **2003**, *349*, 17.

36. (a) Gwost, D.; Caulton, K. G. *Chem. Commun.* **1973**, *3*, 64. (b) Gwost, D.; Caulton, K. G. *Inorg. Chem.* **1973**, *12*, 2095.

37. (a) Sarma, M.; Kalita, A.; Kumar, P.; Singh, A.; Mondal, B. *J. Am. Chem. Soc.* **2010**, *132*, 7846. (b) Sarma, M.; Singh, A.; Gupta G, S.; Das, G.; Mondal, B. *Inorg. Chim. Acta* **2010**, *363*, 63. (c) Sarma, M.; Mondal, B. *Inorg. Chem.* **2011**, *50*, 3206.

38. (a) Suarez-Varela, J.; Moreno, J. M.; Ben, M. I.; Lloret, F.; Mrozinski, J.; Kivekas, R.; Colacio, E. *Cryst. Growth Des.* **2009**, *9*, 4102. (b) Ou, G.-C.; Jiang, L.; Feng, X.-L.; Lu, T.-B. *Dalton Trans.* **2009**, 71. (c) Bharadwaj, P. K.; Potenza, J. A.; Schugar, H. J. *Inorg. Chem.* **1988**, *27*, 3172.

39. (a) Wang, H.; Chen, Y.; Li, J.; Bai, L. *Inorg. Chim. Acta* **1988**, *148*, 261. (b) Dominguez-Vera, J. M.; Suarez-Varela, J.; Ben, M.; Ikram, C. E. *Eur. J. Inorg. Chem.* **2005**, *10*, 1907. (c) Diaz, C.; Ribas, J.; El Fallah, M. S.; Solans, X.; Font-Bardia, M. *Inorg. Chim. Acta* **2001**, *312*, 1.

40. (a) Diaz, G.; Bustos, C.; Shepherd, R. E. *Chim. Acta* **1987**, *133*, 23. (b) Freiberg, M.; Meyerstein, D.; Yamamoto, Y. *Dalton Trans.* **1982**, 1137. (c) Liang, B.-F.; Chung, C.-S. *Inorg. Chem.* **1980**, *19*, 572.

41. (a) Al-Shatti, N.; Segal, M. G.; Sykes, A. G. *Dalton Trans.* **1977**, 1766. (b) Bryan, P. S.; Dabrowiak, J. C. *Inorg. Chem.* **1975**, *14*, 299. (c) Liang, B.F.; Chung, C.S. *Dalton Trans.* **1980**, 1349.

42. (a) Muralidharan, S.; Ferraudi, G. *Inorg. Chem.* **1981**, *20*, 2306. (b) John, E.; Bharadwaj, P. K.; Krogh-Jespersen, K.; Potenza, J. A.; Schugar, H. J. *J. Am. Chem. Soc.* **1986**, *108*, 5015. (c) Siddiqui, S.; Shepherd, R. E. *Inorg. Chem.* **1986**, *25*, 3869.

43. (a) Endicott, J. F.; Rillema, D. P.; Papaconstantinou, E. *Inorg. Chem.* **1971**, *10*, 1739. (b) Ferraudi, G.; Muralidharan, S. *Inorg. Chem.* **1981**, *20*, 4262. (c) Ronco, S.; Van Vlierberge, B.; Ferraudi, G. *Inorg. Chem.* **1988**, *27*, 3453.

44. (a) Holwerda, R. A. *J. Inorg. Biochem.* **1988**, *33*, 131. (b) Woodin, K. S.; Heroux, K. J.; Boswell, C. A.; Wong, E. H.; Weisman, G. R.; Niu, W.; Tomellini, S. A.; Anderson, C. J.; Zakharov, L. N.; Rheingold, A. L. *Eur. J. Inorg. Chem.* **2005**, 4829. (c) Chen, J. W.; Wu, D. S.; Chung, C.-S. *Inorg. Chem.* **1986**, *25*, 1940.

45. (a) Liang, B.-F.; Tsay, Y. K.; Chung, C.-S. *Dalton Trans.* **1983**, 995. (b) Castellani, C. B.; Fabbrizzi, L.; Licchelli, M.; Perotti, A.; Poggi, A. *Chem. Commun.* **1984**, 806. (c) Rodriguez-Dieguez, A.; Kivekaes, R.; Sillanpaeae, R.; Cano, J.; Lloret, F.; McKee, V.; Stoeckli- Evans, H.; Colacio, E. *Inorg. Chem.* **2006**, *45*, 10537.

46. Clay, R.; Murray-Rust, J.; Murray-Rust, P. *Dalton Trans.* **1979**, 1135.

47. (a) Addison, A. W.; Hendriks, H. M. J.; Reedijk, J.; Thompson, L. K. *Inorg. Chem.* **1981**, *20*, 103. (b) Sorrell, T. N.; Jameson, D. L. *Inorg. Chem.* **1982**, *21*, 1014.

48. Olson, D. C.; Vasilevskis, J. *Inorg. Chem.* **197**1, *10*, 463.

49. Ghachtouli, S. E.; Cadiou, C.; Déchamps-Olivier, I.; Chuburu, F.; Aplincourt, M.; Turcry, V.; Baccon, M. L.; Handel, H. *Eur. J. Inorg. Chem.* **2005**, 2658.

50. (a) Cabbiness, D. K.; Margerum, D. W. *J. Am. Chem. Soc.* **1969**, *91*, 6540. (b) Liang, B.-F.; Chung, C.-S. *Inorg. Chem.* **1980**, *19*, 572.

51. Khin, C.; Lim, M. D.; Tsuge, K.; Iretskii, A.; Wu, G.; Ford, P. C. *Inorg. Chem.* **2007**, *46*, 9323.

52. Wright, A. M.; Wu, G.; Hayton, T. W. *J. Am. Chem. Soc.* **2010**, *132*, 14336.

53. Diaz, A.; Ortiz, M.; Sanchez, I.; Cao, R.; Mederos, A.; Sanchiz, J.; Brito, F. *J. Inorg. Biochem.* **2003**, *95*, 283.

54. Deka, R. C.; Vetrivel, R.; Pal, S. *J. Phys. Chem. A* **1999**, *103*, 5978.

55. *SMART, SAINT and XPREP*; Siemens Analytical X-ray Instruments Inc.: Madison, WI, 1995.

56. Sheldrick, G. M. *SHELXS-97*; University of Gottingen: Gottingen, Germany, 1997.

57. Farrugia, L. J. *J. Appl. Crystallogr.* **1997**, *30*, 565.

58. Delly, B. *J. Chem. Phys.* **1990**, *92*, 508.

59. Hay, R. W.; Lawrance, A. G.; Curtis, N. F. *Perkin Trans.* **1975**, *1*, 59.

60. Curtis, N. F. *Aust. J. Chem.* **198**6, *39*, 239.

61. (a) Liang, B.F.; Chung, C. *Inorg. Chem.* **1981**, *20*, 2152. (b) Chen, J.W.; Wu, D.S.; Chung, C.-S. *Inorg. Chem.* **1986**, *25*, 1940.

Chapter 3

Synthesis of a copper(II)–nitrosyl complex and its reaction with water: Example of copper(I)-(η^2-O, O)nitrite complex derived from copper(II)-nitrosyl

Abstract

Copper(II) complex, **3.1**, of a bidentate ligand, $\mathbf{L_3}$ [$\mathbf{L_3}$ = *bis*(2-ethyl-4-methyl-imidazol-5-yl) methane] has been synthesized and structurally characterized. Addition of NO to a degassed acetonitrile solution of **3.1** yielded the corresponding copper(II)-nitrosyl complex, **3.2**. In acetonitrile, complex **3.2**, on reaction with water afforded corresponding copper(I)-nitrite complex, **3.3**. Single crystal structure of complex **3.3** reveals the bidentate nitrite (η^2-O, O) bonding. This is the first example of structurally characterized copper(I)-(η^2-O, O) nitrite complex with N-donor ligand. The sequence of the formation of these complexes is just the reverse of the key steps of the postulated nitrite reduction cycle by CuNiRs.

3.1 Introduction

Most of the roles played by NO in biological systems are attributed to the formation of nitrosyl complexes of metallo-proteins, mainly iron or copper.[1–3] For instance, in bacterial denitrification by copper containing nitrite reductases (Cu-NiRs), copper(II)–nitrosyl and copper(I) nitrite are postulated as the key intermediate based on the results of biochemical and spectroscopic studies (Scheme 3.1).[4–10] However, these intermediate have not been

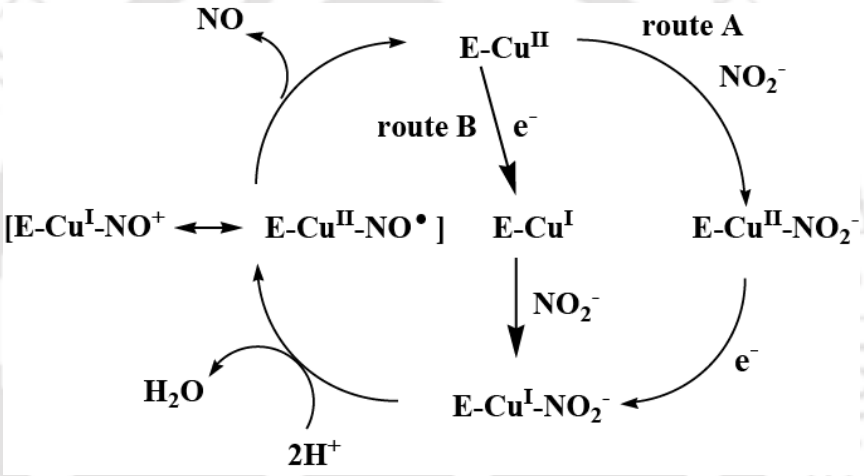

Scheme 3.1

detected in the catalytic cycle because of their high reactivity. Solomon et al, based on density functional theory calculations, reported that binding (O-bound) to copper(I) is found to play the key role in activating the nitrite bond.[11] Hence, the isolation and characterization of these intermediates, even with small molecule models, might be the key to understand the reaction mechanism of the nitrite reductases.

Since the first report of the structurally characterized copper(I) nitrite complex, [(^{i}Pr$_3$tacn)Cu^I(NO_2)] (^{i}Pr$_3$tacn = 1,4,7-triisopropyl-1,4,7-triazacyclononane), as the model for CuNiR by Tolman et al, a number of complexes have been reported.[12–16] However, the

examples of monomeric copper(I)–nitrite (O-bound) complexes are rare and known examples are with typical soft-base phosphine ligands.[16,17]

This chapter describes a copper(II) complex with ligand **L_3** (Figure 3.1) which affords corresponding stable copper(II)–nitrosyl on reaction with NO. The copper(II)–nitrosyl complex in the presence of water results in copper(I)–nitrite (O-bound).

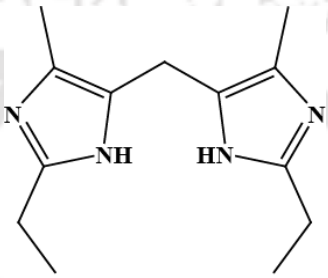

(L_3)

Figure 3.1 Ligand used for the present study.

3.2 Results and discussion

Copper(II) complex, **3.1**, was synthesized with the bidentate ligand, **L_3** [**L_3** = *bis* (2-ethyl-4-methyl-imidazol-5yl) methane], as its perchlorate salt. The single crystal structure of complex **3.1** was determined. The perspective ORTEP view for **3.1** is shown in figure 3.2. The single crystal structure of **3.1** revealed that the copper(II) centre is coordinated by four nitrogen donor atoms from two **L_3** in a distorted square-planar geometry. The crystallographic table and important bond lengths and angles are given in appendix II (Tables A2.1, A2.2 and A2.3, respectively). Complex **3.1** in acetonitrile solvent exhibits a broad *d–d* band at λ_{max} (ε/M^{-1} cm^{-1}), 685 nm (120), along with relatively strong intra-ligand absorptions in the UV region (Figure 3.3). It shows magnetic moment corresponding to one unpaired electron (μ_{obs}, 1.60 BM). It exhibits a characteristic EPR spectrum in acetonitrile at 77 K (Figure 3.4).

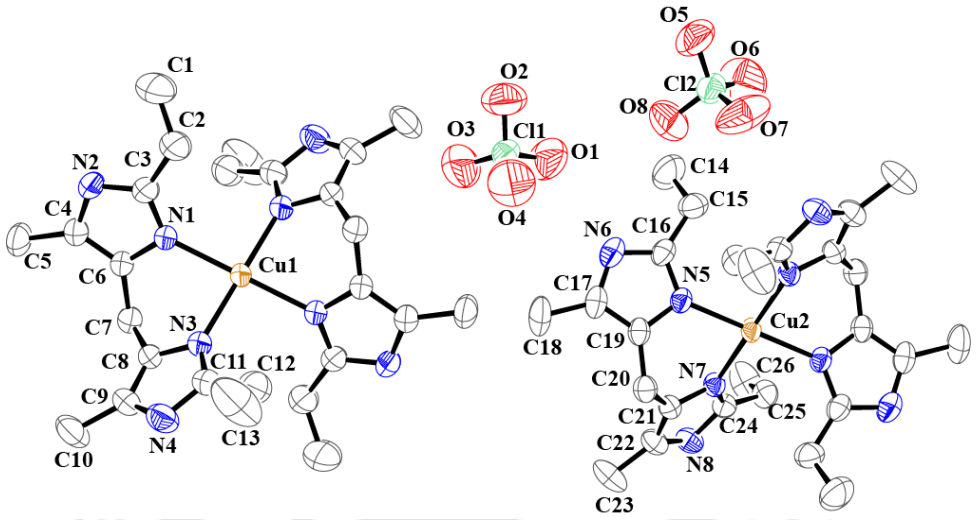

Figure 3.2 ORTEP diagram of complex **3.1** (50% thermal ellipsoid plot). Hydrogen atoms and solvent molecules are not shown for clarity.

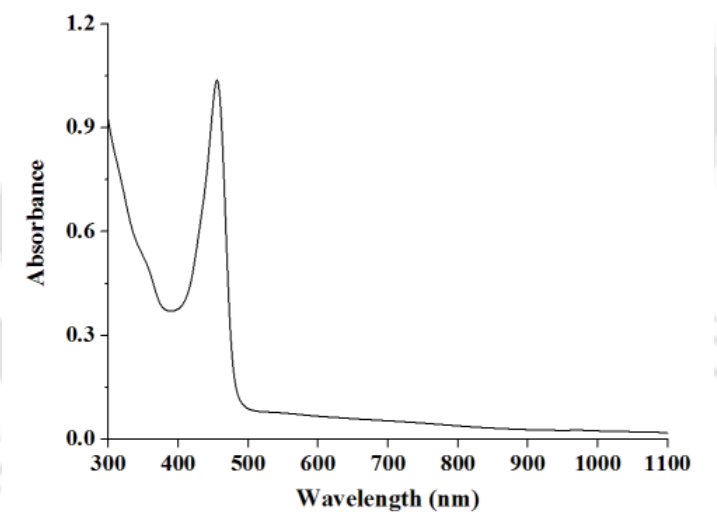

Figure 3.3 UV-visible spectrum of complex **3.1** in acetonitrile at room temperature.

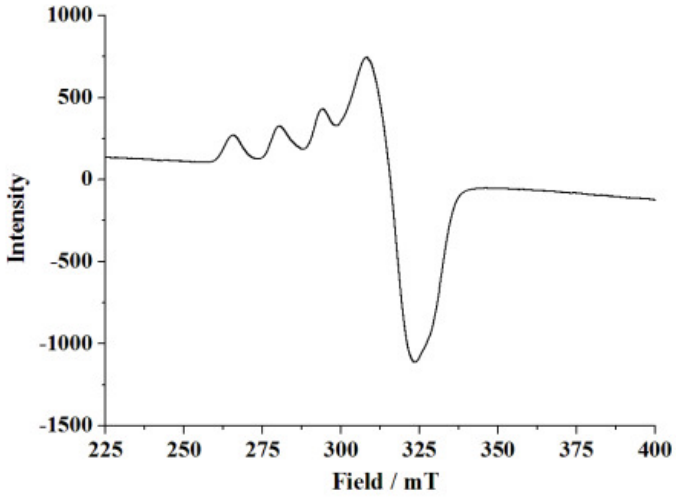

Figure 3.4 X-Band EPR spectrum of complex **3.1** in acetonitrile at 77 K.

3.3 Nitric oxide reactivity

Addition of NO to a degassed acetonitrile solution of complex **3.1** resulted in the corresponding [Cu^{II}–NO] complex, **3.2** (Scheme 3.2). Micro-analytical data and ESI-mass spectroscopy also support the formulation (Figure 3.5). It absorbs at λ_{max} (ε/M^{-1} cm^{-1}), 704 nm (110) (Figure 3.6) in acetonitrile solvent. It is found to be EPR silent (Figure 3.7). In the FT-IR spectrum, it exhibits a vibration at 1662 cm^{-1}, which is attributed to the coordinated nitrosyl stretching frequency.[18]

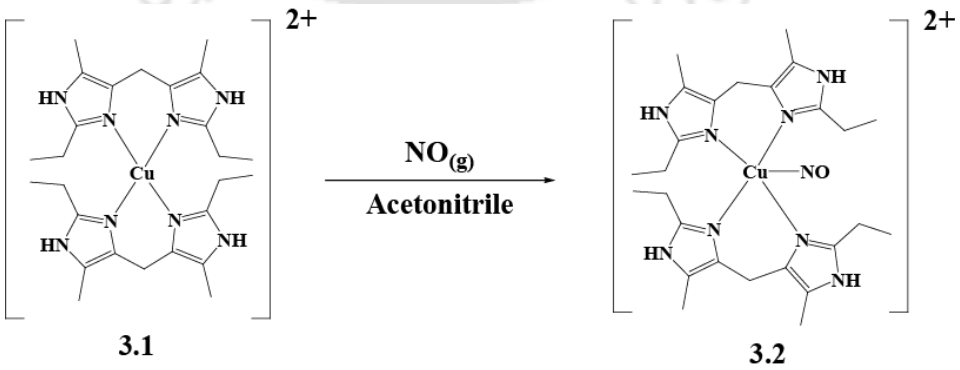

3.1 3.2

Scheme 3.2

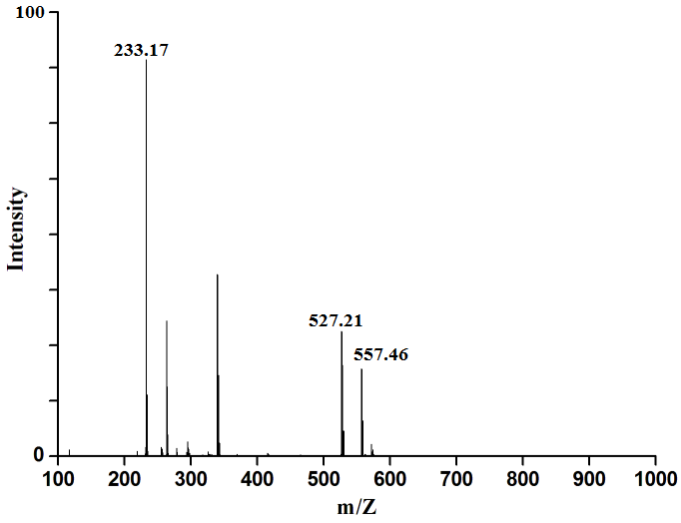

Figure 3.5 ESI-Mass spectrum of complex **3.2** in methanol.

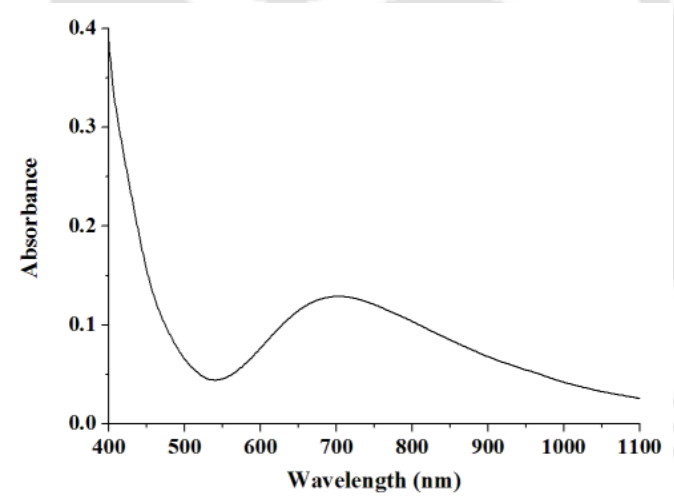

Figure 3.6 UV-visible spectrum of complex **3.2** in acetonitrile solvent at room temperature.

The frequency of this vibration was found to shift to 1631 cm^{-1} on ^{15}NO labelling experiment which further confirms its assignment as ν_{NO} (Figure 3.8). In the case of the $[Cu(TREN)(CH_3CN)]^{2+}$ [TREN = N,N-*bis*(2-aminoethyl)ethane-1,2-diamine] complex, the ν_{NO} of $[Cu^{II}–NO]$ was found to appear at 1650 cm^{-1}.[18] It would be worth mentioning here that for the air-stable solid copper–nitrosyl of copper(II)–dithiocarbamate, the ν_{NO} appears

at 1682 cm^{-1}.[18] Recently, Hayton et al reported the appearance of ν_{NO} band at 1933 cm^{-1} for structurally characterized copper(II)–nitrosyl complex.[18]

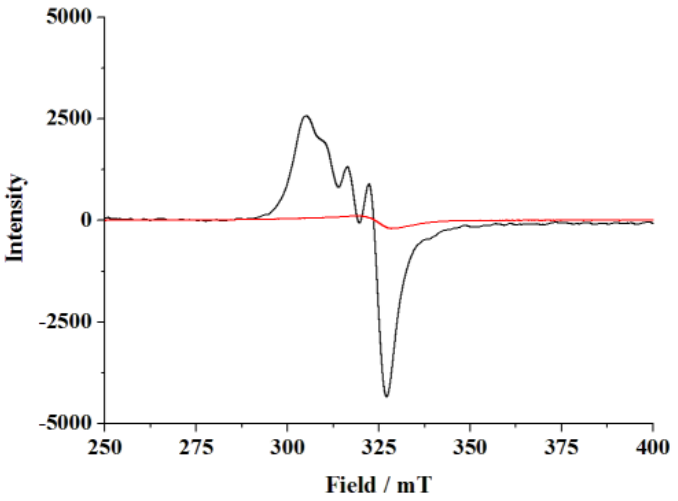

Figure 3.7 X-band EPR spectra of the complex **3.1** (black trace), complex **3.2** (red trace) in acetonitrile at room temperature.

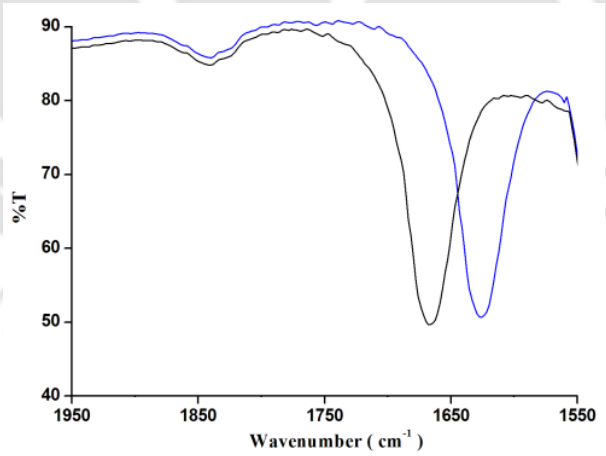

Figure 3.8 FT-IR spectra of complex **3.2** derived from ^{14}NO (black) and ^{15}NO (blue) in acetonitrile solution. Only ν_{NO} frequency is shown for clarity.

The ^{1}H-NMR spectrum of complex **3.2** in CD_3CN displayed the expected number of signals (Figure 3.9). Complex **3.2** is stable at room temperature in the absence of moisture

and has been isolated as a solid. It should be noted that application of vacuum to the acetonitrile solution of complex **3.2** resulted in the decrease of the ν_{NO} band intensity in the FT-IR spectrum indicating the loss of NO ligand from the complex (Appendix II, Figure A2.10).[18] However, we have not succeeded to grow X-ray quality crystals. It is important to note that in all earlier examples, the [Cu^{II}–NO] complexes were found to be unstable, except the two reported by Diaz and Hayton et al.[18]

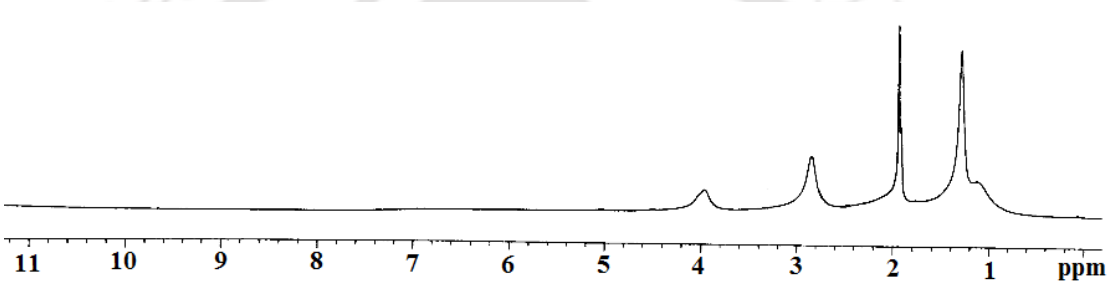

Figure 3.9 ^{1}H-NMR spectrum of complex **3.2** in CD_3CN.

From the DFT calculations, it has been found that for complex **3.2**, the calculated geometry is square pyramidal with the NO group coordinated to the copper at an equatorial site. It should be noted that for the structurally characterized copper(II)–nitrosyl complex, [Cu $(CH_3NO_2)_5(NO)][PF_6]_2$, the NO group was reported to be coordinated to the copper centre in a bent geometry [Cu–N–O, 121.0(3)°] at an equatorial site.[18] In the case of complex **3.2**, the calculated geometry also suggests a bent geometry for NO coordination to the copper centre with an angle of 119.64°. The Cu–$N_{(NO)}$ and N–O distances are calculated to be 2.055 Å and 1.146 Å, respectively. These distances are little longer than the structurally reported one.[18] It would be interesting to note that the DFT analysis suggests that the Cu–NO bond is formed by the overlapping of the d_{Z^2} orbital of Cu and π* orbital of NO ligand

and is purely sigma in nature (Figure 3.10). The HOMO and LUMO energy values were also calculated in the presence of solvent. It has been observed that both HOMO and LUMO orbitals are localized on the imidazole ring of the ligand (Appendix II, Figures A2.12, and A2.13). The NBO calculations suggested the [Cu^{II}–NO] electronic distribution rather than [Cu^{I}–NO^{+}] for complex **3.2**.

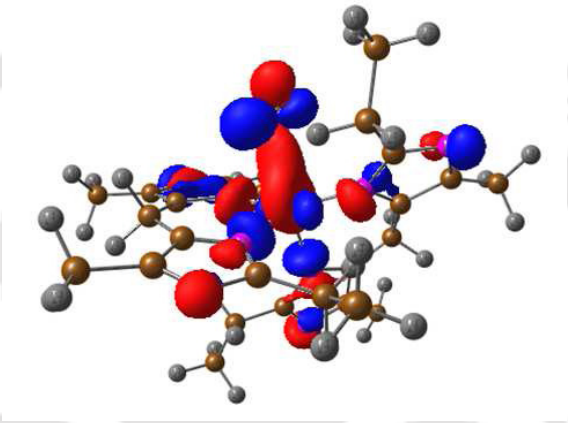

Figure 3.10 HOMO-2 orbital of complex **3.2** that represents the Cu-NO bond.

Complex **3.2** was found to react with water to result into the reduction of the copper(II) centre to copper(I) with a concomitant oxidation of coordinated NO to nitrite yielding a copper(I)–nitrite complex, **3.3** (Scheme 3.3).

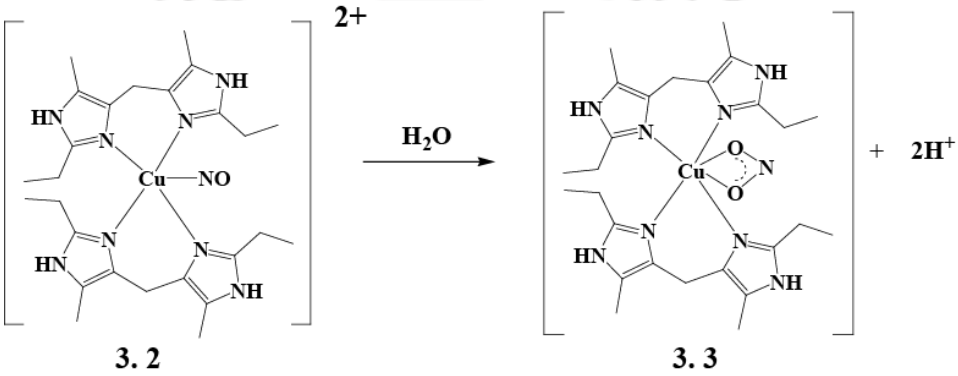

Scheme 3.3

The reduction of copper(II) to copper(I) has been monitored by the UV-visible spectroscopic studies (Figure 3.11). The reaction mixture after the complete reduction was found to be EPR silent, as expected (Appendix II, Figure A2.20). In solution FT-IR study in acetonitrile solvent, the stretching frequency at 1662 cm^{-1} was found to disappear on addition of water (Figure 3.12). The formation of complex **3.3** was further authenticated by its single crystal X-ray structure determination. The ORTEP view of complex **3.3** is shown in figure 3.13. It would be worth mentioning here that in complex **3.3**, a bidentate nitrite binding (O-bound) to copper(I) is observed as suggested by Solomon et al for CuNiR.[11] The crystallographic table and important bond lengths and angles are given in appendix II (Tables A2.1, A2.2 and A2.3, respectively). UV-visible and ^{1}H-NMR studies also suggest the formation of complex **3.3** (Appendix II, Figures A2.15, and A2.19).

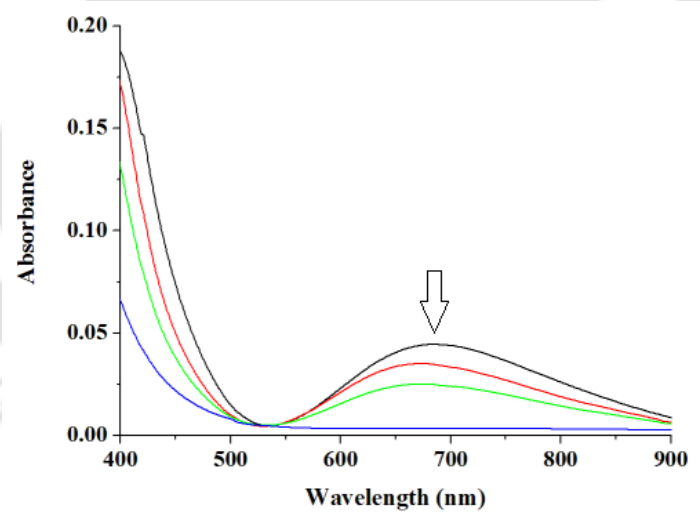

Figure 3.11 UV-visible spectroscopic monitoring of the reaction of complex **3.2** with water in acetonitrile. Black and blue traces represent complexes **3.2** and **3.3**, respectively; whereas, red and green ones represent the intermediate steps for the gradual decomposition of complex **3.2** to **3.3**.

The release of proton during the formation of complex **3.3** was qualitatively established by the decrease of pH of the reaction mixture. In the ESI-mass spectroscopy, the molecular

ion peak of complex **3.3** was found to appear at 573.26 (Appendix II, Figure A1.17). This peak was found to shift to 575.21, as expected, when ^{18}O-labeled water was used (Appendix II, Figure A1.18) suggesting that water is involved in the reaction.

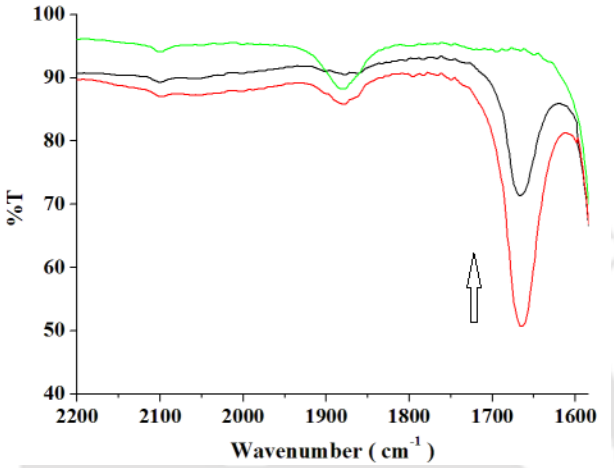

Figure 3.12 Solution FT-IR spectroscopic monitoring of the reaction of complex **3.2** with water in acetonitrile. Only the gradual decay of ν_{NO} at 1662 cm^{-1} in presence of water is shown for clarity.

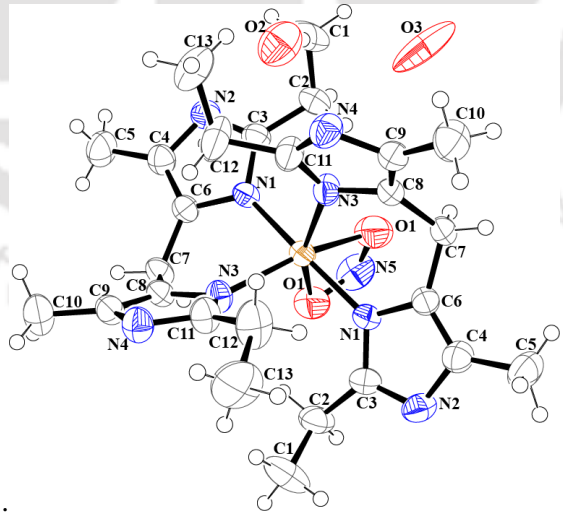

Figure 3.13 ORTEP diagram of complex **3.3** (50% thermal ellipsoid plot).

3.4 Conclusion

The present work demonstrates an example of formation of stable copper(II)–nitrosyl from the reaction of copper(II) complex and NO. The copper(II)–nitrosyl complex, in acetonitrile solvent, in the presence of water affords the corresponding copper(I)–nitrite (O-bound) complex. The sequence of the formation of these complexes, essentially, is just the reverse of the key steps of the postulated nitrite reduction cycle by copper containing nitrite reductases. Furthermore, though it has been observed that copper(I)–nitrite complexes with aliphatic or aromatic nitrogen donor prefer to have an N-bound bonding mode, the present study demonstrates the first example of a copper(I)–nitrite (O-bound) complex with N-donor ligand.

3.5 Experimental section

3.5.1 Materials and methods

All reagents and solvents were purchased from commercial sources and were of reagent grade. Acetonitrile was distilled from calcium hydride. Deoxygenation of the solvent and solutions was effected by repeated vacuum/purge cycles or bubbling with nitrogen for 30 minutes. NO gas was purified by passing through KOH and P_2O_5 column. UV−visible spectra were recorded on a Perkin-Elmer lambda 25 UV−visible spectrophotometer. FT-IR spectra were taken on a Perkin-Elmer spectrophotometer with either sample prepared as KBr pellets or in solution in a potassium bromide cell. Solution electrical conductivity was checked using a Systronic 305 conductivity bridge. ^{1}H- NMR spectra were obtained with a 400 MHz Varian FT-spectrometer. Chemical shifts (ppm) were referenced either with an internal standard (Me_4Si) for organic compounds or to the residual solvent peaks. The X-band Electron Paramagnetic Resonance (EPR) spectra of the complexes and of the reaction

mixtures were recorded on a JES-FA200 ESR spectrometer. Elemental analyses were obtained from a Perkin-Elmer Series II Analyzer. The magnetic moment of complexes were measured on a Cambridge Magnetic Balance. Mass spectra of the compounds in methanol were recorded in a Waters Q-Tof Premier and Aquity instrument.

Single crystals were grown by slow diffusion followed by slow evaporation technique. The intensity data were collected using a Bruker SMART APEX-II CCD diffractometer, equipped with a fine focus 1.75 kW sealed tube MoKα radiation (λ = 0.71073 Å) at 273(3) K, with increasing ω (width of 0.3° per frame) at a scan speed of 3 s/ frame. The SMART software was used for data acquisition. Data integration and reduction were undertaken with the SAINT and XPREP software.[19] Structures were solved by direct methods using SHELXS-97 and refined with full matrix least-squares on F^2 using SHELXL-97.[20]All non-hydrogen atoms were refined anisotropically. Structural illustrations have been drawn with ORTEP-3 for Windows.[21] The disorder present in the crystal structure has been tried to be minimized by use of SHELXL.

DFT calculations were performed on complex **3.2**. The complex was fully optimized using PW91 functional and DNP basis sets in the presence of solvent acetonitrile. The Conductor-like Screening Model (COSMO) as incorporated into the DMol^3 program with dielectric constant of 37.5 was adopted to study the solvent effect. NBO calculations were performed on the optimized cluster to identify the electronic distribution on the complex.

3.5.2 Synthesis of ligand L_3

The ligand $\mathbf{L_3}$ was synthesized by a method adapted from Morteza Shiri.[22] A 100 ml, two-necked, round-bottomed flask equipped with a magnetic stirring bar, and a rubber septum was charged with 2.20g (20 mmol) of 2-ethyl-4-methyl-imidazole, and 30 ml of methanol.

To the stirred solution 0.45g (15 mmol) of formaldehyde was added over a period of 5 minutes and the resulting mixture was made alkaline (pH ~14) by adding KOH. The reaction mixture was then allowed to stirr at room temperature. After 3-4 h ligand **L_3** precipitated out from the reaction mixture as white solid. The white precipitate was washed with water, dried in vacuum. Yield: 1.97 g (85%). It was characterized by elemental analysis, FT-IR, ^{1}H- NMR and ^{13}C-NMR spectroscopy. Elemental analyses: Calcd. (%) for $C_{13}H_{20}N_4$: C, 67.21; H, 8.68; N, 24.12. Found (%): C, 67.19; H, 8.68; N, 24.02. FT-IR (in KBr): 2964, 2842, 1614, 1529, 1455, 1071 cm^{-1}; ^{1}H-NMR (400 MHz, $CDCl_3$): δ_{ppm}, 3.53(2H), 2.44(4H), 1.87(6H), 1.08(6H). ^{13}C-NMR (100 MHz, $CDCl_3$): δ_{ppm}, 149.2, 129.1, 127.2, 23.3, 22.6, 13.7, 10.6. Mass: (m+H$^+$)/z: Calcd. 233.16; Found, 233.17.

3.5.3 Synthesis of complex 3.1, [Cu (L_3)$_2$](ClO$_4$)$_2$

Copper(II) perchlorate hexahydrate (0.740 g, 2 mmol) was dissolved in 20 ml distilled methanol. To this solution, 0.928 g (4 mmol) of the ligand **L_3** was added slowly with constant stirring. The color of the solution turned into dark brown from light blue. The stirring was continued for 1h at room temperature. The volume of the solution then reduced to ~5 ml. To this, 10 ml of diethylether was added to make a layer on it and kept overnight on freezer. This resulted into microcrystalline complex **3.1**. Yield: 1.25 g (85%). Elemental Analyses: Calcd. For $C_{26}H_{40}Cl_2CuN_8O_8$: C, 42.95; H, 5.55; N, 15.41. Found (%): C, 42.91; H, 5.54; N, 15.36. FT-IR: 2976, 1633, 1455, 1150, 1114, 625 cm^{-1}; magnetic moment, 1.60 BM. ESI-Mass: Calcd. 527.19; Found, 527.24.

3.5.4 Synthesis of complex 3.2, [Cu (L_3)$_2$(NO)](ClO$_4$)$_2$

To 20 ml of distilled and degassed acetonitrile solution of complex **3.1** (0.5 g), freshly

prepared NO was bubbled for 1 minute. The color of the solution turned dark green. The excess of NO was removed by vacuum and purging nitrogen gas and 10 ml of degassed benzene was added to this under nitrogen atmosphere. The reaction mixture was kept in freezer for two days. This resulted into the precipitate of complex **3.2** as green powder. Yield: 0.364 g (70%). Elemental Analyses: Calcd. for $C_{26}H_{40}Cl_2CuN_9O_9$: C, 41.25; H, 5.32; N, 16.65. Found (%): C, 41.28; H, 5.30; N, 16.70. FT-IR (KBr pellet): 2921, 1662, 1620, 1475, 1384, 1242, 1108, 625 cm^{-1}. ESI-Mass: Calcd. 557.20; Found, 557.46.

3.5.5 Synthesis of complex 3.3, [Cu $(L_3)_2(NO_2)$]

To 15 ml of distilled and degassed acetonitrile solution of complex **3.2** (0.5 g) quantitative amount of distilled water was added at room temperature with constant stirring under nitrogen environment. The green color of the solution turned colorless. It was kept on freezer. After three days, yellow color crystals of complex **3.3** were obtained. Yield: 0.265 g (63%). Elemental analyses for $C_{26}H_{40}CuN_9O_2$, Calcd.(%): C, 54.38; H, 7.02; N, 21.95. Found (%): C, 54.36; H, 7.04; N, 21.91. FT-IR (KBr pellet): 2976, 1639, 1535, 1455, 1377, 1322, 1267, 1175, 967, 789 cm^{-1}. ESI-Mass: Calcd. 573.24; Found, 573.26 (when normal water used to prepare the complex) and 575.21 (when ^{18}O-lebeled water was used).

3.6 References

1. Ignarro, L. J., Ed. *Nitric Oxide: Biology and Pathobiology* Academic Press: San Diego, CA, 2000.

2. (a) Moncada, S.; Palmer , R. M. J.; Higgs, E. A. *Pharmacol. Rev*. **1991**, 43, 109. (b) Butler, A. R.; Williams, D. L. *Chem. Soc. Rev.* **1993**, *22*, 233. (c) *Methods in Nitric*

Oxide Research Feelisch, M.; Stamler, J. S., Ed. John Wiley and Sons, Chichester, England, 1996.

3. (a) Jia, L.; Bonaventura, C.; Bonaventura,J.; Stamler, J. S. *Nature*, **1996**, *380*, 221. (b) Galdwin, M. T.; Lancaster, J. R. Jr.; Freeman, B. A.; Chechter, A. N. *Nat. Med.*, **2003**, *9*, 496.

4. (a) Strange, R. W.; Murphy, L. M.; Dodd, F. E.; Abraham, Z. H.; Eady, R. R.; Smith, B. E.; Hasnain, S. S. *J. Mol. Biol.* **1999**, *287*, 1001. (b) Kujime, M.; Izumi, C.; Tomura, M.; Hada, M.; Fujii, H. *J. Am. Chem. Soc.*, **1998**, *130*, 6088.

5. (a) Weeg-Aerssens, E.; Tiedje, J. M.; Averill, B. A. *J. Am. Chem. Soc.* **1988**, *110*, 6851. (b) Hulse, C. L.; Averill, B. A.; Tiedje, J.M. *J. Am. Chem. Soc.* **1989**, *111*, 2322. (c) Jackson, M. A.; Tiedje, J. M.; Averill, B. A. *FEBS Lett.* **1991**, *291*, 41. (d) Ye, R. W.; Toro- Suarez, I.; Tiedje, J. M.; Averill, B. A. *J. Biol. Chem.* **1991**, *266*, 12848.

6. (a) Adman, E. T.; Turley, S. K. *Bioinorganic Chemistry of Copper* Karlin, K. D.; Tyeklar, Z., Ed.; Chapman & Hall, New York, 1993, p. 397. (b) Averill, B. A. *Chem. Rev.* **1996**, *96*, 2951. (c) Ferguson, S. J. *Curr. Opin. Chem. Biol.* **1998**, *2*, 182. (d) Wasser, I. M.; de Vries, S.; Monnee-Loccoz, P.; Schrder, I.; Karlin, K. D. *Chem. Rev.* **2002**, *102*, 1201.

7. (a) Hulse, C. L.; Averill, B. A.; Tiedje, J. M. *J. Am. Chem. Soc.* **1989**, *111*, 2322. (b) Ye, R. W.; Toro-Suarez, I.; Tiedje, J. M.; Averill, B. A. *J. Biol. Chem.* **1991**, *266*, 12848.

8. (a) Kataoka, K.; Furusawa, K.; Takagi, H.; Yamaguchi, K.; Suzuki, S. *J. Biochem.* **2002**, *197*, 345. (b) Zhao, Y.; Lukoyanov, D. A.; Toropov, Y. V.; Wu, K.; Sharleigh, J.; P.; Scholes, C. P. *Biochemistry* **2002**, *41*, 7464. (c) Strange, R. W.; Murphy, L. M.; Dodd, F. E.; Abraham, Z. H.; Eady, R. R.; Smith, B. E.; Hasnain, S. S. *J. Mol. Biol.* **1999**, *287*, 1001.

9. (a) Tocheva, E. I.; Rosell, F. I.; Mauk, A. G.; Murphy, M. E. P. *Science* **2004**, *304*, 867. (b) Antonyuk, S. V.; Strange, R. W.; Sawers, G.; Eady, R. R.; Hasnain, S. *Proc. Natl. Acad. Sci. U. S. A*. **2005**, *102*, 12041. (c) Tocheva, E. I.; Rosell, F. I.; Mauk, A. G.; Murphy, M. E. P. *Biochemistry*, **2007**, *46*, 12366.

10. (a) Murphy, M. E. P.; Turley, S.; Adman, E. T. *J. Biol. Chem.* **1997**, *272*, 28455. (b) Boulanger, M. J.; Kukimoto, M.; Nishiyama, M.; Horinouchi, S.; Murphy, M. E. P. *J. Biol. Chem.* **2000**, *275*, 23957. (c) Zhao, Y.; Lukoyanov, D. A.; Toropov, Y. V.; Wu, K.; Shapleigh, J. P.; Scholes, C. P. *Biochemistry* **2002**, *41*, 7464.

11. Ghosh, S.; Dey, A.; Sun, Y.; Scholes, C. P.; Solomon, E. I. *J. Am. Chem. Soc.* **2009**, *131*, 277.

12. (a) Halfen, J. A.; Tolman, W. B. *J. Am. Chem. Soc.* **1994**, *116*, 5475. (b) Halfen, J. A.; Mahapatra, S.; Wilkinson, E. C.; Gengenbach, A. J.; Young, V. G. Jr.; Que, L. Jr.; Tolman, W. B. *J. Am. Chem. Soc.* **1996**, *118*, 763.

13. (a) Jiang, F.; Conry, R. R.; Bubacco, L.; Tyeklar, Z.; Jacobson, R. R.; Karlin, K. D.; Peisach, J. *J. Am. Chem. Soc.* **1993**, *115*, 2093. (b) Komeda, N.; Nagao, H.; Adachi, G.; Suzuki, M.; Uehara, A.; Tanaka, K. *Chem. Lett.* **1993**, 1521.

14. (a) Ruggiero, C. E.; Carrier, S. M.; Tolman, W. B. *Angew. Chem., Int. Ed. Engl.* **1994**, *33*, 895.(b) Stibrany, R. T.; Potenza, J. A.; Schugar, H. J. *Inorg. Chim. Acta* **1996**, *243*, 33. (c) Monzani, E.; Koolhaas, G. J. A. A.; Spandre, A.; Leggieri, E.; Casella, L.; Gullotti, M.; Nardim, G.; Randaccio, L.; Fontani, M.; Zanello, P.; Reedijk, J. *J. Biol. Inorg. Chem.* **2000**, *5*, 251.

15. (a) Halfen, J. A.; Mahapatra, S.; Olmstead, M. M.; Tolman, W. B. *J. Am. Chem. Soc.* **1994**, *116*, 2173. (b) Yokoyama, H.; Yamaguchi, K.; Sugimoto, M.; Suzuki, S. *Eur. J. Inorg. Chem.* **2005**, 1435. (c) Nairn, A. K.; Archibald, S. J.; Bhalla, R.; Boxwell, C. J.; Whitwood, A. C.; Walton, P. H. *Dalton Trans.* **2006**, 1790.

16. (a) Kujime, M.; Izumi, C.; Tomura, M.; Hada, M.; Fujii, H. *J. Am. Chem. Soc.* **2008**, *130*, 6088. (b) Kujime, M.; Izumi, C.; Tomura, M.; Hada, M.; Fujii, H. *J. Am. Chem. Soc.* **2008**, *130*, 6088. (c) Chuang, W. J.; Lin, I.J.; Chen, H.Y.; Chang,Y.L.; Hsu, S. C. N. *Inorg. Chem.* **2010**, *49*, 5377.

17. (a) Halfen, J. A.; Tolman, W. B. *Acta Crystallogr., Sect. C:* **1995**, *51*, 215. (b) Chen, C.S.; Yeh, W.Y. *Chem. Commun.* **2010**, *46*, 3098.

18. (a) Sarma, M.; Singh, A.; Gupta, S. G.; Das, G.; Mondal, B. *Inorg. Chim. Acta* **2010**, *363*, 63. (b) Tsumore, N.; Xu, Q. *Bull. Chem. Soc. Jpn.* **2002**, *75*, 1861. (c) Diaz, A.; Ortiz, M.; Sanchez, I.; Cao, R.; Mederos, A.; Sanchiz, J.; Brito, F. *J. Inorg. Biochem.* **2003**, *95*, 283. (d) Wright, A. M.; Wu, G.; Hayton, T. W. *J. Am. Chem. Soc.* **2010**, *132*, 14336. (e) Sarma, M.; Mondal, B. *Inorg. Chem.* **2011**, *50*, 3206. (f) Tran, D.; Skelton, B. W.; White, A. H.; Leverman, L. E.; Ford, P. C. *Inorg. Chem.* **1998**, *37*, 2505. (g) Lim, M. D.; Capps, K. B.; Karpessian, T.; Ford, P. C. *Nitric Oxide, Biol. Chem.* **2005**, *12*, 244.

19. *SMART, SAINT* and *XPREP*; Siemens Analytical X-ray Instruments Inc.: Madison, WI, 1995.

20. Sheldrick, G. M. *SHELXS-97*; University of Gottingen: Gottingen, Germany, 1997.

21. Farrugia, L. J. *J. Appl. Crystallogr.* **1997**, *30*, 565.

22. Shiri, M.; Zolfigol, M. A.; Kruger, H. G.; Tanbakouchian, Z. *Chem. Rev.* **2010**, *110,* 2250.

Chapter 4

Reaction of a copper(II)–nitrosyl complex with hydrogen peroxide: putative formation of a copper(I)–peroxynitrite intermediate

Abstract

The reaction of a copper(II)–nitrosyl complex, **3.2** with hydrogen peroxide at - 20 °C in acetonitrile results in the formation of the corresponding copper(I)–peroxynitrite intermediate. The reduction of the copper(II) centre was monitored by UV-visible spectroscopic studies. Formation of the peroxynitrite intermediate has been confirmed by its characteristic phenol ring nitration reaction as well as isolation of corresponding copper(I)–nitrate, **4.1**. On air oxidation, **4.1** resulted in the corresponding copper(II)–nitrate, **4.2**. Thus, these results demonstrate a possible decomposition pathway for H_2O_2 and NO through the formation of a peroxynitrite intermediate in biological systems.

4.1 Introduction

NO has attracted enormous research interest since it has been identified to play the key roles in many physiological processes like neurotransmission, vasodilation etc.[1,2] It has been found that NO can also behave as a cytotoxic effector and/or a pathogenic mediator when produced at high rates.[3] The cytotoxicity of NO is believed to be related to the formation of some secondary intermediates like peroxynitrite or nitrogen dioxide. The formation of these secondary intermediates from NO requires the presence of oxidants like superoxide radicals, hydrogen peroxide and transition metal centres.[3] Peroxynitrite is a strong oxidizing/nitrating agent generated by the near diffusion controlled reactions of NO with superoxide anions and is considered as the mediator for oxidative/nitrative stress injury.[4] It has been found that transition metal ions are also important for generation, stabilization, activation for substrate oxidation and thermal isomerization of peroxynitrite.[5] Heme proteins have been well studied in this regard. However, the role of copper ions in peroxynitrite generation and reactivity is not studied so extensively.[5–7] Only a few examples of kinetic studies of interactions of peroxynitrite with copper salts and copper complex mediated decomposition of peroxynitrite are known.[6,7] The examples of discrete metal–peroxynitrite complexes are rare; only a cobalt–peroxynitrite complex is known to be discretely characterized.[8] However, they are proposed to form as transient intermediates in the reaction of metal–nitrosyl and oxygen or metal superoxide and NO.[6,9]

In our recent study of the interaction of NO with copper(II) ions, we have observed the formation of copper(II)–nitrosyl intermediates.[10] All these copper(II)–nitrosyl intermediates are proposed to have $\{CuNO\}^{10}$ electronic configuration with an electrophilic NO coordinated to the metal centre.[10] Anbar and Taube suggested that reaction of NO^+ with H_2O_2 leads to the formation of peroxynitrite.[11] Hence, it would be

logical to think that the reaction of $\{CuNO\}^{10}$ species with H_2O_2 may afford a metal–peroxynitrite complex. In this context, this chapter describes the reaction of a copper(II)–nitrosyl complex with hydrogen peroxide to induce reduction of the copper(II) centre with simultaneous formation of a peroxynitrite intermediate.

4.2 Results and discussion

The copper(II)–nitrosyl complex, **3.2** absorbs at λ_{max} (ε/M^{-1} cm^{-1}), 704 nm (110) (Figure 4.1) in acetonitrile solution. It is found to be EPR silent. In the FT-IR spectroscopy, it exhibits a vibration at 1662 cm^{-1}, which is assigned as the coordinated nitrosyl stretching frequency.[10]

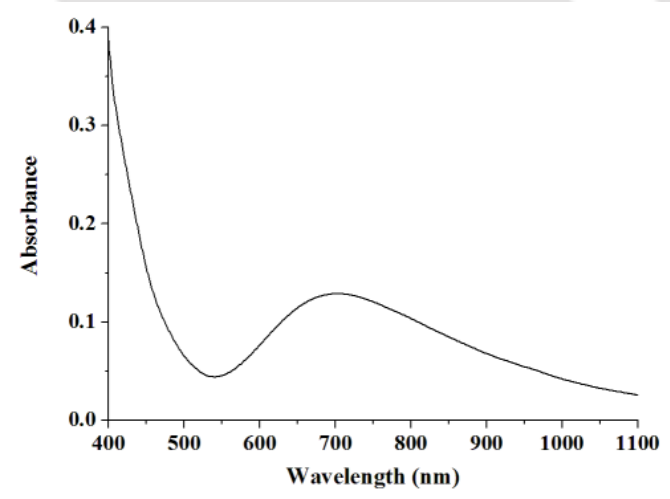

Figure 4.1 UV-visible spectrum of complex **3.2** in acetonitrile solvent at room temperature.

Stoichiometric addition of pre-cooled hydrogen peroxide to a cold (- 20 °C) solution of complex **3.2** resulted in the formation of a colorless solution. This has been formulated as a copper(I)–peroxynitrite complex. The *d*–*d* transition band of complex **3.2** having λ_{max} at

704 nm was found to decrease in intensity with time upon addition of H_2O_2 suggesting the formation of copper(I) from copper(II) (Figure 4.2).

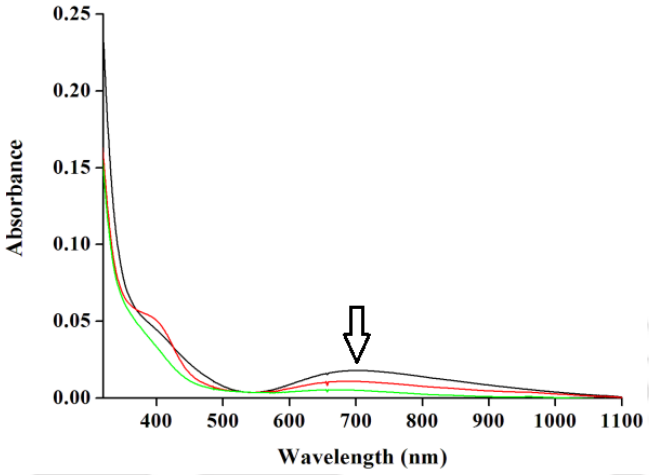

Figure 4.2 UV-visible monitoring of the reaction of complex **3.2** with hydrogen peroxide in acetonitrile at - 20 °C (black trace represents the spectrum of complex **3.2** and green represents that of the colorless intermediate).

In solution FT-IR studies at room temperature, the intensity of the ν_{NO} band at ~1662 cm^{-1} was found to be diminished upon addition of H_2O_2 with the appearance of NO_3^- stretching at ~1384 cm^{-1} (Figure 4.3). The reduction of the copper(II) centre to copper(I), in this case was further authenticated by isolation and X-ray single crystal structure determination of the final copper(I) product, $[(L_3)_2Cu(NO_3)]$, **4.1**. The perspective ORTEP view for **4.1** is shown in figure 4.4. The crystallographic table and important bond lengths and angles are given in appendix III (Tables A3.1, A3.2 and A3.3, respectively). The ^{1}H-NMR spectrum of complex **4.1** in methanol-d_4 displayed the expected number of signals (Figure 4.5). The colorless solution on exposure to air resulted in the corresponding copper(II) complex, $[(L_3)_2Cu(NO_3)](ClO_4)$, **4.2**. The formation of complex **4.2** was confirmed by various

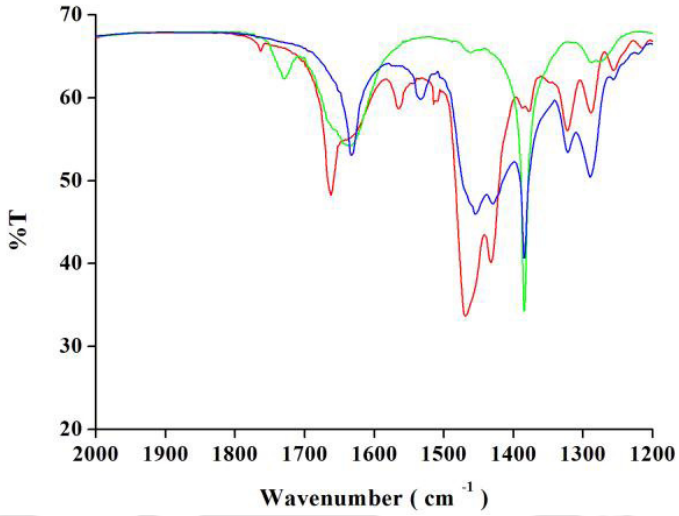

Figure 4.3 FT-IR spectra of complexes **3.2**(red), **4.1**(green), **4.2**(blue) in KBr.

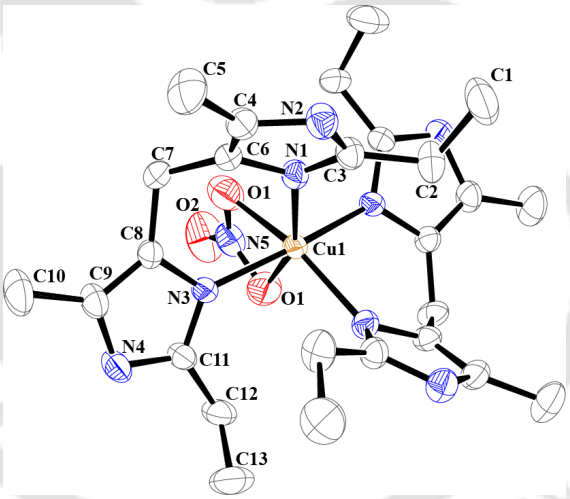

Figure 4.4 ORTEP diagram of complex **4.1** (solvent molecules and hydrogen are removed for clarity; 50% thermal ellipsoid plot).

spectroscopic analyses as well as by determination of its X-ray single crystal structure. The ORTEP view of complex **4.2** is shown in figure 4.5. The crystallographic table and important bond lengths and angles are given in appendix III (Tables A3.1, A3.2 and A3.3, respectively).

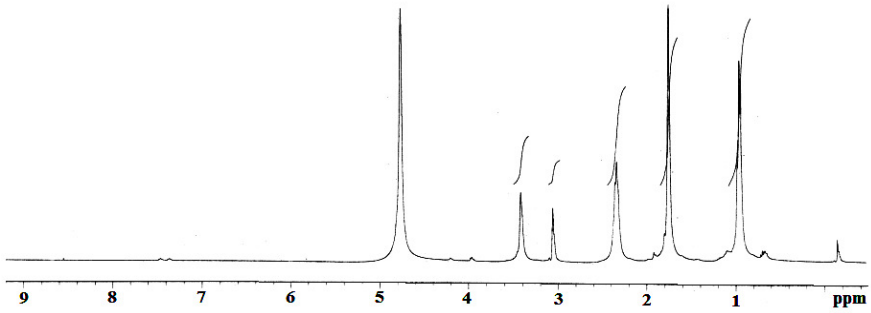

Figure 4.5 ^{1}H-NMR spectrum of complex **4.1** in methanol-d_4.

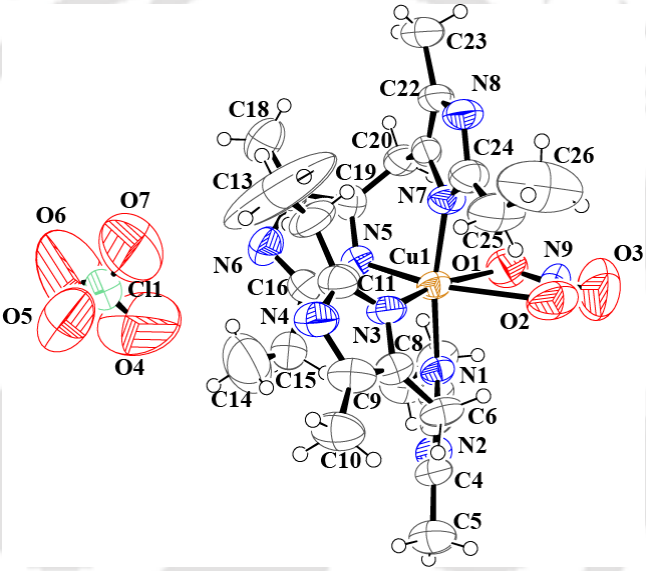

Figure 4.5 ORTEP diagram of complex **4.2** (50% thermal ellipsoid plot).

The formation of complex **4.1** essentially suggests the formation of a peroxynitrite intermediate in the course of the reaction (Scheme 4.1) as nitrate is the common decomposition/ isomerisation product of peroxynitrite.[5] On the other hand, addition of 2,4-di-*tertiary*butyl phenol in the above mentioned colorless solution was observed to afford phenol ring nitration (yield, ~65%), which is a characteristic reaction of the peroxynitrite complexes.[3,6] Thus, the isolation of complex **4.1** and phenol ring nitrosation indicate the presence of a copper(I)–peroxynitrite complex in the colorless solution formed in the

reaction of complex **3.2** with hydrogen peroxide. It should be noted that addition of H_2O_2 to the parent copper(II) complex, **3.1**, followed by NO purging was not observed to result in the same reaction (Appendix III, Figure A3.6). By contrast, in a recent report, Cu^{2+}/H_2O_2 was found to catalyze tyrosine nitration induced by NO with molecular oxygen.[3] There, NO was oxidized by O_2 to form NO_2, and the role of Cu^{2+}/H_2O_2 was to generate $^{\bullet}OH/Cu^{2+}–^{\bullet}OH$ topromote $Tyr^{\bullet}$ formation then leading to nitrated tyrosine.

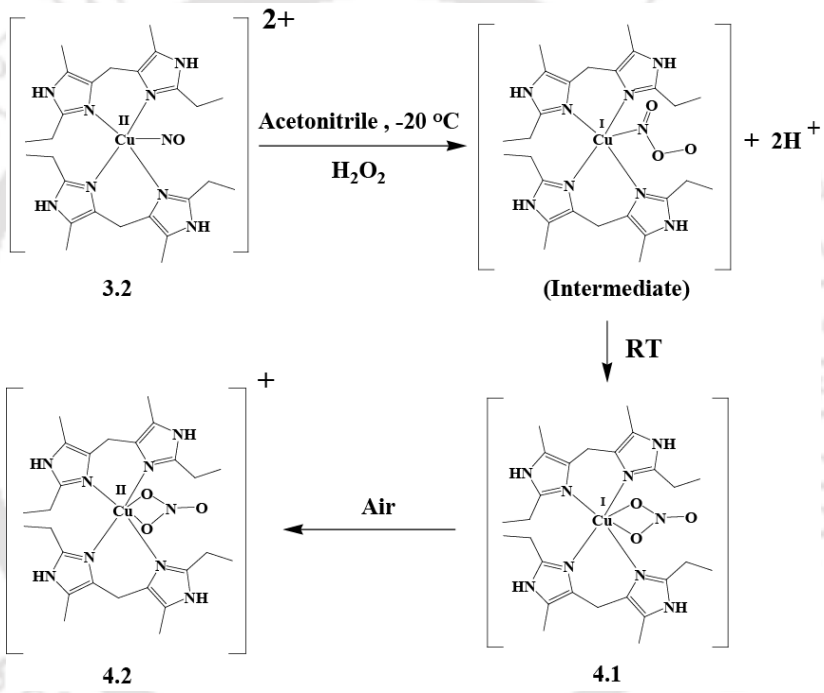

Scheme 4.1

It would be worth mentioning that NO is reported to react with alkaline H_2O_2 in the absence of oxygen to give peroxynitrite.[12] However, Blough and Zafiriou have not evidenced the formation of peroxynitrite in direct addition of NO to degassed alkaline solutions of H_2O_2.[13] In addition, it has been found that a thermal reaction between NO and H_2O_2 occurs at room temperature but the rate is so slow in neutral solutions; on the other hand, it was quite fast at pH 12.[13] It has been observed that since NO is not a nitrosating

agent, the formation of peroxynitrite by the reaction of NO and H_2O_2 probably requires oxygen, and proceeds through nitrosating intermediates that are formed during the autoxidation of NO; for instance, they observed the formation of peroxynitrite in the reaction of N_2O_3 and hydroperoxo anions.[14]

It is not very clear (i) whether the reaction of H_2O_2 is taking place directly in the electrophilic NO centre or (ii) first it reacts with the copper(II) centre followed by NO. However, since addition of H_2O_2 to the precursor copper(II) complex followed by NO purging resulted in neither reduction of copper(II) nor peroxynitrite formation, it is assumed that the first option is most likely to take place. It should be noted that when stoichiometric amount of potassium superoxide was added into the pre-cooled solution of complex **3.2**, no reduction of the copper(II) centre was observed (Appendix III, Figure A3.5), though the formation of the peroxynitrite intermediate complex was evidenced from the phenol ring nitration reaction as well as by the X-ray single crystal structure determination of the end product, $[(L_3)_2Cu(NO_3)](ClO_4)$, **4.2**.

4.3 Conclusion

The present chapter demonstrates a possible pathway of decomposition of both hydrogen peroxide as well as NO formed in biological systems. The reaction of a copper(II)–nitrosyl complex, **3.2**, with hydrogen peroxide was found to result in the reduction of the copper(II) centre to copper(I) leading to the formation of a copper(I)–peroxynitrite intermediate.

4.4 Experimental section

4.4.1 Materials and methods

All reagents and solvents were purchased from commercial sources and were of reagent

grade. Acetonitrile was distilled from calcium hydride. Deoxygenation of the solvent and solutions was effected by repeated vacuum/purge cycles or bubbling with nitrogen for 30 minutes. NO gas was purified by passing through KOH and P_2O_5 column. UV-visible spectra were recorded on a Perkin Elmer lambda 25 UV-visible spectrophotometer. FT-IR spectra were taken on a Perkin Elmer spectrophotometer with either sample prepared as KBr pellets or in solution in a potassium bromide cell. Solution electrical conductivity was checked using a Systronic 305 conductivity bridge. ^{1}H- NMR spectra were obtained with a 400 MHz Varian FT-spectrometer. Chemical shifts (ppm) were referenced either with an internal standard (Me_4Si) for organic compounds or to the residual solvent peaks. The X-band Electron Paramagnetic Resonance (EPR) spectra of the complexes and of the reaction mixtures were recorded on a JES-FA200 ESR spectrometer. Elemental analyses were obtained from a Perkin-Elmer Series II Analyzer. The magnetic moment of complexes were measured on a Cambridge Magnetic Balance. Mass spectra of the compounds in methanol were recorded in a Waters Q-Tof Premier and Aquity instrument.

Single crystals were grown by slow diffusion followed by slow evaporation technique. The intensity data were collected using a Bruker SMART APEX-II CCD diffractometer, equipped with a fine focus 1.75 kW sealed tube MoKα radiation (λ = 0.71073 Å) at 273(3) K, with increasing ω (width of 0.3° per frame) at a scan speed of 3 s/ frame. The SMART software was used for data acquisition. Data integration and reduction were undertaken with the SAINT and XPREP software.[15] Structures were solved by direct methods using SHELXS-97 and refined with fullmatrix least-squares on F^2 using SHELXL-97.[16] All non-hydrogen atoms were refined anisotropically. Structural illustrations have been drawn with ORTEP-3 for Windows.[17] The disorder present in the crystal structure has been tried to be minimized by use of SHELXL.

4.4.2 Synthesis of complex 4.1, $[Cu(L_3)_2(NO_3)]$

Complex **3.2** (1.514 g, 2 mmol) was dissolved in 20 ml of degassed acetonitrile and the solution was cooled to -20 °C. To this cold solution, pre-cooled hydrogen peroxide (70% v/v; 4 ml) was added and the solution turned colorless. It was then stirred at room temperature for 1h; layered with degassed benzene (20 ml) and kept in freezer. Colorless crystals of complex **4.1** were obtained from this solution after 2 days. Yield: 0.827 g (~70%). FT-IR (KBr pellet): 2976, 1630, 1535, 1384 cm^{-1}. ESI-Mass: Calcd. 589.25; Found, 527.28.

4.4.3 Synthesis of complex 4.2, $[Cu(L_3)_2(NO_3)](ClO_4)$

Complex **3.2** (1.514 g; 2 mmol) was dissolved in 20 ml of degassed acetonitrile and the solution was cooled to -20 °C. To this cold solution, pre-cooled hydrogen peroxide (70% v/v; 4 ml) was added and the solution turned colorless. It was then opened to air and stirred at room temperature for 2h to ensure the complete conversion of copper(I) to copper(II). Then the volume of the solution was reduced to 10 ml and layered with benzene. The mixture was then kept in freezer for overnight which resulted in green crystalline complex **4.2**. Yield: 1.172 g (~85%). UV-visible (acetonitrile): λ_{max} (ε / M^{-1} cm^{-1}) 720 nm (108) and 391 nm (340). FT-IR (KBr pellet): 2982, 1630, 1466, 1384, 1089, 625 cm^{-1}. Molar conductance: 244 S cm^2 mol^{-1}; magnetic moment, 1.64 BM.

4.4.4 Isolation of 2, 4-di-*tertiary*-butyl-6-nitrophenol

Complex **3.2** (1.514 g; 2 mmol) was dissolved in 20 ml of degassed acetonitrile and the solution was cooled to -20 °C. To this cold solution, pre-cooled hydrogen peroxide (70% v/v; 4 ml) was added and the solution turned colorless. To this, a pre-cooled solution (5

ml) of 2, 4-di-*tertiary*-butyl phenol (0.8 molar) was added and stirred for 1 h at -20 °C. The reaction mixture was then warmed to room temperature and dried under reduce pressure. The solid mass was then subjected to column chromatography using silica gel column to obtain pure 2,4-di-*tertiary*-butyl-6-nitrophenol. Yield: 0.326 g (~65%). ^{1}H-NMR (400 MHz, $CDCl_3$): δ_{ppm}, 7.88, 7.56, 4.85, 1.41, 1.29. Mass: $(m+H^+)/z$: Calcd. 251.15; Found, 251.32.

4.5 References

1. Ignarro, L. J., Ed. *Nitric Oxide: Biology and Pathobiology* Academic Press: San Diego, CA, 2000.

2. (a) Moncada, S.; Palmer, R. M. J.; Higgs, E. A.; *Pharmacol. Rev.* **1991**, *43*, 109. (b) Butler, A. R.; Williams, D. L. *Chem. Soc. Rev.* **1993**, *22*, 233. (c) Feelisch, M. Ed.; Stamler, J. S. *Methods in Nitric Oxide Research* John Wiley and Sons, Chichester, England, 1996. (d) Jia, L.; Bonaventura, C.; Bonaventura, J.; Stamler, J. S. *Nature* **1996**, *380*, 221. (e) Galdwin, M. T.; Lancaster Jr., J. R.; Freeman, B. A. A. N. *Nat. Med*. **2003**, *9*, 496.

3. (a) Radi, R. *Proc. Natl. Acad. Sci. U. S. A.* **2004**, *101*, 4003. (b) Qiao, L.; Lu, Y.; Liu, B.; Girault, H. H. *J. Am. Chem. Soc*. **2011**, *133*, 19823.

4. (a) Goldstein, S.; Lind, J.; Merenyi, G. *Chem. Rev.* **2005**, *105*, 2457. (b) Pacher, P.; Beckman, J. S.; Liaudet, L. *Physiol. Rev.* **2007**, *87*, 315.

5. (a) Herold, S.; Koppenol, W. H. Coord. *Chem. Rev.* **2005**, *249*, 499. (b) Ford, P. C.; Lorkovic, I. M. *Chem. Rev.* **2002**, *102*, 993.

6. (a) Maiti, D.; Lee, D.H.; Sarjeant, A. N. N.; Pau, M. Y. M.; Solomon, E. I.; Gaoutchenova, K.; Sundermeyer, J.; Karlin, K. D. *J. Am. Chem. Soc.* **2008**, *130*, 6700. (b) Park, G. Y.; Deepalatha, S.; Puiu, S. C.; Lee, D.H.; Mondal, B.; Sarjeant, A. N. N.; del Rio, D.; Pau, M. Y. M.; Solomon, E. I.; Karlin, K. D. *J. Biol. Inorg. Chem.* **2009**, *14*, 1301. (c) Hughes, M. N.; Nicklin, H. G.; Sackrule, W. A. C. *J. Chem. Soc. A* **1971**, 3722.

7. (a) Geletii, Y. V.; Bailey, A. J.; Boring, E. A.; Hill, C. L. *Chem. Commun.* **2001**, 1700. (b) Babich, O. A.; Gould, E. S. *Res. Chem. Intermed.* **2002**, *28*, 575. (c) Pellei, M.; Lobbia, G. G.; Santini, C.; Spagna, R.; Camalli, M.; Fedeli, D.; Falcioni, G. *Dalton Trans.* **2004**, 2822. (d) Kohnen, S.; Halusiak, E.; Mouithys-Mickalad, A.; Deby-Dupont, G.; Deby, C.; Hans, P.; Lamy, M.; Noels, A. F. *Nitric Oxide* **2005**, *12*, 252.

8. Wick, P. K.; Kissner, R.; Koppenol, W. H. *Helv. Chim. Acta* **2000**, *83*, 748.

9. (a) Clarkson, S. G.; Basolo, F. *Inorg. Chem.* **1973**, *12*, 1528. (b) Roncaroli, F.; Videla, M.; Slep, L. D.; Olabe, J. A. *Coord. Chem. Rev.* **2007**, *251*, 1903.

10. (a) Kalita, A.; Kumar, P.; Deka, R. C.; Mondal, B. *Chem. Commun.* **2012**, *48*, 1251. (b) Sarma, M.; Mondal, B. *Dalton Trans.* **2012**, *41*, 292. (c) Kalita, A.; Kumar, P.; Deka, R. C.; Mondal, B. *Inorg. Chem.* **2011**, *50*, 11868. (d) Sarma, M.; Mondal, B. *Inorg. Chem.* **2011**, *50*, 3206. (e) Sarma, M.; Kalita, A.; Kumar, P.; Singh, A.; Mondal, B. *J. Am. Chem. Soc.* **2010**, *132*, 7846.

11. Anbar, M.; Taube, H. *J. Am. Chem. Soc.* **1954**, *76*, 6243.

12. Halfpenny, E.; Robinson, P. L. *J. Chem. Soc. A* **1952**, 928.

13. Blough, N. V.; Zafiriou, O. C. *Inorg. Chem.* **1985**, *24*, 3502.

14. (a) Goldstein, S.; Czapski, G. *Inorg. Chem.* **1996**, *35*, 5935. (b) Goldstein, S.; Czapski, G. *J. Am. Chem. Soc.* **1995**, *117*, 12078. (c) Ford, P. C.; Wink, D. A.; Stanbury, D. M. *FEBS Lett.* **1993**, *326*, 1.

15. *SMART, SAINT* and *XPREP*; Siemens Analytical X-ray Instruments Inc.: Madison, WI, 1995.

16. Sheldrick, G. M. *SHELXS-97*; University of Gottingen: Gottingen, Germany, 1997.

17. Farrugia, L. J. *J. Appl. Crystallogr.* **1997**, *30*, 565.

Chapter 5

Reaction of a copper(II)–nitrosyl complex with hydrogen peroxide: Mimicking of tyrosine nitration

Abstract

Copper(II) complex, **5.1**, with the histidine-derived ligand $\mathbf{L_4}$ have been synthesized and characterized. The single crystal structure determination reveals a di-phenolato bridged di-copper(II) core in **5.1**. Addition of NO to the acetonitrile solution of **5.1** afforded corresponding mono-nuclear copper(II)-nitrosyl complex, **5.2**. In presence of H_2O_2, **5.2** results in the formation of corresponding copper(I)-peroxynitrite. The formation of peroxynitrite intermediate is evident from its characteristic phenol ring nitration reaction which resembles the tyrosine nitration in biological systems. Further, formation of nitrate as the decomposition product from **5.2** at room temperature also supports the involvement of peroxynitrite intermediate.

5.1 Introduction

Reactive nitrogen species (RNS) constitute a major class of intermediates involved in oxidative reactions in biological systems.[1] When produced at low or moderate concentrations, they stimulate signal transduction; but a higher concentration, they can induce oxidative damage of DNA, lipids and proteins.[2] Tyrosine nitration by RNS has attracted a considerable research interest as it can alter protein functions and can be useful as a diagnostic biomarker for cardiovascular, Alzheimer and Perkinson's diseases.[3] It is well known that tyrosine nitration occurs either by peroxynitrite ($^{-}$OONO) or by NO_2.[4] Peroxynitrite is known to generate *in vivo* by a diffusion control reaction between NO and superoxide (O_2^{-}) anion.[5] The presence of 3-nitrotyrosine in biological fluids indicates that peroxynitrite is capable of nitrating tyrosin in presence of Lewis acid like Cu^{2+} or Fe^{3+} and metalloproteins such as SOD.

The general idea of endogeneous generation of peroxynitrite and its cytotoxicity though an attractive and well-supported hypothesis, it should be noted that the evidence of the presence of peroxynitrite in biological systems is indirect and potentially ambiguous. For instance, it has been found that NO derived from activated macrophages can be quantitatively converted to peroxynitrite in SOD catalyzed nitration of phenolic substrates.[6] Nathan et al reported the enhancement of cytotoxicity associated with the activated macrophages upon addition of SOD and blocked by the addition of H_2O_2 scavenging enzyme.[7]

Recently, in small molecule models we have shown that copper(II)-nitrosyl complex can react with H_2O_2 to generate peroxynitrite intermediate.[8] In the present study, we would like to explore this idea of the reaction of copper(II)-nitrosyl complex/intermediate with H_2O_2

to afford phenol ring nitration which is a part of the ligand framework. For the present study we have prepared a histidin based ligand, $\mathbf{L_4}$, with a phenolic group (Figure 5.1).

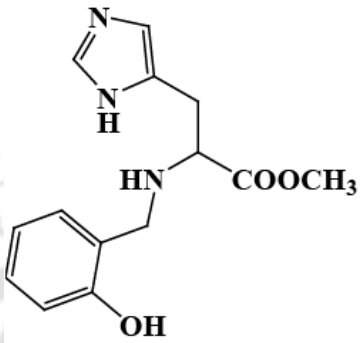

($\mathbf{L_4}$)

Figure 5.1 Ligand used for the present study.

5.2 Results and discussion

Ligand $\mathbf{L_4}$ was synthesized from the reaction of L-histidine methyl ester dihydrochloride and salicylaldehyde in presence of lithium hydroxide as base followed by the reduction of intermediate imine by $NaBH_4$ (Experimental section). The ligand was characterized by various spectroscopic techniques (Experimental section). The copper(II) complex, **5.1**, was synthesized from the reaction of copper (II) perchlorate hexahydrate with ligand, $\mathbf{L_4}$. It was characterized by various analytical techniques (Experimental section). The single crystal structure of the complex was determined. The perspective ORTEP view is shown in figure 5.2. The crystallographic table and important bond lengths and angles are given in appendix IV (Tables A4.1, A4.2 and A4.3, respectively). The crystal structure revealed that complex **5.1** is a di-phenolato bridged dicopper(II) system. Two nitrogen donor atoms from the ligand and two oxygen atoms from two bridging phenolato groups resulted in a distorted square planar coordination geometry around each copper(II) centre. The fifth

coordination site is occupied by carbonyl oxygen from the ester group present in the ligand framework. The octahedral coordination of each copper(II) centre is completed by the solvent water molecule. The Cu-$O_{(carbonyl)}$ and Cu-$O_{(water)}$ distances, 2.530(2) and 2.546(2) Å, respectively, are within the range of reported distances.[9] The average Cu-N distances in complex **5.1,** (Cu-N1/Cu-N2), 2.027(2)/1.956(2)Å are also in the range observed in the reported complexes.[9] The phenolato oxygen atoms are coordinated to the copper(II) centre through the equatorial position at an average distance of 1.963(1) Å which is in the range observed for other equatorial Cu-$O_{(phenolato)}$ distances.[10] The Cu-$O_{(phenolato)}$-Cu angle is ~ 100.5 °. It should be noted that in earlier reported compounds, this was observed in the range of 91°-104°. The two copper (II) centres are separated by 3.03 Å. This is comparable to the values for other reported complexes by Thompson et al (e.g. ranging from 2.997 to 3.1184 Å) and Ray et al.[11] The C-$O_{(phenolato)}$ distance, 1.354(3) Å is very close to the C–O single bond distance, indicating the phenolato character of the bridging oxygen centres.[12]

Complex **5.1** in acetonitrile solvent, exhibited broad *d-d* band at λ_{max}(ε/ $M^{-1}cm^{-1}$), 660 nm (244), along with relatively strong intra-ligand absorptions in the UV region (Figure 5.3). The phenolato-copper(II) charge transfer transition was found to appear at 421 nm.

The acetonitrile solution of complex **5.1** was found to be silent in X-band EPR studies (Appendix IV, Figure A4.6). This has been attributed to the antiferromagnetic coupling of the two paramagnetic copper(II) centres through phenlato bridges. It is further supported by very low resultant magnetic moment of the solid complex **5.1**

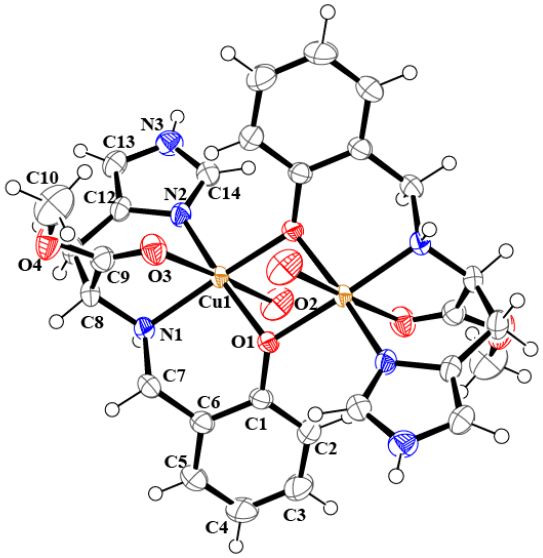

Figure 5.2 ORTEP diagram of complex **5.1** (Solvent molecules and perchlorate are removed for clarity; 50% thermal ellipsoid plot).

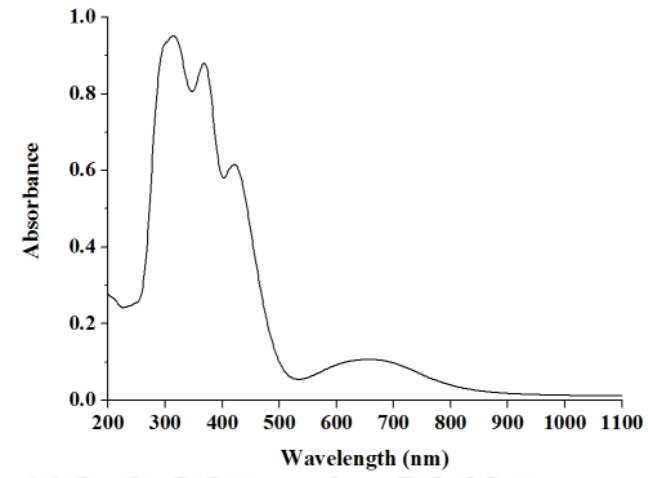

Figure 5.3 UV-visible spectrum of complex **5.1** in acetonitrile solution at room temperature.

5.3 Nitric oxide reactivity

Purging of NO to a degassed acetonitrile solution of complex **5.1** resulted into the darkening in color. In UV-visible spectroscopy, the *d-d* band (λ_{max}, 660 nm) of complex **5.1** was found to be blue shifted with λ_{max} at 645 nm (Figure 5.4). This has been attributed

to the formation of corresponding mononuclear [Cu^{II}-NO] complex, **5.2**. Because of thermal instability and moisture sensitivity, complex **5.2** could not be isolated as solid unlike complex **3.2** (Chapter 3).[8] However, studies on solution FT-IR, X-band EPR and ESI-mass spectroscopy support its formulation as corresponding mononuclear [Cu^{II}-NO] intermediate complex. It is found to be EPR silent (Appendix IV, Figure A4.9).

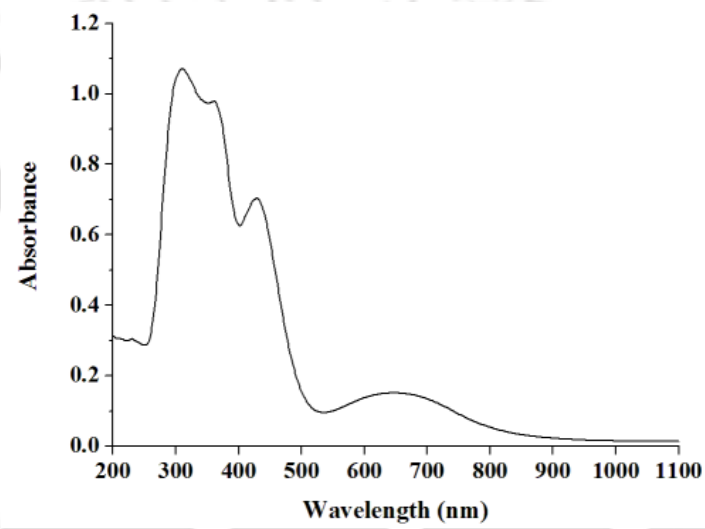

Figure 5.4 UV-visible spectrum of complex **5.2** in acetonitrile solution at room temperature.

In the FT-IR spectrum, it exhibits a vibration at 1846 cm^{-1}, which is attributed to the coordinated nitrosyl stretching frequency (Figure 5.5).[13] The frequency of this vibration was found to shift to 1815 cm^{-1} on ^{15}NO labelling experiment which further confirms its assignment as ν_{NO}.[8] It should be noted that in case of the solid isolated [Cu^{II}-NO], this frequency was reported to appear at 1662 cm^{-1}(Chapter 3, complex **3.2**).[8] For $[Cu(TAEA)(CH_3CN)]^{2+}$ [TAEA = *tris*(2- aminoethyl)amine] complex, the ν_{NO} of [Cu^{II}-NO] was found to appear at 1650 cm^{-1}.[13] In early report on the air-stable solid copper-nitrosyl of copper(II)-dithiocarbamate, the ν_{NO} for the NO coordinated to copper appears at

1682 cm^{-1}.[13] Hayton et al reported the appearance of ν_{NO} band at 1933 cm^{-1} for copper(II)-nitrosyl.[13] Application of vacuum to the acetonitrile solution of complex **5.2** was found to result in the decrease of the ν_{NO} band intensity in FT-IR spectrum indicating the loss of NO ligand from the complex (Appendix IV, Figure A4.10).[13] This intermediate complex **5.2** was found to be stable in solution under nitrogen atmosphere for few hours. It is important to note that in all earlier examples, the [Cu^{II}-NO] complexes were found to be very unstable, except the examples reported by Diaz and Hayton et al[13] and the very recent one from our laboratory.

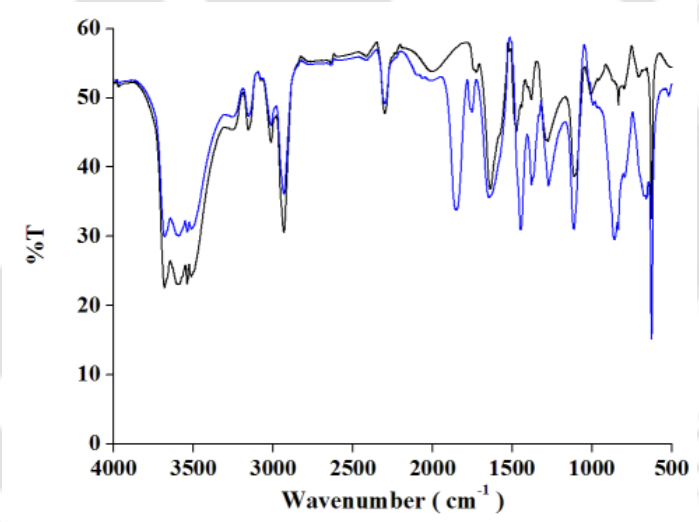

Figure 5.5 Solution FT-IR spectra of complexes **5.1** (black) and **5.2** (blue) in acetonitrile solvent at room temperature.

The mononuclear nature of complex **5.2** was further confirmed from the ESI-mass spectral studies. The observed mass of complex **5.2** in acetonitrile solution was found to corroborate with the mononuclear unit, rather than the dinuclear dinitrosyl (Figure 5.6).

In our study on copper(II)-nitrosyl intermediates having $\{CuNO\}^{10}$ electronic configuration, it has been observed the reaction of copper(II)-nitrosyl complex with

hydrogen peroxide induces the reduction of copper(II) centre with a simultaneous formation of peroxynitrite intermediate (Chapter 4).

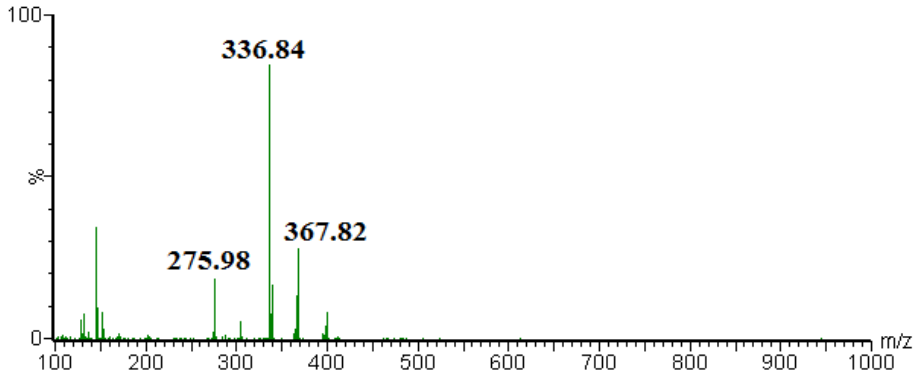

Figure 5.6 ESI-mass spectrum of complex **5.2** in acetonitrile

From a freshly generated complex **5.2**, excess of NO was removed by purging argon gas and the solution was cooled to -20 °C. To this cold solution, stoichiometric addition of pre-cooled hydrogen peroxide was found to turn it into a colorless solution. This has been attributed to the formation of corresponding copper(I)-peroxynitrite complex. The intensity of the *d-d* transition band of complex **5.2** having λ_{max} at 645 nm was found to decrease with time upon addition of H_2O_2 suggesting the reduction of copper(II) (Figure 5.7).

The ν_{NO} band at ~1846 cm^{-1} in solution FT-IR of complex **5.2,** was found to diminish upon addition of H_2O_2 with the appearance of NO_3^- stretching at ~1384 cm^{-1} (Appendix IV, Figure A4.11). In chapter 4, similar observation was noticed with complex **3.2**. The colorless solution, when allowed to stay in presence of air, it became green. FT-IR spectral analysis of the crude product indicates the presence of nitrate (NO_3^-). It should be noted that the ligand $\mathbf{L_4}$, was found to be undergo phenol ring nitration to yield $\mathbf{L_4}'$ (yield, ~40%). These essentially suggest the formation of peroxynitrite intermediate in course of the reaction (Scheme 5.1).[8]

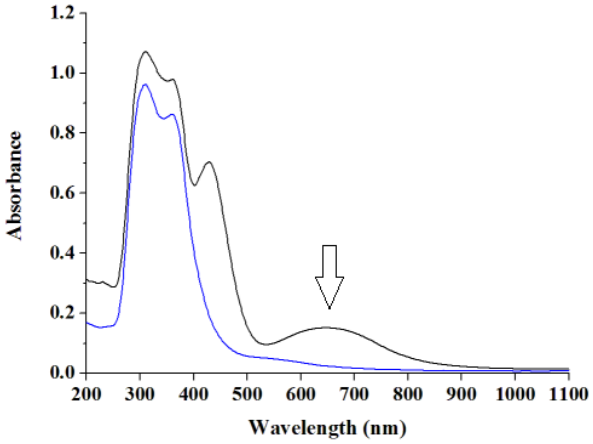

Figure 5.7 UV-visible spectra of complex **5.2** (black) and after reaction with H_2O_2 (blue) in acetonitrile solvent.

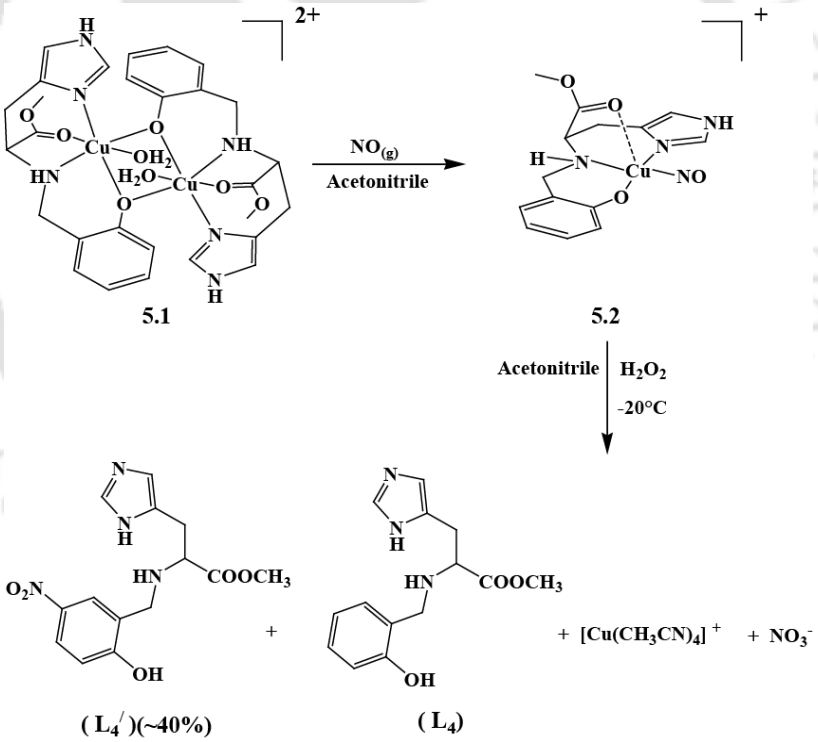

Scheme 5.1

It should be noted that addition of H_2O_2 to the parent copper(II) complex, **5.1** followed by NO purging was not observed to result to the same reaction. Thus, the appearance of NO_3^-

stretching frequency in FT-IR spectrum and phenol ring nitrosation indicate the presence of copper(I)-peroxynitrite complex in the colorless solution formed in the reaction of complex **5.2** with H_2O_2. It would be worth mentioning that NO is reported to react with alkaline H_2O_2 in absence of oxygen to give peroxynitrite.[14]

However, Blough and Zafiriou have not evidenced the formation of peroxynitrite in direct addition of NO to degassed alkaline solutions of H_2O_2.[15] In addition, it has been found that a thermal reaction between NO and H_2O_2 occurs at room temperature but the rate is so slow in neutral solutions; on the other hand, it was quite fast at pH 12.[15] It was observed that since NO is not a nitrosating agent, the formation of peroxynitrite by the reaction of NO and H_2O_2 probably requires oxygen, and proceeds through nitrosating intermediates that are formed during the autoxidation of NO; for instance, they observed the formation of peroxynitrite in the reaction of N_2O_3 and hydroperoxo anion.[16]

Recently both copper(II) and copper(II)-peptide complexes were reported to catalyze the tyrosine nitration in the presence of nitrite and hydrogen peroxide.[17] This copper-mediated tyrosine nitration has been explained by a mechanism considering the generation of hydroxyl radicals (•OH) and/or copper(II)-bound •OH (Cu^{2+}- •OH) from Cu^{2+} and H_2O_2 through a Fenton-like reaction. These radicals may be scavenged by both NO_2^- to form $•NO_2$ and tyrosine to form tyrosine radicals (Tyr•), resulting in tyrosine nitration. Cu^{2+}/H_2O_2 was also found to catalyze the tyrosine nitration induced by NO and oxygen. •NO was oxidized by O_2 to form $•NO_2$, and the role of Cu^{2+}/H_2O_2 was to generate •OH/Cu^{2+}-•OH to promote Tyr• formation.[17]

It is not very clear that (i) whether the reaction of H_2O_2 is taking place directly to the electrophillic NO centre or (ii) first it reacts with copper(II) centre followed by NO. However, since addition of H_2O_2 to the precursor copper(II) complex followed by NO

purging did not result neither reduction of copper(II) nor peroxynitrite formation, it is assumed that the first option is most likely to take place. It should be noted that when stoichiometric amount of potassium superoxide is added into the pre-cooled solution of complex **5.2**, no reduction of copper(II) centre was observed; though the formation of the peroxynitrite intermediate complex was evidenced from the phenol ring nitrosation of the ligand.

5.4 Conclusion

Thus, the present chapter describes the formation of copper(I)-peroxynitrite through the reaction of [Cu^{II}-NO] complex and H_2O_2. This mechanism is clearly different than what was proposed by Girault et al for the Cu^{2+}/H_2O_2 mediated tyrosine nitration in presence of NO_2^-. The peroxynitrite intermediate was found to induce nitration at the phenol ring present in the ligand framework which resembles the tyrosine nitration in biological systems. Thus, this work supports the possibility of the occurrence of decomposition of both hydrogen peroxide as well as NO formed in the biological systems which has been proposed in chapter 4.

5.5 Experimental section

5.5.1 Materials and methods

All reagents and solvents were purchased from commercial sources and were of reagent grade. Acetonitrile was distilled from calcium hydride. Deoxygenation of the solvent and solutions were effected by repeated vacuum/purge cycles or bubbling with nitrogen for 30 minutes. NO gas was purified by passing through KOH and P_2O_5 column. UV-visible spectra were recorded on a Perkin Elmer Lamda 25 UV-visible spectrophotometer. FT-IR

spectra were taken on a Perkin-Elmer spectrophotometer with either sample prepared as KBr pellets or in solution in a potassium bromide cell. Solution electrical conductivity was checked using a Systronic 305 conductivity bridge. ^{1}H-NMR spectra were obtained with a 400 MHz Varian FT spectrometer. Chemical shifts (ppm) were referenced either with an internal standard (Me_4Si) for organic compounds or to the residual solvent peaks. The X-band Electron Paramagnetic Resonance (EPR) spectra of the complexes and of the reaction mixtures were recorded on a JES-FA200 ESR spectrometer. The magnetic moment of complexes are measured on a Cambridge Magnetic Balance. Mass spectra of the compounds were recorded in a Waters Q-Tof Premier and Aquity instrument. Single crystals were grown by slow diffusion followed by slow evaporation technique. The intensity data were collected using a Bruker SMART APEX-II CCD diffractometer, equipped with a fine focus 1.75 kW sealed tube MoKa radiation (λ = 0.71073 Å) at 273(3) K, with increasing ω (width of 0.3° per frame) at a scan speed of 3 s/frame. The SMART software was used for data acquisition.[18] Data integration and reduction was undertaken with SAINT and XPREP software. Structures were solved by direct methods using SHELXS-97 and refined with full-matrix least squares on F^2 using SHELXL-97.[19] All non-hydrogen atoms were refined anisotropically. Structural illustrations have been drawn with ORTEP-3 for Windows.[20]

5.5.2 Synthesis of ligand L_4

To a solution of L-histidine methyl ester dihydrochloride (2.421 g, 10 mmol) in 50 ml methanol was added lithium hydroxide monohydrate (0.84 g, 20 mmol) into a 100 ml round bottom flask equipped with a magnetic stirring bar. To this solution salicylaldehyde (1.22 g, 10 mmol) was added drop wise with constant stirring. The reaction mixture was

then allowed to stir at room temperature for 5 h. The resulting reddish-yellow solution was then reduced by $NaBH_4$ (0.95 g, 25 mmol). Removal of solvent under reduced pressure affords a crude mass. It was dissolved in water (50 ml) and neutralized by addition of dilute acetic acid and then extracted with chloroform (50 m × 4 portions).

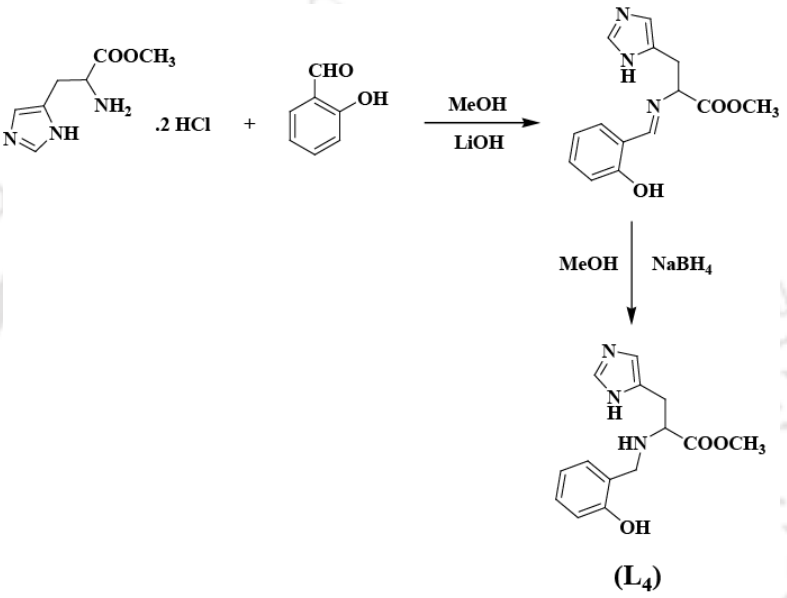

(L_4)

Scheme 5.2

Chloroform extract was dried under reduced pressure and the reddish yellow oil thus obtained was subjected to chromatographic purification using silica gel column to yield the pure ligand, **L_4** as yellow oil. Yield: 2.21 g (80%). Elemental Analyses: Calcd. for $C_{14}H_{17}N_3O_3$: C, 61.08; H, 6.22; N, 15.26. Found (%): C, 61.03; H, 6.27; N, 15.21. FT-IR (in KBr): 1730, 1654, 1455, 12154, 754 cm^{-1}. ^{1}H-NMR (400 MHz, $CDCl_3$) δ_{ppm}: 7.50 (s, 1H), 7.13-7.09 (t, 1H), 6.94-6.92 (d, 1H), 6.78 (s, 4H), 6.76-6.73 (t, 1H), 6.71 (d, 1H), 3.98-3.95 (d, 2H), 3.68 (s, 4H), 3.04-2.86 (d, 2H). ^{13}C-NMR (100 MHz, $CDCl_3$) $\delta_{ppm:}$ 30.61, 50.75, 52.35, 60.24, 116.47, 116.84, 119.49, 123.01, 129.12, 133.84, 135.49, 157.54 and 174. ESI-Mass (m+1), Calcd. 276.13; Found: 276.12.

5.5.3 Synthesis of complex 5.1, $[Cu_2 (L_4)_2(H_2O)_2](ClO_4)_2$

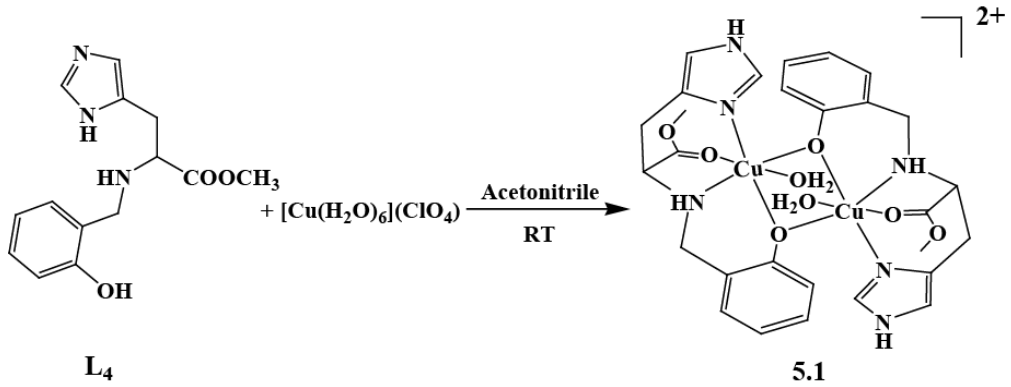

L_4 5.1

Scheme 5.3

Copper(II) perchlorate hexahydrate (1.482 g, 4 mmol) was dissolved in 20 ml acetonitrile. To this solution, 1.101 g (4 mmol) of the ligand L_4 was added slowly with constant stirring. The color of the solution turned into green from light blue. The stirring was continued for 1h at room temperature. The volume of the solution then reduced to ~5 ml. To this, 10 ml of benzene was added to make a layer on it and kept it overnight on freezer. This resulted into microcrystalline complex **5.1**. Yield: 1.55 g (~85%). FT-IR (in KBr): 2936, 1721, 1630, 1599, 1485, 1263, 1118, 625 cm^{-1}; magnetic moment, 0.38 BM /Cu^{II}. Molar conductivity, 275 S mol^{-1} cm^{-1}.

5.5.4 Isolation of L_4'

To 20 ml of distilled and degassed acetonitrile solution of complex **5.1** (0.5 g), freshly prepared NO was bubbled for 1 minute. The color of the solution turned dark green. The excess of NO was removed by purging argon gas and the solution was cooled to -20 °C. To this cold solution, pre-cooled hydrogen peroxide (70% v/v; 0.05ml) was added and the

solution turned colorless. The reaction mixture was then warmed to room temperature and dried under reduce pressure. Water (5 ml) was added to the dried mass followed by the addition of 5 ml of saturated Na_2S solution. The black precipitate of CuS was filtered out. The crude organic part was then extracted from the aqueous layer using $CHCl_3$ (25 ml × 4 portions). The crude product, obtained after removal of solvent, was then purified by column chromatography using neutral alumina column and hexane / ethyl acetate solvent mixture to get the pure modified ligand $\mathbf{L_4'}$**.** Yield: 0.14 g (~40%). Elemental Analyses: Calcd. (%) for $C_{14}H_{16}N_4O_5$: C, 52.50; H, 5.03; N, 17.49. Found (%): C, 52.48; H, 5.08; N, 17.44. FT-IR (in KBr): 2967, 1630, 1545, 1510, 1431, 1340, 1269, 1203, 853 cm^{-1}. ^{1}H-NMR (400 MHz, $CDCl_3$) δ_{ppm}: 7.68-66 (d, 1H), 7.45 (s, 1H), 6.96-6.95 (d, 1H), 6.86 (s, 1H), 6.05 (s, 1H), 3.98-3.95 (d, 2H), 3.72 (s, 4H), 3.05-2.89 (d, 2H). ^{13}C-NMR (100 MHz, $CDCl_3$) $\delta_{ppm:}$ 174.87, 162.18, 141.81, 135.71, 134.01, 125.02, 120.76, 120.26, 116.82, 60.72, 52.81, 50.94, 30.78. ESI-Mass $(m+H^+)/z$: Calcd. 321.11; Found: 321.13.

5.6 References

1. Wiseman, H.; Halliwell, B. *Biochem. J.* **1996**, *313*, 17.

2. (a) Apel, K.; Hirt, H. *Annu. Rev. Plant Biol.* **2004**, *55*, 373. (b) Radi, R. *Proc. Natl. Acad. Sci. U.S.A.* **2004**, *101*, 4003.

3. (a) Shishehbor, M. H.; Aviles, R. J.; Brennan, M. L.; Fu, X. M.; Goormastic, M.; Pearce, G. L.; Gokce, N.; Keaney, J. F.; Penn, M. S.; Sprecher, D. L.; Vita, J. A.; Hazen, S. L. *J. Am. Med. Assoc.* **2003**, *289*, 1675. (b) Good, P. F.; Werner, P.; Hsu, A.; Olanow, C. W.; Perl, D. P. *Am. J. Pathol.* **1996**, *149*, 21. (c) Danielson, S. R.; Held, J. M.; Schilling, B.; Oo, M.; Gibson, B. W.; Andersen, J. K. *Anal. Chem.* **2009**, *81*, 7823.

4. (a) Gunaydin, H.; Houk, K. N. *Chem. Res. Toxicol.* **2009**, *22*, 894. (b) Van der Vliet, A.; Eiserich, J. P.; Halliwell, B.; Cross, C. E. *J. Biol. Chem.* **1997**, *272*, 7617.

5. (a) Goldstein, S.; Lind, J.; Merenyi, G. *Chem. Rev.* **2005**, *105*, 2457. (b) Schopfer, M. P.; Wang, J.; Karlin, K. D. *Inorg. Chem.* **2010**, *49*, 6267. (c) Surmeli, N. B.; Litterman, N. K.; Miller, A. F.; Groves, J. T. *J. Am. Chem. Soc.* **2010**, *132*, 17174.

6. Ischiropoulos, H.; Zhu, L.; Beckman, J. S. *Arch. Biochem. Biophys.* **1992**, *298*, 446.

7. Nathan, C. F.; Silverstein, S. C.; Brukner, L. H.; Cohn, Z. A. *J. Exp. Med.* **1979**, *149*, 100.

8. Kalita, A.; Kumar, P.; Mondal, B. *Chem. Commun.* **2012**, *48*, 4636.

9. (a) Zeyrek, C. T.; Elmali, A.; Elerman, Y.; Svoboda, I.; Fuess, H.; *Z. Naturforsch* **2000**, *55b*, 1067. (b) Rajendiran, T. M.; Kannappan, R.; Venkatesan, R.; Rao, P. S.; Kandaswami, M. *Polyhedron* **1999**, *18*, 3085. (b) O'Connor, C. J. *Prog. Inorg. Chem.* **1982**, *29*, 203. (c) Elmali, A.; Zeyrek, C. T.; Elerman, Y. *J. Mol. Struct.* **2004**, *693*, 225.

10. (a) Thakurta, S.; Chakraborty, J.; Rosair, G.; Tercero, J.; El Fallah, M. S.; Garribba, E.; Mitra, S. *Inorg. Chem.* **2008**, *47*, 6227. (b) Chakraborty, J.; Samanta, B.; Pilet, G.; Mitra, S. S.; *Inorg. Chem. Commun.* **2007**, *10*, 40. (c) Majumder, A.; Rosair, G.; Mallick, A.; Chattopadhyay, N.; Mitra, S. *Polyhedron* **2006**, *25*, 1753. (d) Blackman, A. G. *Polyhedron* **2005**, *24*, 1. (e) Mukherjee, A.; Saha, M. K.; Nethaji, M.; Chakravarty, A. R. *Polyhedron* **2004**, *23*, 2177.

11. (a) Sinha Ray, M.; Mukhopadhyay, G.; Drew, M. G. B.; Chaudhuri, T.-H. Lu, S.; Ghosh, A. *Inorg. Chem. Commun.* **2003**, *6*, 961. (b) Kavlakoglu, E.; Elmali, A.;

Elerman, Y.; Fuess, H.; *Z. Naturforsch.* **2000**, *55b*, 561. (c) Burk, P.L.; Osborn, J.A.; Youinou, M.-T.; Agnus, Y.; Louis, R.; Weiss, R. *J. Am. Chem. Soc.* **1981**, *103*, 1273. (d) Nishida, Y.; Kida, S.J. *J. Chem. Soc., Dalton Trans.* **1986**, 2633.

12. Dutta, G.; Debnath, R. K.; Kalita, A.; Kumar, P.; Sarma, M.; Boomi Shaknar, R.; Mondal, B. *Polyhedron* **2011**, *30*, 293.
13. (a) Sarma, M.; Singh, A.; Gupta, S. G.; Das, G.; Mondal, B. *Inorg. Chim. Acta* **2010**, *363*, 63. (b) Tsumore, N.; Xu, Q. *Bull. Chem. Soc. Jpn.* **2002**, *75*, 1861. (c) Diaz, A.; Ortiz, M.; Sanchez, I.; Cao, R.; Mederos, A.; Sanchiz, J.; Brito, F. *J. Inorg. Biochem.* **2003**, *95*, 283. (d) Wright, A. M.; Wu, G.; Hayton, T. W. *J. Am. Chem. Soc.* **2010**, *132*, 14336, (e) Sarma, M.; Mondal, B. *Inorg. Chem.* **2011**, *50*, 3206. (f) Tran, D.; Skelton, B. W.; White, A. H.; Leverman, L. E.; Ford, P. C. *Inorg. Chem.* **1998**, *37*, 2505. (g) Lim, M. D.; Capps, K. B.; Karpessian, T.; Ford, P. C. *Nitric Oxide, Biol. Chem*. **2005**, *12*, 244.
14. Anbar, M.; Taube, H. *J. Am. Chem. Soc.* **1954**, *76*, 6243.
15. Halfpenny, E.; Robinson, P. L. *J. Chem. Soc. A*, **1952**, 928.
16. Blough, N. V.; Zafiriou, O. C. *Inorg. Chem*. **1985**, *24*, 3502.
17. Qiao, L.; Lu, Y.; Liu, B.; Girault, H. H. *J. Am. Chem. Soc.* **2011**, *133*,19823.
18. *SMART, SAINT* and *XPREP*; Siemens Analytical X-ray Instruments Inc.: Madison, WI, 1995.
19. Sheldrick, G. M. *SHELXS-97*; University of Gottingen: Gottingen, Germany, 1997.
20. Farrugia, L. J. *J. Appl. Crystallogr.* **1997**, *30*, 565.

Appendix I

Table A1.1 Crystallographic data for complexes **2.1, 2.2** and $\mathbf{L_2'}$.

	Complex **2.1**	Complex **2.2**	$\mathbf{L_2'}$
Formulae	$C_{16}\ H_{36}\ Cl_2\ Cu\ N_4\ O_8$	$C_{16}\ H_{36}\ Cl_2\ Cu\ N_4\ O_8$	$C_8\ H_{16}\ N_4\ O_2$
Mol. wt.	546.94	546.94	200.25
Crystal system	Monoclinic	Monoclinic	Monoclinic
Space group	P 2_1/n	P 2_1/n	P 2_1/c
Temperature /K	296(2)	296(2)	296(2)
Wavelength /Å	0.71073	0.71073	0.71073
a /Å	8.4581(4)	9.9191(4)	5.9207(7)
b /Å	9.1705(4)	10.4189(4)	15.3528(17)
c /Å	15.5388(7)	11.9274(4)	12.8203(15)
α/°	90.00	90.00	90.00
β/°	98.063(2)	97.283(2)	114.452(8)
γ/°	90.00	90.00	90.00
V/ $Å^3$	1193.35(9)	1222.71(8)	1060.8(2)
Z	2	2	4
Density/Mgm^{-3}	1.522	1.475	1.254
Abs. Coeff. /mm^{-1}	1.187	1.158	0.093
Abs. correction	None	None	None
F(000)	574.0	566.0	432
Total no. of reflections	2956	3411	2563
Reflections, $I > 2\sigma(I)$	2466	2360	817
Max. 2θ/°	28.35	30.01	28.42
Ranges (h, k, l)	-9≤h ≤11 -11≤ k ≤12 -20≤ l ≤20	-13≤ h ≤12 -14≤ k ≤14 -14≤l ≤16	-7≤ h ≤7 -20≤k ≤20 -17≤ l ≤15
Complete to 2θ (%)	99.3	95.5	96.4
Refinement method	Full-matrix least-squares on F^2	Full-matrix least-squares on F^2	Full-matrix least-squares on F^2
Goof (F^2)	0.999	1.030	1.626
R indices [$I > 2\sigma(I)$]	0.0366	0.0457	0.0969
R indices (all data)	0.0430	0.0639	0.2077

Table A1.2 Selected bond lengths (Å) for complexes **2.1**, **2.2** and $\mathbf{L_2'}$.

	Complex **2.1**	Complex **2.2**	$\mathbf{L_2'}$
Cu(1)-N(1)	2.046(1)	1.999(2)	-
Cu(1)-N(2)	2.027(2)	2.010(3)	-
C(1)-N(1)	1.504(3)	1.509(4)	1.477(6)
C(5)-N(2)	1.496(2)	1.518(4)	-
C(5)-N(3)	-	-	1.450(7)
N(1)-N(2)	-	-	1.318(7)
N(2)-O(1)	-	-	1.226(6)

Table A1.3 Selected bond angles (°) for complexes **2.1**, **2.2** and $\mathbf{L_2'}$.

	Complex **2.1**	Complex **2.2**	$\mathbf{L_2'}$
N(1)-Cu(1)-N(2)	94.24(6)	79.41(9)	-
N(1)-Cu(1)-N(1)	180.00(6)	180.00(9)	-
Cu(1)-N(1)-C(1)	122.7(1)	110.2(2)	-
N(1)-C(1)-C(4)	108.2(2)	109.9(3)	108.7(4)
N(1)-N(2)-O(1)	-	-	114.2(5)
N(1)-C(8)-C(7)	-	-	111.8(5)
N(2)-C(7)-C(8)	107.7(2)	110.1(3)	-
C(4)- C(5)-C(6)	109.5(2)	110.5(3)	111.9(5)

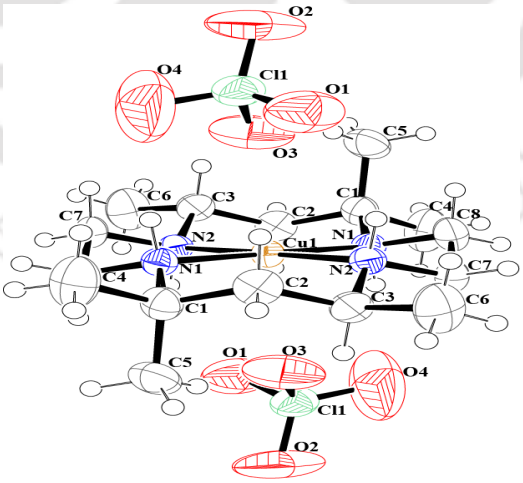

Figure A1.1 ORTEP diagram of complex **2.1**. (50% thermal ellipsoid plot).

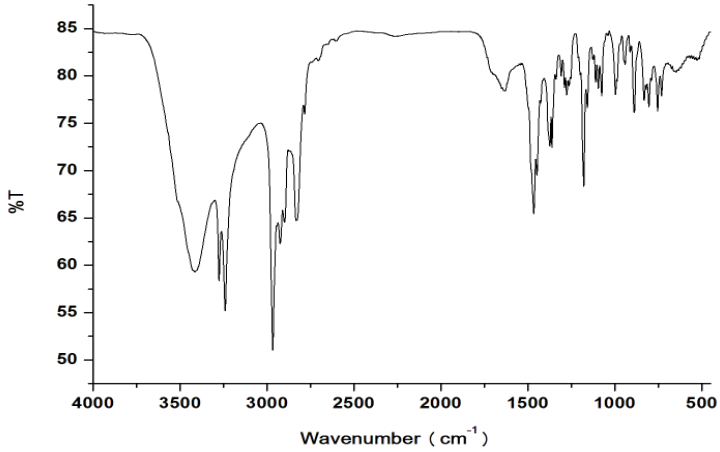

Figure A1.2 FT-IR spectrum of $\mathbf{L_1}$ in KBr.

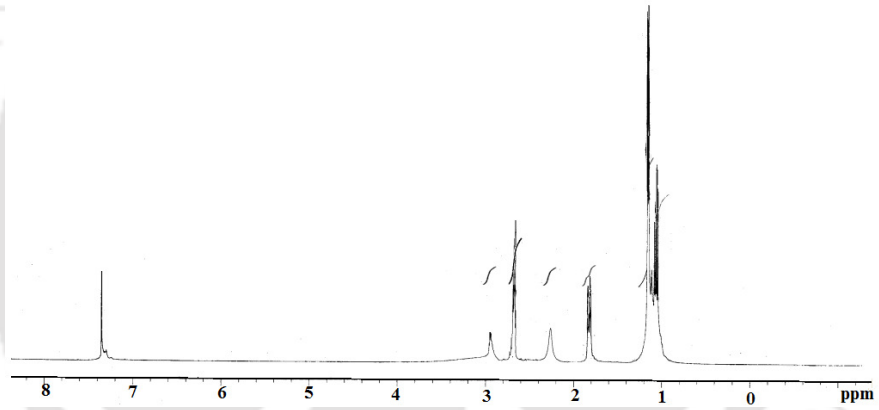

Figure A1.3 ^{1}H-NMR spectrum of $\mathbf{L_1}$ in $CDCl_3$.

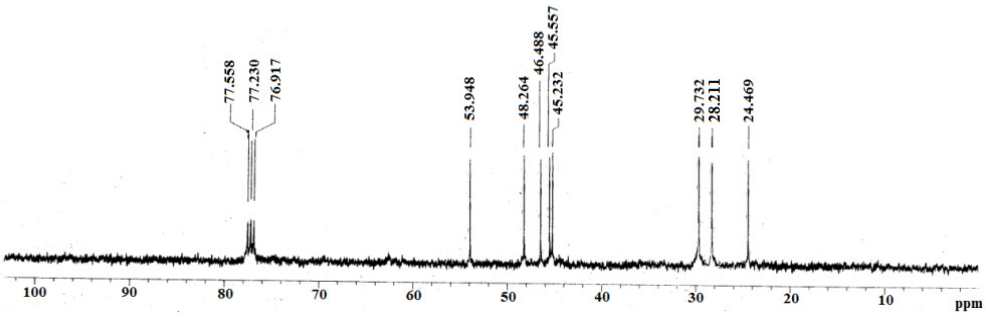

Figure A1.4 ^{13}C-NMR spectrum of $\mathbf{L_1}$ in $CDCl_3$.

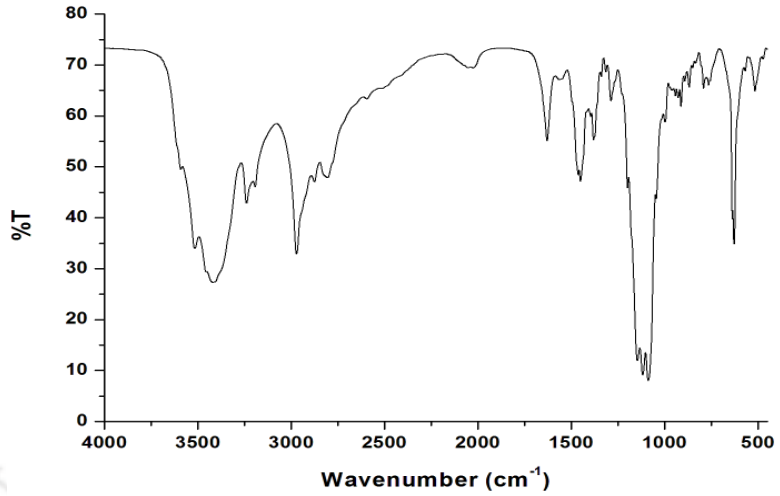

Figure A1.5 FT-IR spectrum of complex **2.1** in KBr.

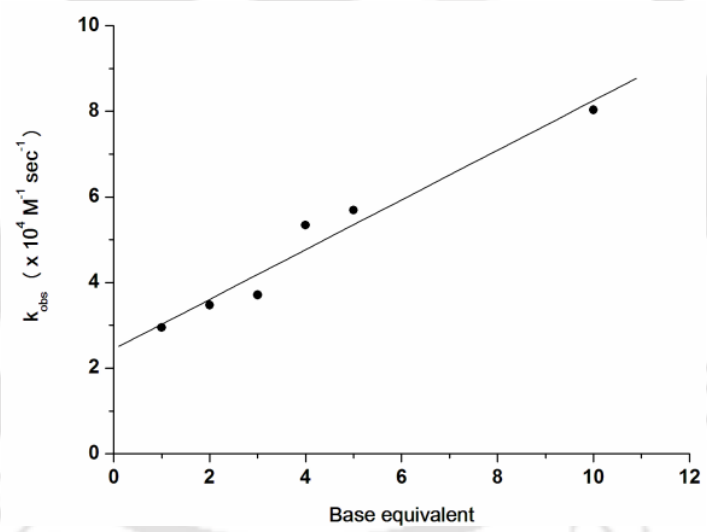

Figure A1.6 Plot of k_{obs} *vs.* equivalent of base added to a methanol/water (4:1) solution of complex **2.1** at 298K.

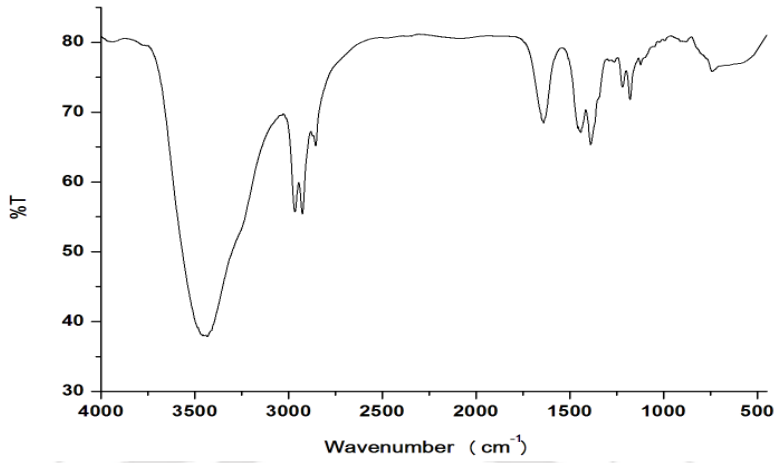

Figure A1.7 FT-IR spectrum of $\mathbf{L_1}'$ in KBr.

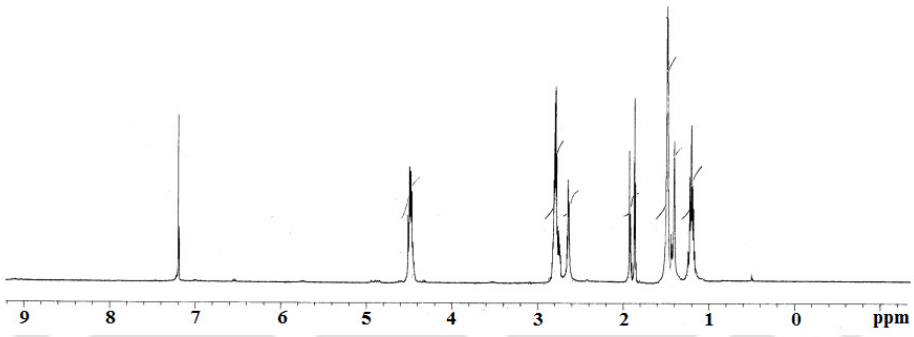

Figure A1.8 ^{1}H-NMR spectrum of $\mathbf{L_1}'$ in $CDCl_3$.

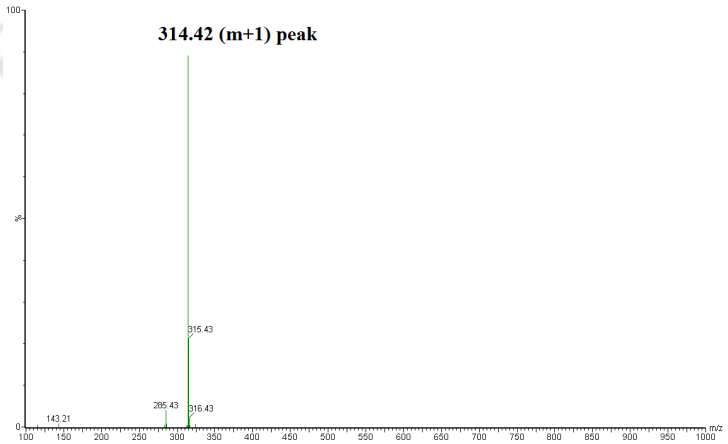

Figure A1.9 ESI-mass spectrum of $\mathbf{L_1}'$ in methanol.

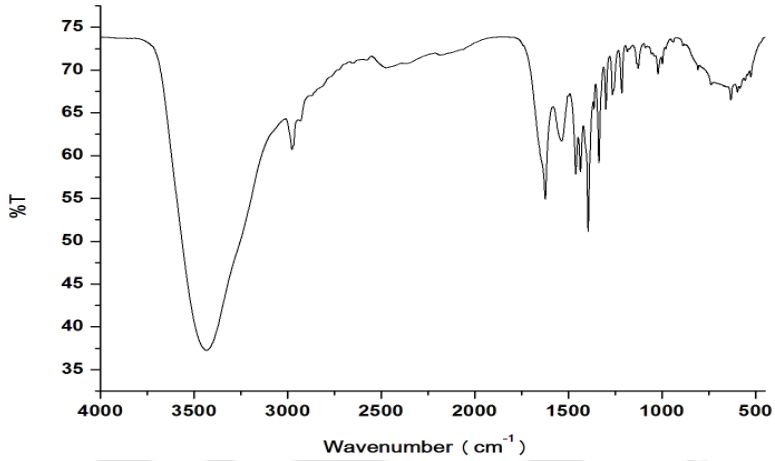

Figure A1.10 FT-IR spectrum of $\mathbf{L_2}$ in KBr.

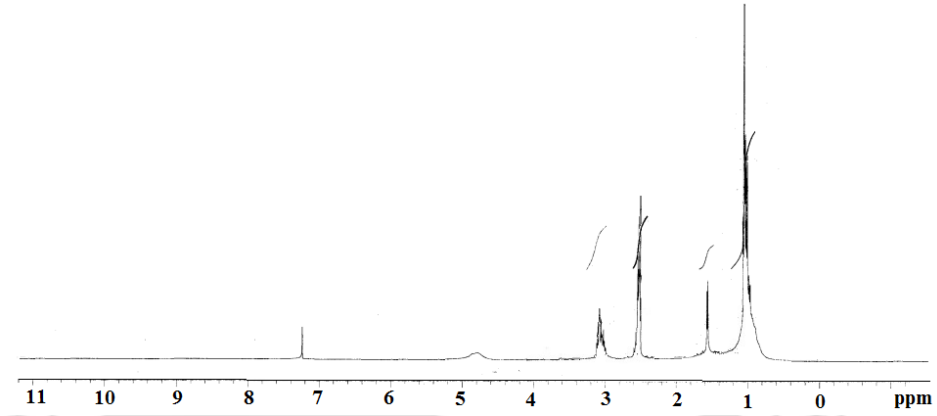

Figure A1.11 ^{1}H-NMR spectrum of $\mathbf{L_2}$ in $CDCl_3$.

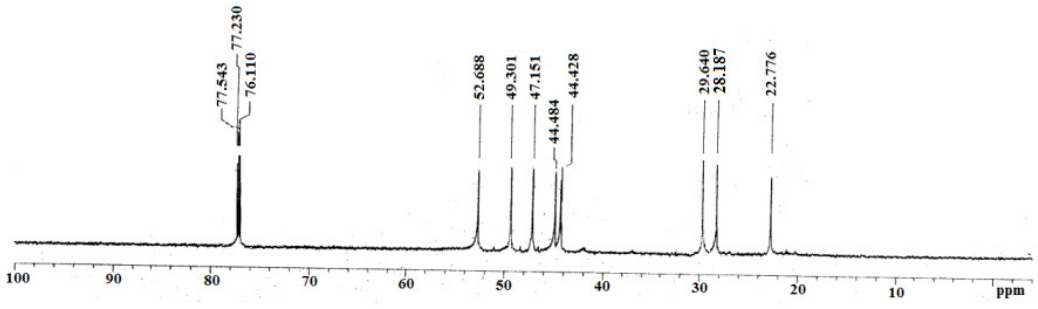

Figure A1.12 ^{13}C-NMR spectrum of $\mathbf{L_2}$ in $CDCl_3$.

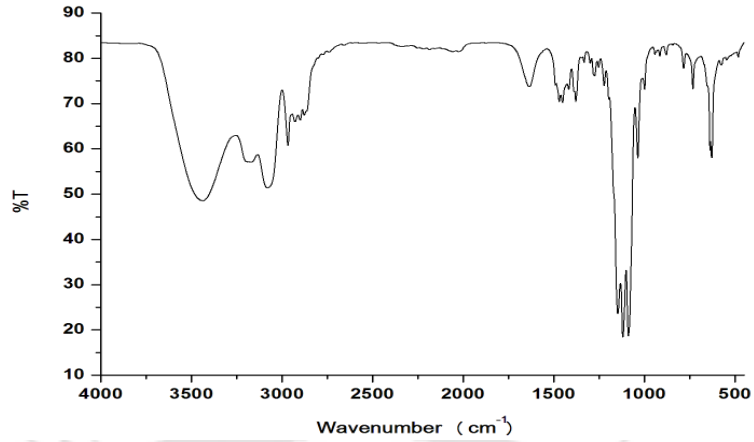

Figure A1.13 FT-IR spectrum of complex **2.2** in KBr.

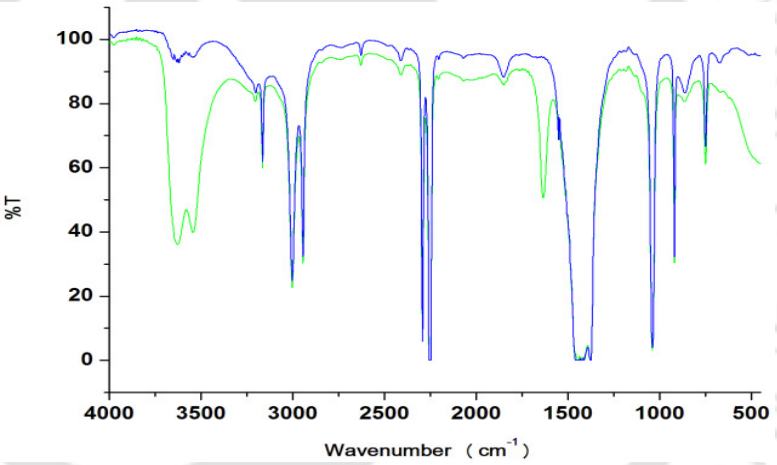

Figure A1.14 Solution FT-IR spectra of complex **2.2**(blue line) and after reaction with NO (green line) in acetonitrile solution at room temperature.

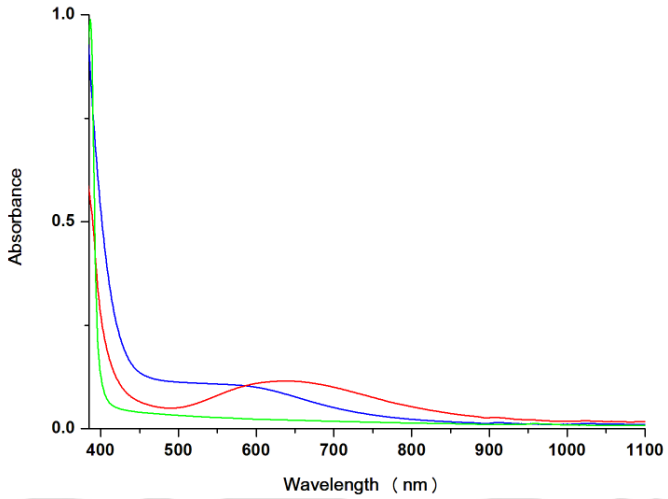

Figure A1.15 UV-visible spectra of the reaction of complex **2.2** (blue line) with NO in methanol solution at room temperature. Red and green line represent the [Cu^{II}-NO] intermediate and complete reduction to copper(I), respectively.

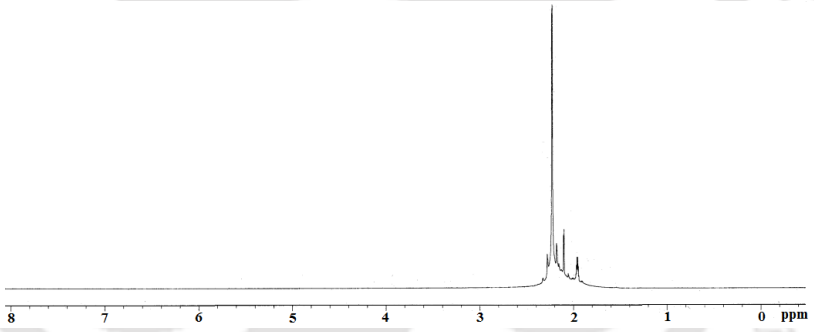

Figure A1.16 ^{1}H-NMR spectrum of complex **2.2** in CD_3CN.

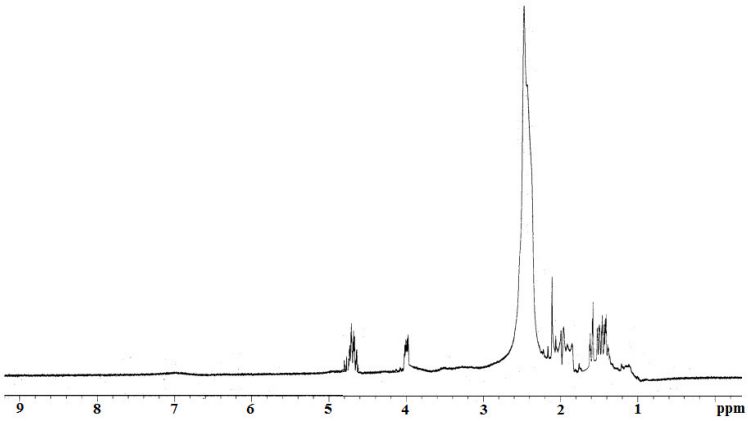

Figure A1.17 ^{1}H-NMR spectrum of complex **2.2** after purging NO in CD_3CN.

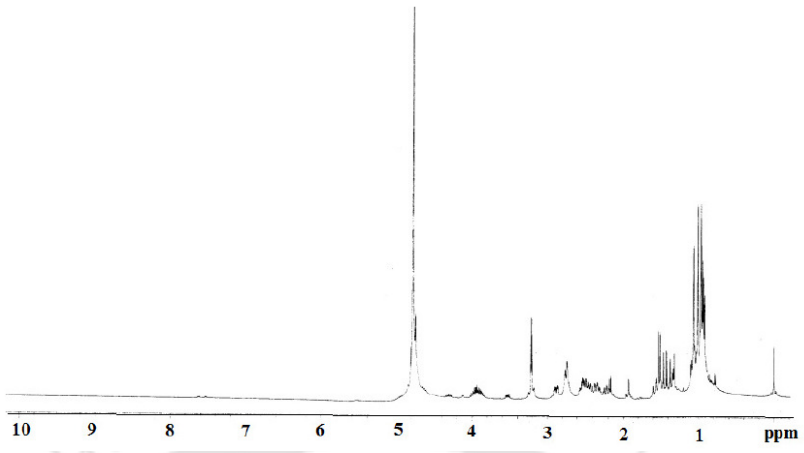

Figure A1.18 ^{1}H-NMR spectrum of the reaction mixture obtained from the reaction of complex **2.2** with NO in methanol.

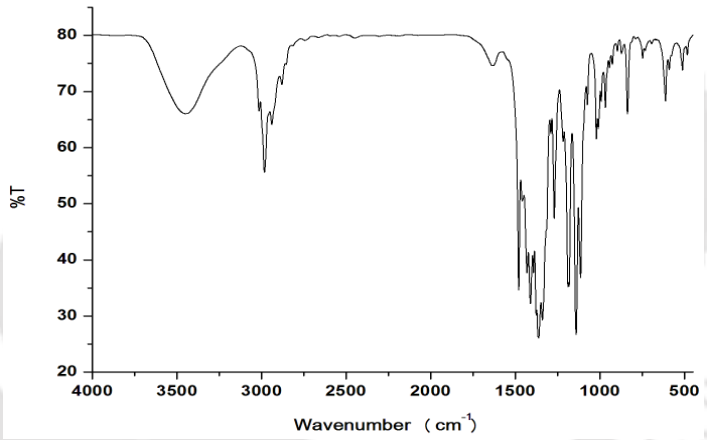

Figure A1.19 FT-IR spectrum of $\mathbf{L_2}'$ in KBr.

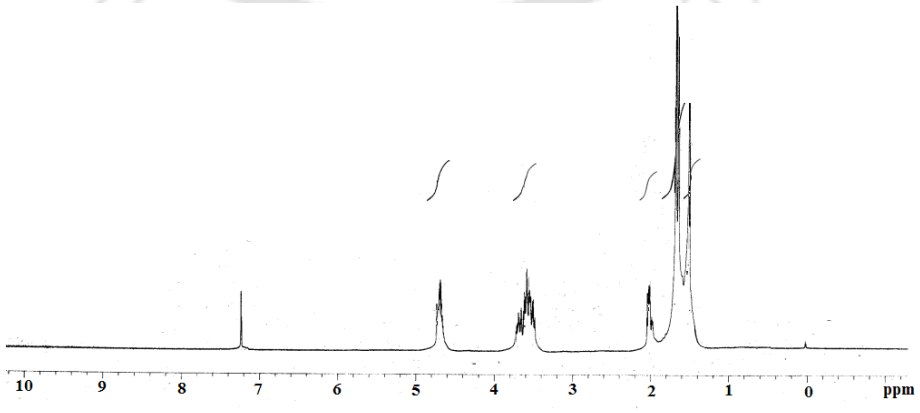

Figure A1.20 ^{1}H-NMR spectrum of $\mathbf{L_2}'$ in $CDCl_3$.

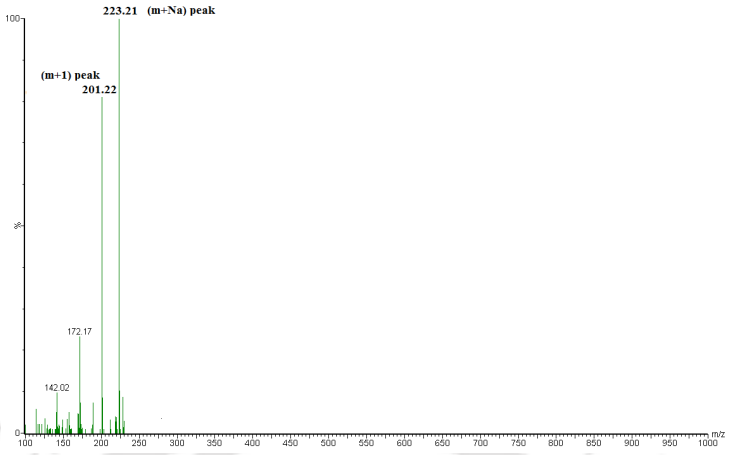

Figure A1.21 ESI-mass spectrum of $\mathbf{L_2}'$ in methanol.

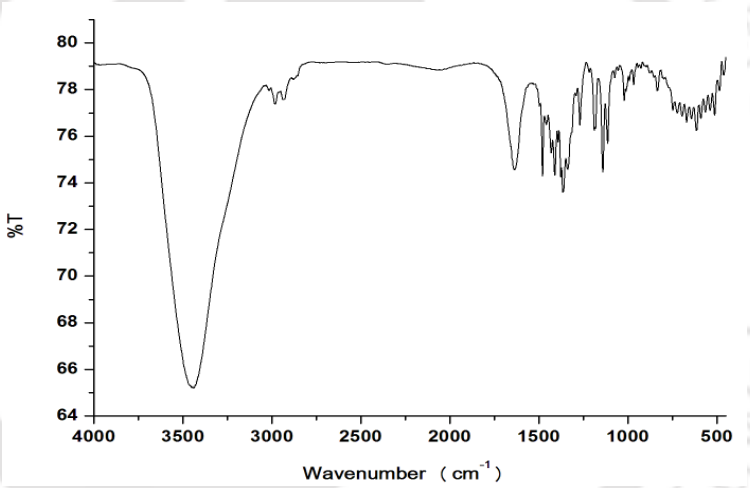

Figure A1.22 FT-IR spectrum of $\mathbf{L_2}''$ in KBr.

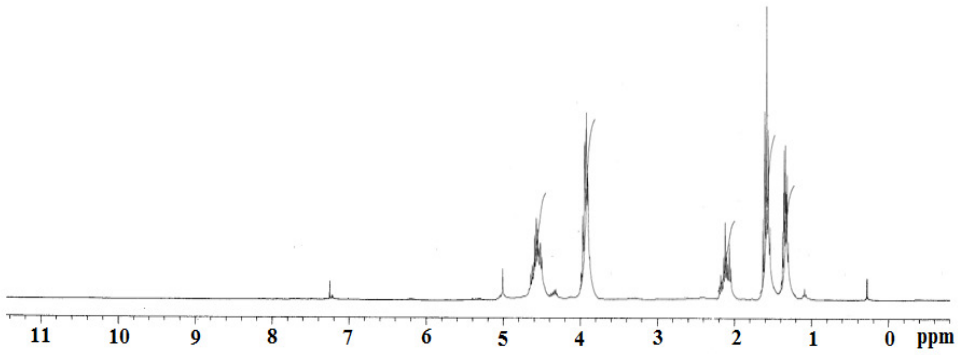

Figure A1.23 ^{1}H-NMR spectrum of $\mathbf{L_2}''$ in $CDCl_3$.

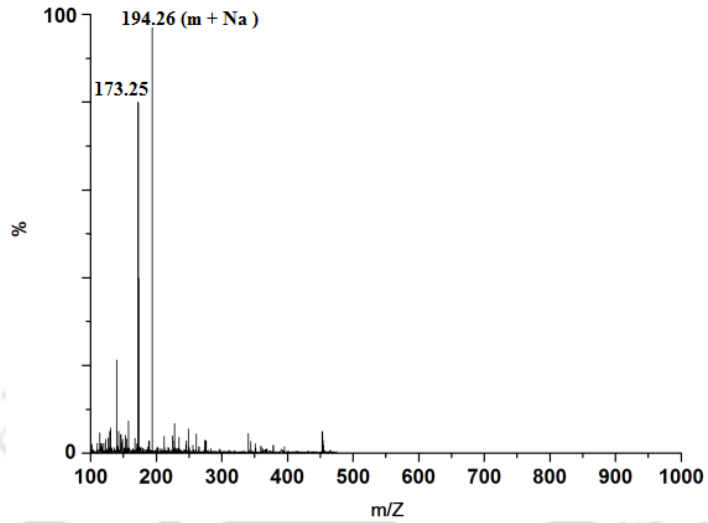

Figure A1.24 ESI-mass spectrum of $\mathbf{L_2}''$ in methanol.

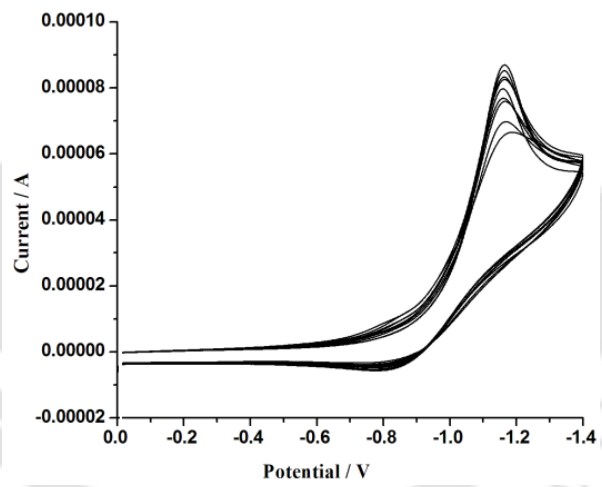

Figure A1.25 Cyclic voltammogram (multiple scan) of complex **2.1** in acetonitrile solvent. Working electrode, Pt; Reference electrode, Ag/Ag^{+}; TBAP supporting electrolyte; scan rate 50 mV/s.

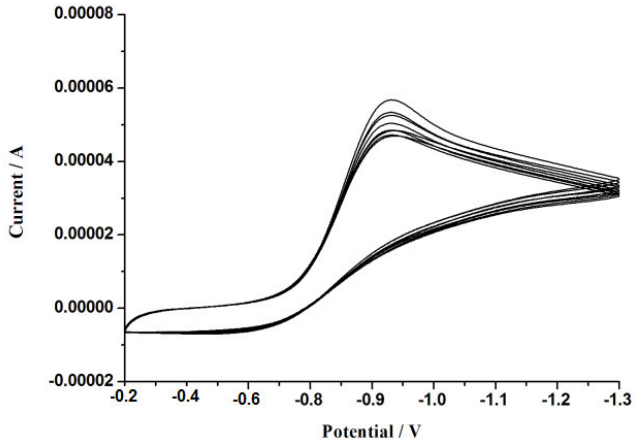

Figure A1.26 Cyclic voltammogram (multiple scan) of complex **2.2** in acetonitrile solvent. Working electrode, Pt; Reference electrode, Ag/Ag^{+}; TBAP supporting electrolyte; scan rate 50 mV/s.

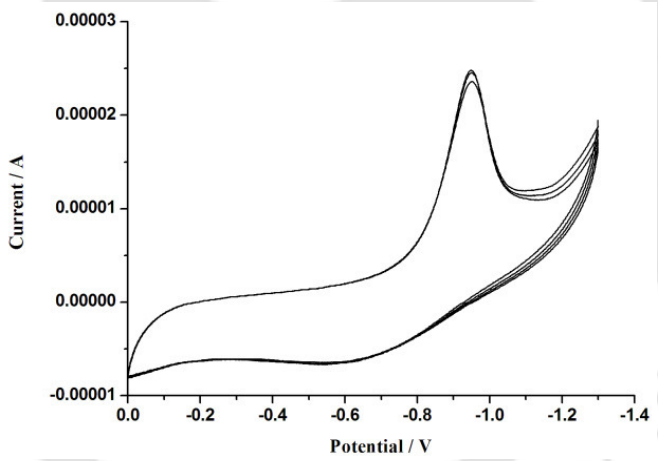

Figure A1.27 Cyclic voltammogram (multiple scan) of complex **2.1** after addition of one equivalent of sodium methoxide in acetonitrile solvent. Working electrode, Pt; Reference electrode, Ag/Ag^{+}; TBAP supporting electrolyte; scan rate 50 mV/s.

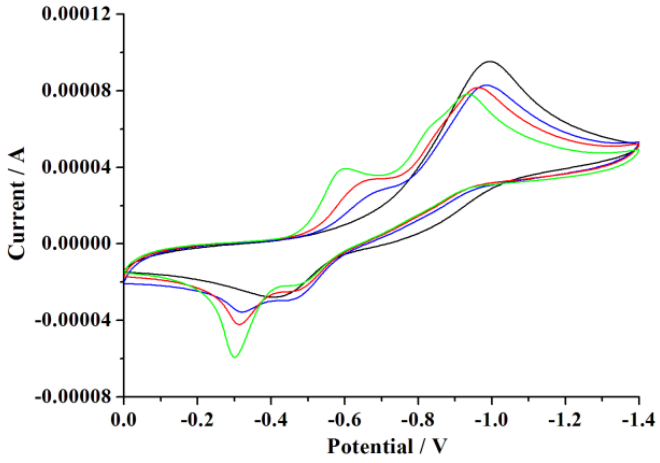

Figure A1.28 Cyclic voltammograms of complex **2.1** in acetonitrile at (i) 20 mV/s (green), (ii) 30 mV/s (red); (iii) 40 mV/s (blue) and (iv) 50 mV/s scan rates. Working electrode, Pt; Reference electrode, Ag/Ag^{+}; TBAP supporting electrolyte.

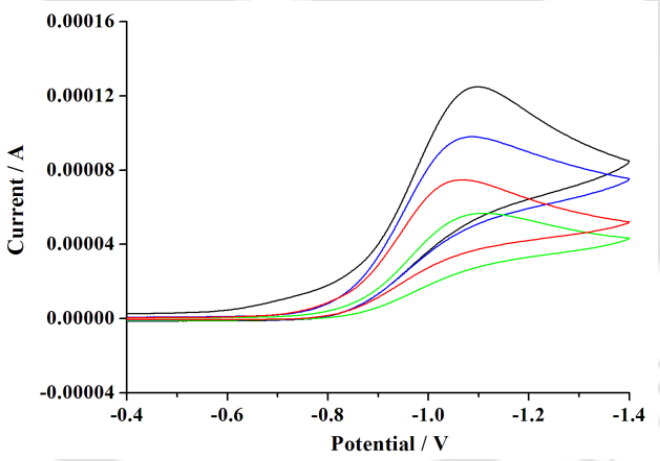

Figure A1.29 Cyclic voltammograms of complex **2.2** in acetonitrile at (i) 20 mV/s (green), (ii) 30 mV/s (red); (iii) 40 mV/s (blue) and (iv) 50 mV/s scan rates. Working electrode, Pt; Reference lectrode, SCE; TBAP supporting electrolyte.

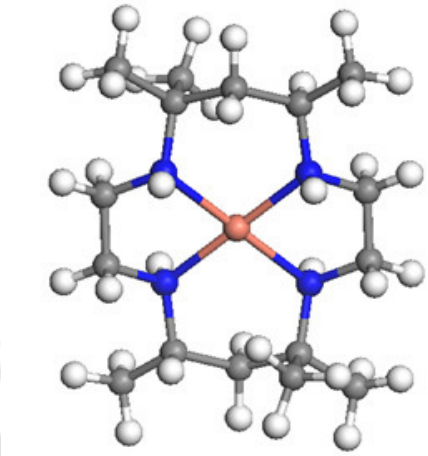

Figure A1.30 DFT optimized structure of complex **2.1**.

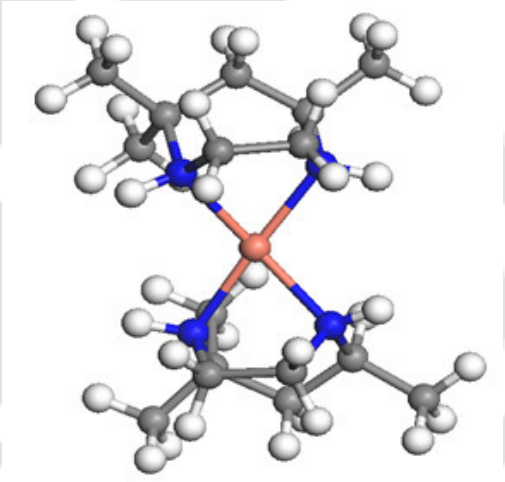

Figure A1.31 DFT optimized structure of complex **2.2**.

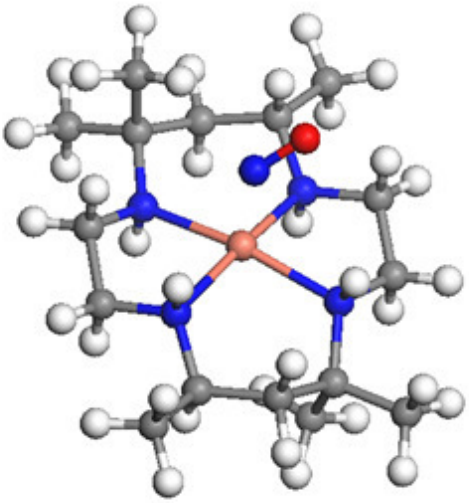

Figure A1.32 DFT optimized structure of [Cu^{II}-NO] from complex **2.1**.

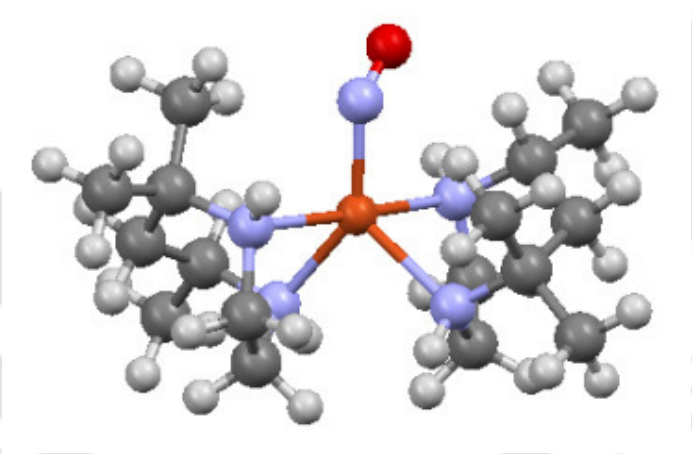

Figure A1.33 DFT optimized structure of [Cu^{II}-NO] from complex **2.2**.

Appendix II

Table A2.1 Crystallographic data for complexes **3.1** and **3.3**.

	Complex **3.1**	Complex **3.3**
Formulae	C_{30} H_{42} Cl_2 Cu N_{10} O_8	C_{26} H_{36} Cu N_9 O_6
Mol. wt.	805.19	634.19
Crystal system	Triclinic	Monoclinic
Space group	P -1	P 2/c
Temperature /K	296(2)	293(2)
Wavelength /Å	0.71073	0.71073
a /Å	9.3488(6)	9.4710(2)
b /Å	11.1223(7)	9.4545(2)
c /Å	18.8929(11)	18.3295(5)
α/°	77.839(3)	90.00
β/°	86.532(3)	90.0540(10)
γ/°	82.881(3)	90.00
V/ $Å^3$	1904.4(2)	1641.29(7)
Z	2	2
Density/Mgm^{-3}	1.404	1.283
Abs. Coeff. /mm^{-1}	0.773	0.716
Abs. correction	None	None
F(000)	838	664.0
Total no. of reflections	9262	4113
Reflections, $I > 2\sigma(I)$	6429	3330
Max. 2θ/°	28.32	28.38
Ranges (h, k, l)	-12≤ h ≤12 -14≤ k ≤14 -24≤ l ≤24	-12≤ h ≤12 -12≤ k ≤12 -24≤ l ≤ 24
Complete to 2θ (%)	97.5	99.8
Refinement method	Full-matrix least-squares on F^2	Full-matrix least-squares on F^2
Goof (F^2)	1.039	1.100
R indices [$I > 2\sigma(I)$]	0.0576	0.0582
R indices (all data)	0.0847	0.0674

Table A2.2 Selected bond lengths (Å) for complexes **3.1** and **3.2**.

	Complex **3.1**	Complex **3.3**
Cu(1)-N(1)	2.035(2)	1.984(2)
Cu(1)-N(3)	1.995(3)	2.148(2)
Cu(1)-O(1)	-	2.353(3)
C(2)-C(1)	1.484(7)	1.530(5)
C(2)-C(3)	1.495(5)	1.488(4)
C(3)-N(1)	1.328(4)	1.329(3)
C(3)-N(2)	1.351(4)	1.353(4)
C(4)-N(2)	1.379(4)	1.380(4)
C(6)-N(1)	1.397(4)	1.401(3)
C(4)-C(5)	1.490(4)	1.507(5)
C(4)-C(6)	1.358(4)	1.340(4)
C(7)-C(6)	1.489(5)	1.486(4)
C(7)-C(8)	1.490(5)	1.501(4)
N(9)-O(1)	-	1.263(4)
C(9)-C(10)	1.493(5)	1.482(5)
C(11)-C(12)	1.489(5)	1.500(4)
C(12)-C(13)	1.49(1)	1.514(6)

Table A2.3 Selected bond angles (°) for complexes **3.1** and **3.2**.

	Complex **3.1**	Complex **3.3**
N(1)-Cu(1)-N(3)	86.7(1)	89.15(9)
Cu(1)-N(1)- C(3)	133.4(2)	129.4(2)
Cu(1)-N(1)- C(6)	119.7(2)	124.5(2)
Cu(1)-N(3)- C(8)	121.0(2)	120.0(2)
Cu(1)-N(3)- C(11)	131.5(2)	132.0(2)
C(1)-C(2)-C(3)	114.1(4)	113.5(3)
N(2)-C(3)-N(1)	109.2(3)	110.1(2)
C(3)-N(2)-C(4)	109.3(3)	107.9(3)
C(3)-N(1)-C(6)	106.9(3)	106.0(2)
C(5)- C(4)-C(6)	132.4(3)	132.3(3)
C(4)-C(6)-C(7)	130.8(3)	130.8(2)
C(6)-C(7)-C(8)	109.3(3)	111.9(2)
C(8)-C(9)-C(10)	132.0(3)	132.2(3)
C(8)-N(3)-C(11)	107.0(3)	106.0(2)
C(12)-C(11)-N(3)	128.3(3)	127.4(3)
C(11)-C(12)-C(13)	113.8(4)	114.6(3)

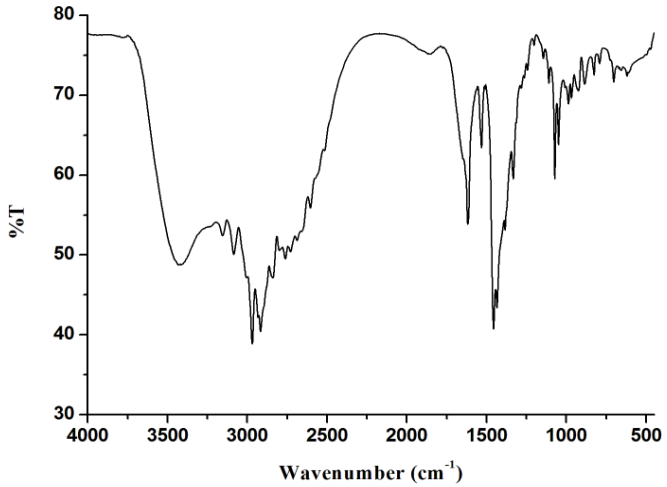

Figure A2.1 FT-IR spectrum of $\mathbf{L_3}$ in KBr.

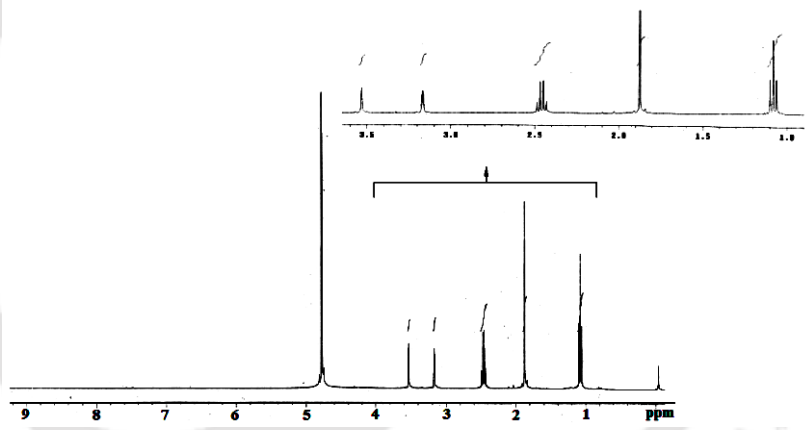

Figure A2.2 ^{1}H-NMR spectrum of $\mathbf{L_3}$ in methanol-d_4.

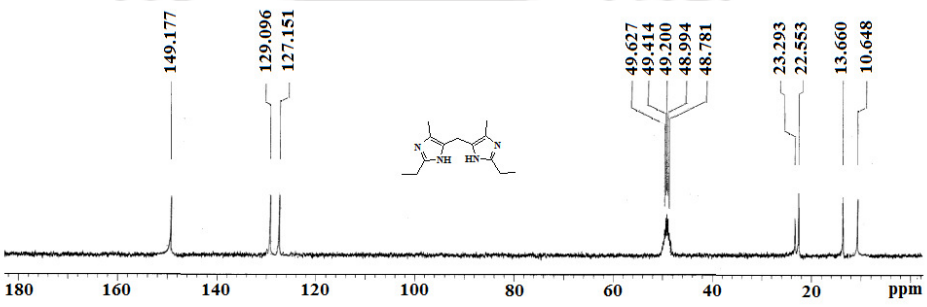

Figure A2.3 ^{13}C-NMR spectrum of $\mathbf{L_3}$ in methanol-d_4.

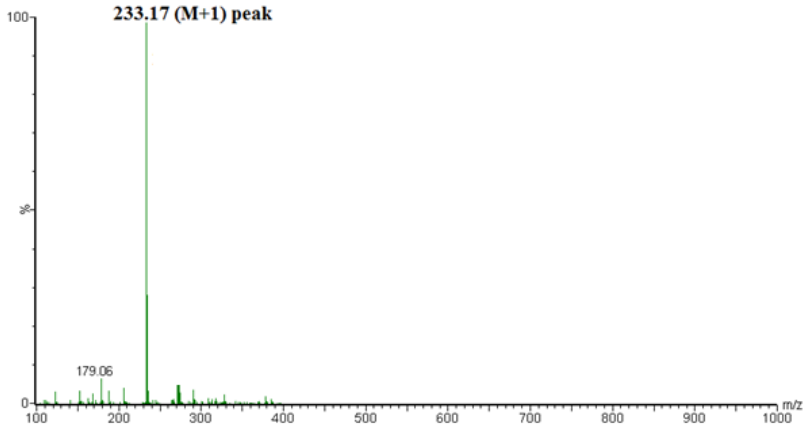

Figure A2.4 ESI-mass spectrum of $\mathbf{L_3}$ in methanol.

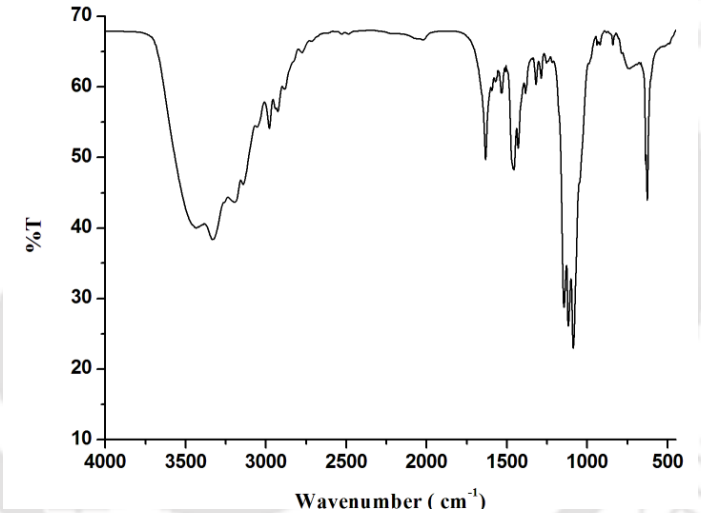

Figure A2.5 FT-IR spectrum of complex **3.1** in KBr.

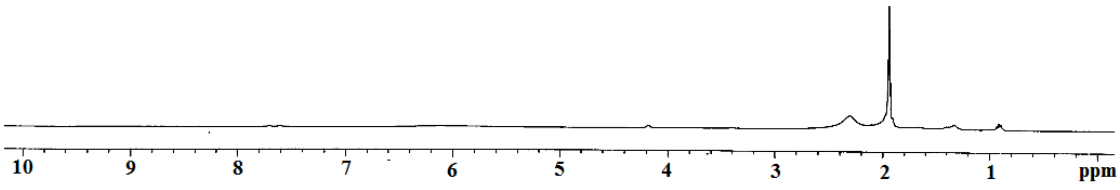

Figure A2.6 ^{1}H-NMR spectrum of complex **3.1** in CD_3CN.

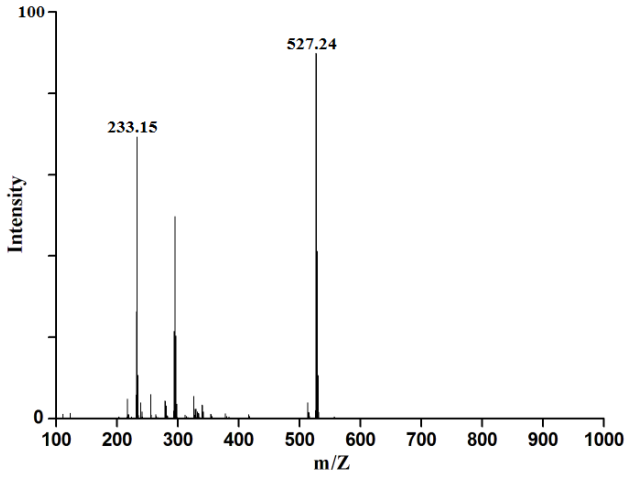

Figure A2.7 ESI-Mass spectrum of complex **3.1** in methanol.

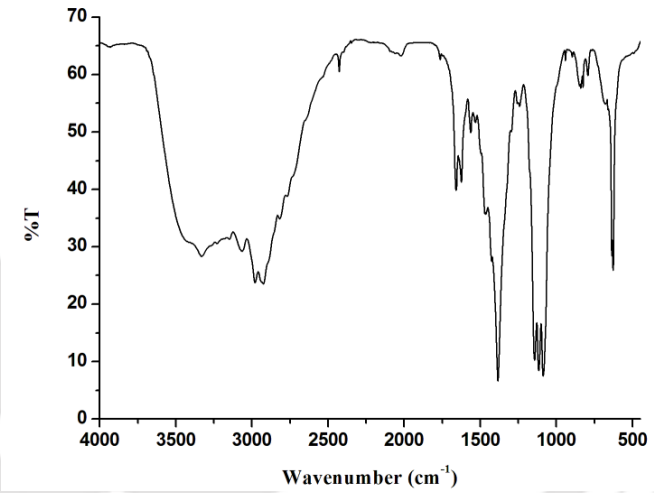

Figure A2.8 FT-IR spectrum of complex **3.2** in KBr.

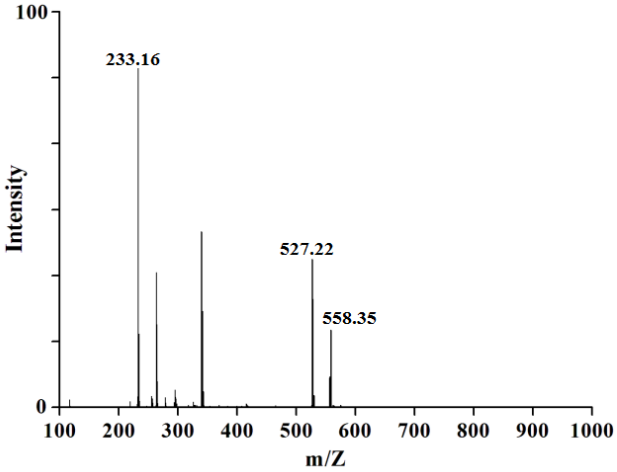

Figure A2.9 ESI-Mass spectrum of ^{15}NO labeled complex **3.2** in methanol.

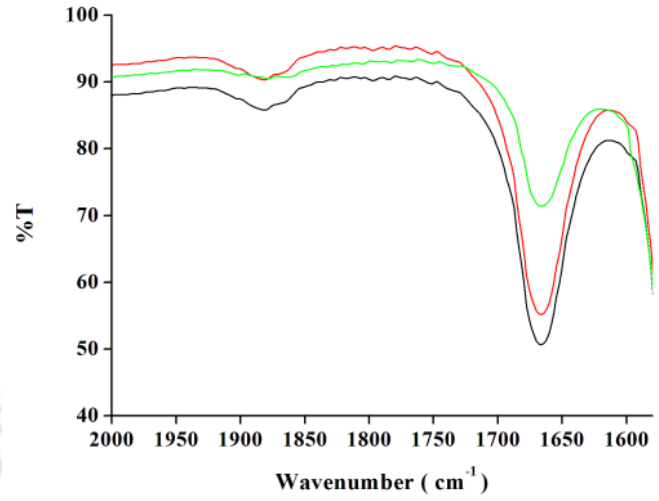

Figure A2.10 FT-IR spectra of complex **3.2** in acetonitrile solution before (black) and after applying vacuum [at 5 minutes (red) and 15 minutes (green)].

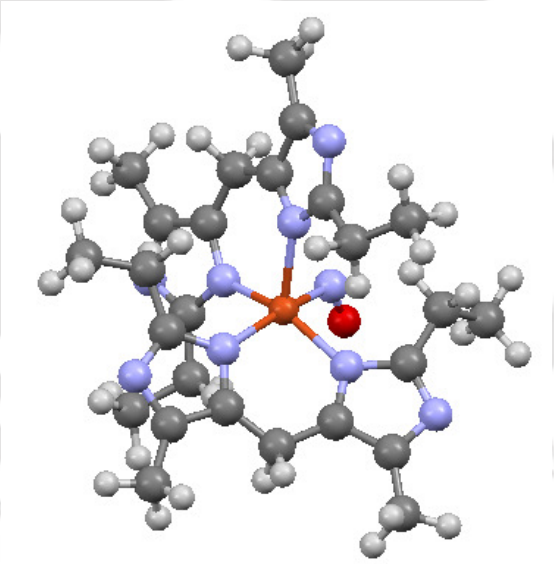

Figure A2.11 DFT optimized structure of complex **3.2**.

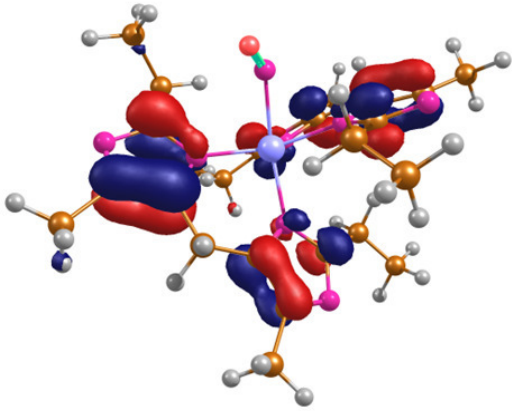

Figure A2.12 HOMO of complex **3.2**.

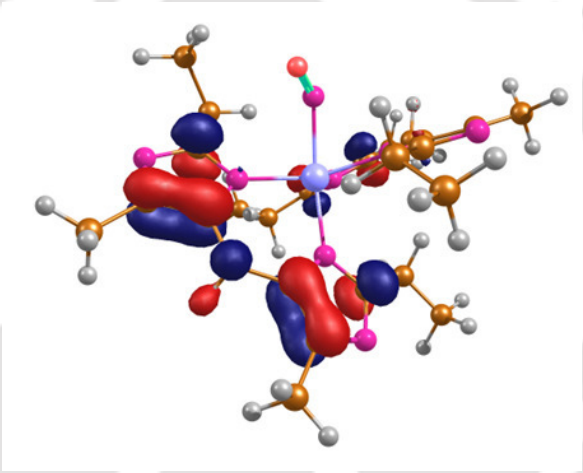

Figure A2.13 LUMO of complex **3.2**.

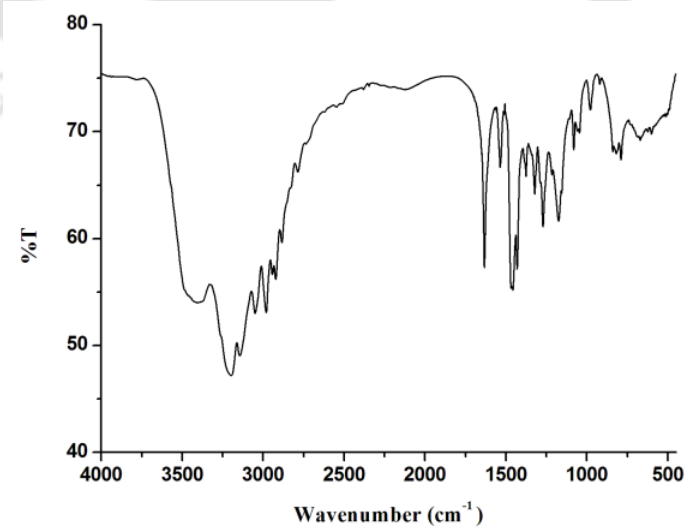

Figure A2.14 FT-IR spectrum of complex **3.3** in KBr.

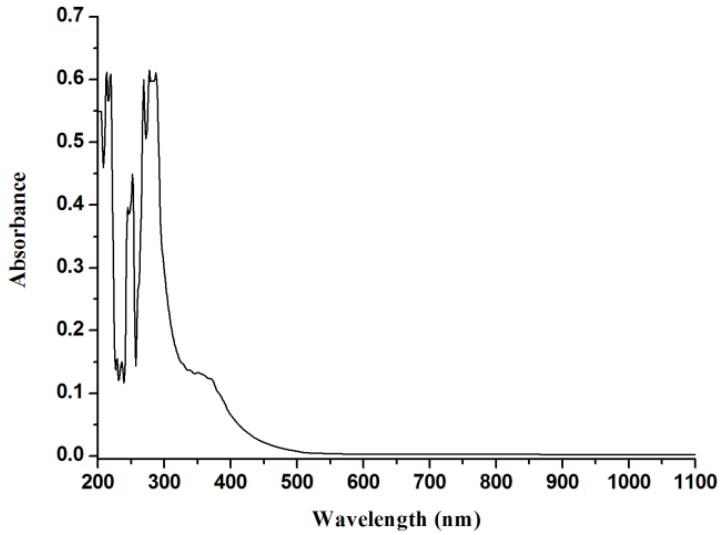

Figure A2.15 UV-visible spectrum of complex **3.3** in acetonitrile solvent at room temperature.

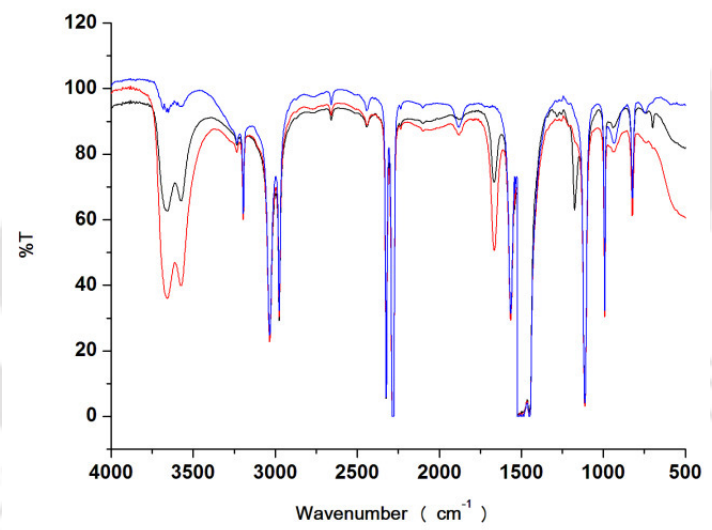

Figure A2.16 Solution FT-IR spectra of complex **3.2** (red line) and after reaction with water in acetonitrile solvent at room temperature.

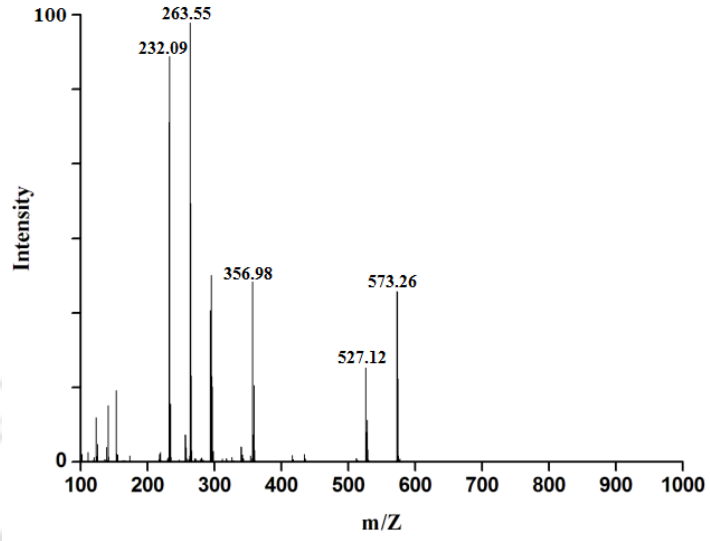

Figure A2.17 ESI-mass spectrum of complex **3.3** obtained from the reaction of complex **3.2** and water in acetonitrile.

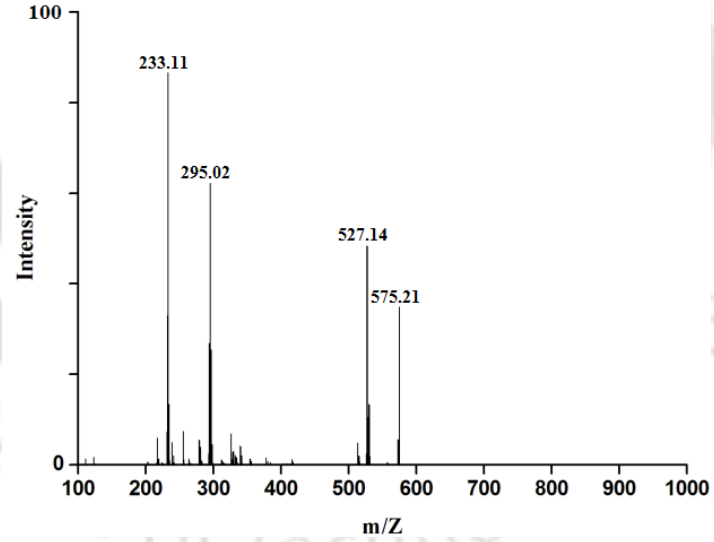

Figure A2.18 ESI-mass spectrum of complex **3.3** obtained from the reaction of complex **3.2** and water (^{18}O-lebeled) in acetonitrile.

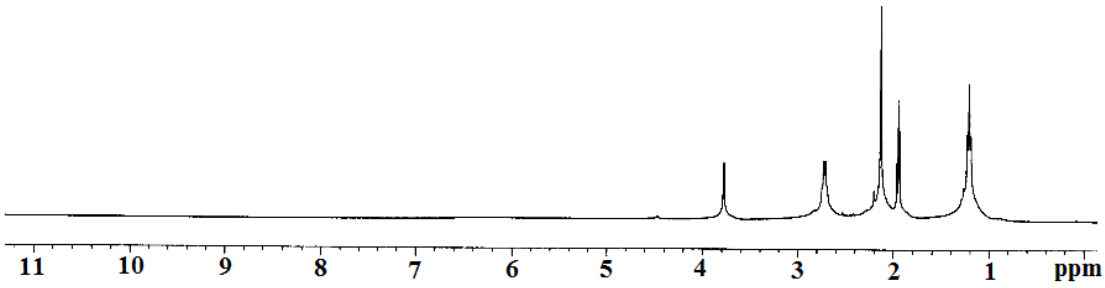

Figure A2.19 ^{1}H-NMR spectrum of complex **3.3** in CD_3CN.

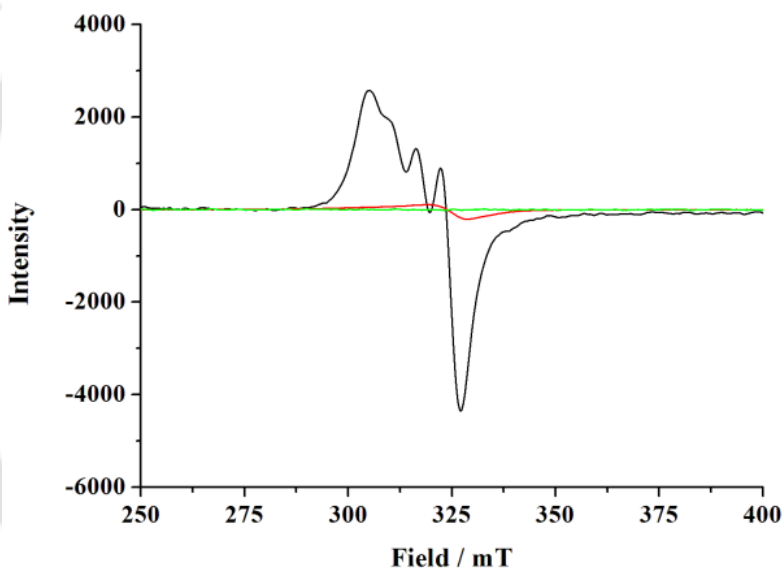

Figure A2.20 X-band EPR spectra of the complex **3.1** (black trace), complex **3.2** (red trace) and after reaction with water (green trace) in acetonitrile at room temperature.

Appendix III

Table A3.1 Crystallographic data for complexes **4.1** and **4.2**.

	Complex **4.1**	Complex **4.2**
Formulae	$C_{26}H_{36}CuN_9O_7$	$C_{26}H_{36}ClCuN_9O_7$
Mol. wt.	650.19	685.64
Crystal system	Monoclinic	Monoclinic
Space group	P 2/c	P 21/c
Temperature /K	296(2)	293(2)
Wavelength /Å	0.71073	0.71073
a /Å	9.3665(10)	19.5792(16)
b /Å	9.6913(11)	9.3484(8)
c /Å	18.1622(18)	18.7219(16)
α/°	90.00	90.00
β/°	90.203(5)	102.510(5)
γ /°	90.00	90.00
V/ Å^3	1648.6(3)	3345.4(5)
Z	2	4
Density/Mgm^{-3}	1.310	1.361
Abs. Coeff. /mm^{-1}	0.716	0.787
Abs. correction	None	None
F(000)	680.0	1428
Total no. of reflections	7344	8345
Reflections, $I > 2\sigma(I)$	5057	3561
Max. 2θ/°	35.54	28.44
Ranges (h, k, l)	-14≤ h ≤15 -15≤ k ≤14 -29≤ l ≤ 29	-26≤ h ≤23 -12≤ k ≤12 -25≤ l ≤ 20
Complete to 2θ (%)	97.3	98.9
Refinement method	Full-matrix least-squares on F^2	Full-matrix least-squares on F^2
Goof (F^2)	1.071	1.055
R indices [$I > 2\sigma(I)$]	0.0664	0.0847
R indices (all data)	0.0838	0.1617

Table A3.2 Selected bond lengths (Å) for complexes **4.1** and **4.2**.

	Complex **4.1**	Complex **4.2**
Cu(1)-N(1)	2.122(2)	1.985(5)
Cu(1)-N(3)	1.984(2)	2.052(6)
Cu(1)-O(1)	2.386(3)	2.208(6)
Cu(1)-O(2)	-	2.637(8)
C(2)-C(1)	1.509(5)	1.49(1)
C(2)-C(3)	1.494(3)	1.49(1)
C(3)-N(1)	1.322(3)	1.332(8)
C(3)-N(2)	1.354(3)	1.333(8)
C(4)-N(2)	1.384(3)	1.386(9)
C(6)-N(1)	1.395(3)	1.401(8)
C(4)-C(5)	1.485(4)	1.47(1)
C(4)-C(6)	1.358(3)	1.35(1)
C(7)-C(6)	1.496(3)	1.494(9)
C(7)-C(8)	1.486(3)	1.49(1)
N(9)-O(1)	-	1.24(1)
C(9)-C(10)	1.497(3)	1.48(1)
C(11)-C(12)	1.490(3)	1.50(1)
C(12)-C(13)	1.504(4)	1.44(3)

Table: A3.3 Selected bond angles (°) for complexes **4.1** and **4.2**.

	Complex **4.1**	Complex **4.2**
N(1)-Cu(1)-N(3)	90.24(7)	90.2(2)
Cu(1)-N(1)- C(3)	130.4(1)	130.7(4)
Cu(1)-N(1)- C(6)	120.0(1)	123.7(4)
Cu(1)-N(3)- C(8)	124.2(1)	123.3(5)
Cu(1)-N(3)- C(11)	129.3(1)	130.4(5)
N(1)-Cu(1)-O(1)	104.87(7)	87.5(2)
N(3)-Cu(1)-O(1)	84.71(7)	161.3(2)
C(1)-C(2)-C(3)	114.2(2)	115.3(7)
N(2)-C(3)-N(1)	110.0(2)	110.5(6)
C(3)-N(2)-C(4)	108.5(2)	109.0(6)
C(3)-N(1)-C(6)	106.7(2)	105.5(6)
C(5)- C(4)-C(6)	131.6(2)	133.2(7)
C(4)-C(6)-C(7)	130.3(2)	130.7(7)
C(6)-C(7)-C(8)	111.7(2)	114.2(6)
C(8)-C(9)-C(10)	132.5(2)	132.2(7)
C(8)-N(3)-C(11)	106.5(2)	105.9(6)
C(12)-C(11)-N(3)	127.4(2)	127.4(8)

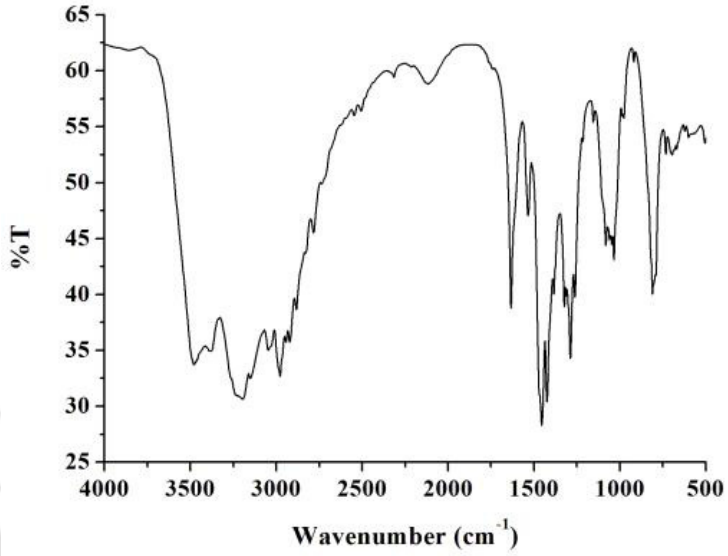

Figure A3.1 FT-IR spectrum of complex **4.1** in KBr.

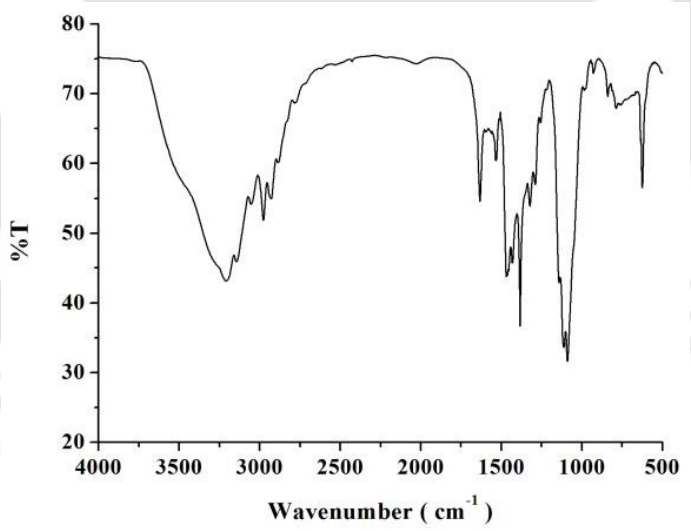

Figure A3.2 FT-IR spectrum of complex **4.2** in KBr.

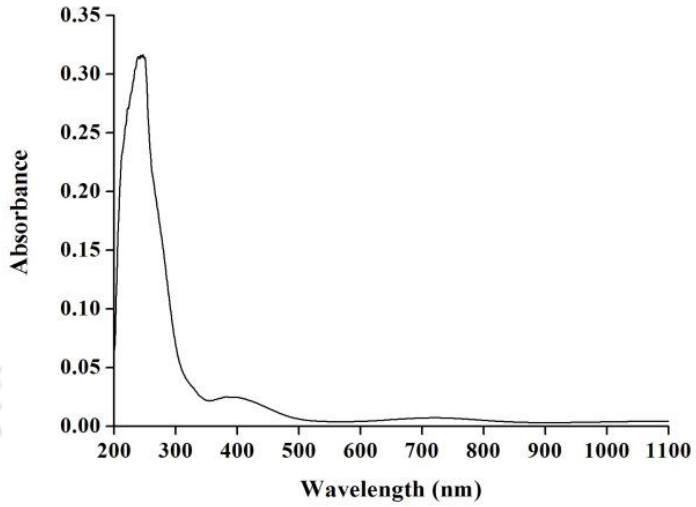

Figure A3.3 UV-visible spectrum of complex **4.2** in acetonitrile.

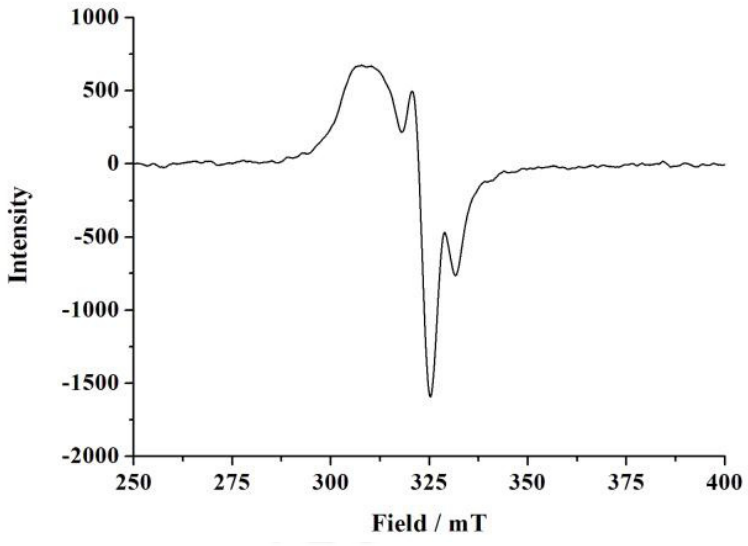

Figure A3.4 X-band EPR spectra of the complex **4.2** in acetonitrile solvent at room temperature.

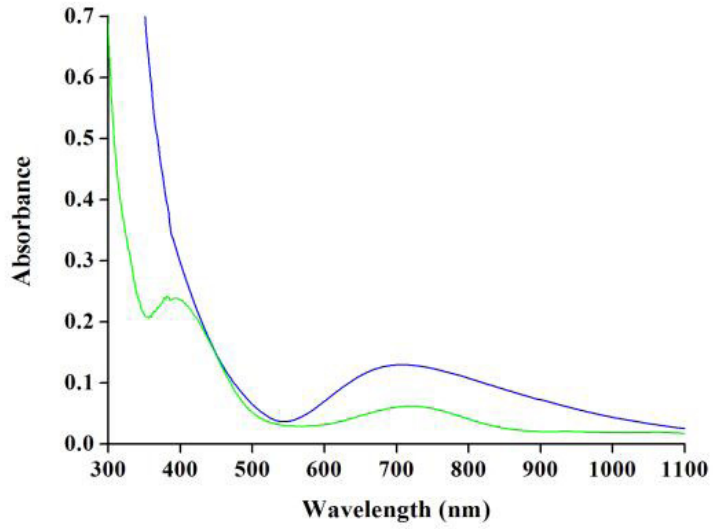

Figure A3.5 UV-visible spectra of complex **3.2** (blue) and after addition of one equivalent of KO_2 (green) in acetonitrile.

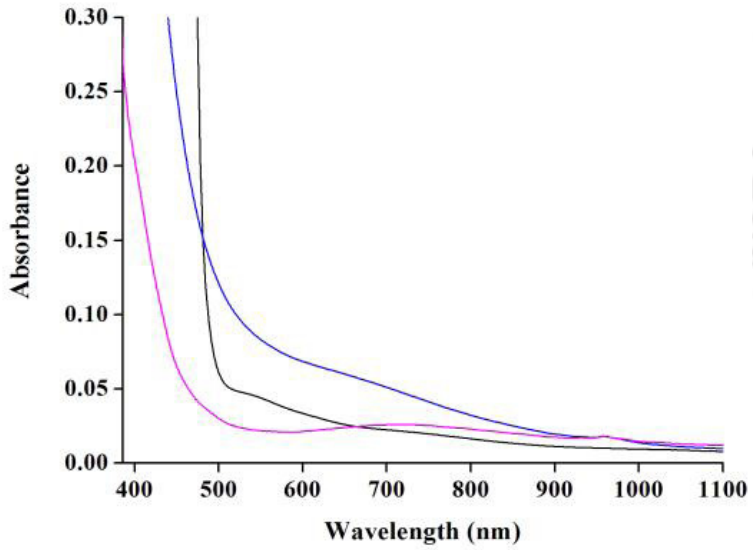

Figure A3.6 UV-visible spectra of complex **3.1** (black), after addition of one equivalent of H_2O_2 (blue) and after addition of NO to the above mixture (pink) in acetonitrile.

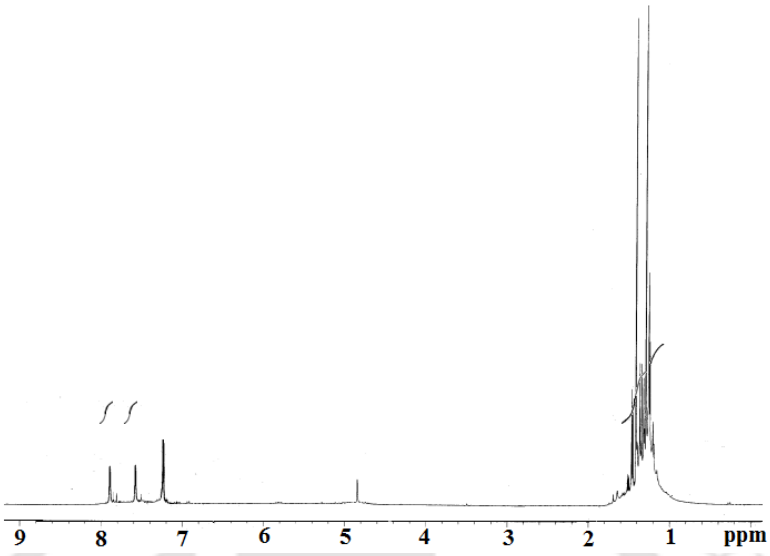

Figure A3.7 ^{1}H-NMR spectrum of 2, 4-di-*tertiary*-butyl-6-nitrophenol in $CDCl_3$.

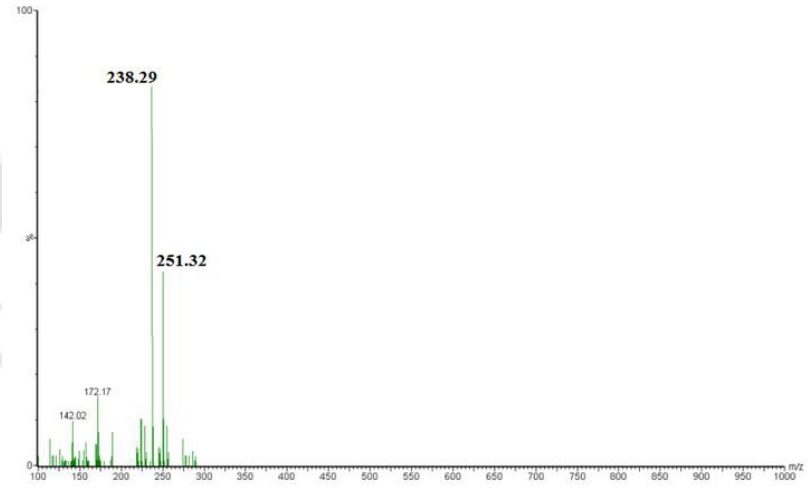

Figure A3.8 ESI-Mass spectrum of 2, 4-di-*tertiary*-butyl-6-nitrophenol in methanol.

Appendix IV

Table A4.1 Crystallographic data for complex **5.1**.

	Complex **5.1**
Formulae	C_{17} H_{23} Cl Cu N_4 O_9
Mol. wt.	526.39
Crystal system	Triclinic
Space group	P -1
Temperature /K	293(2)
Wavelength /Å	0.71073
a /Å	9.8228(2)
b /Å	10.2640(2)
c /Å	11.3496(2)
α/°	89.6260(10)
β/°	82.1540(10)
γ/°	76.9530(10)
V/ $Å^3$	1103.96(4)
Z	2
Density/Mgm^{-3}	1.584
Abs. Coeff. /mm^{-1}	1.166
Abs. correction	None
F(000)	542
Total no. of reflections	5436
Reflections, $I > 2\sigma(I)$	4770
Max. 2θ/°	28.37
Ranges (h, k, l)	$-13 \leq h \leq 13$ $-13 \leq k \leq 13$ $-15 \leq l \leq 15$
Complete to 2θ (%)	98.3
Refinement method	Full-matrix least-squares on F^2
Goof (F^2)	1.086
R indices [$I > 2\sigma(I)$]	0.0454
R indices (all data)	0.0500

Table A4.2 Selected bond lengths (Å) for complex **5.1**.

	Complex **5.1**
Cu(1)-N(1)	2.027(2)
Cu(1)-N(2)	1.956(2)
Cu(1)-O(1)	1.963(1)
Cu(1)-O(2)	2.546(2)
Cu(1)-O(3)	2.530(2)
C(2)-C(1)	1.394(3)
C(4)-C(5)	1.388(4)
C(6)-C(7)	1.498(3)
C(1)-O(1)	1.354(3)
C(7)-N(1)	1.491(3)
C(8)-N(1)	1.477(2)
C(9)-O(3)	1.209(3)
C(9)-O(4)	1.322(3)
C(10)-O(4)	1.447(5)
C(12)-N(2)	1.394(3)
C(13)-N(3)	1.363(3)

Table A4.3 Selected bond angles (°) for complex **5.1**.

	Complex **5.1**
N(1)-Cu(1)-N(2)	90.53(7)
N(1)-Cu(1)-O(1)	93.33(7)
N(1)-Cu(1)-O(2)	104.14(7)
N(1)-Cu(1)-O(3)	73.35(7)
O(2)-Cu(1)-O(3)	177.07(6)
O(1)-Cu(1)-N(2)	171.10(7)
C(1)-C(2)-C(3)	120.1(2)
C(1)-C(6)-C(7)	119.0(2)
C(7)-N(1)-C(8)	111.0(2)
C(11)- C(12)-C(13)	127.9(2)
Cu(1)-N(2)-C(14)	125.9(2)
Cu(1)-O(1)-C(7)	111.7(1)

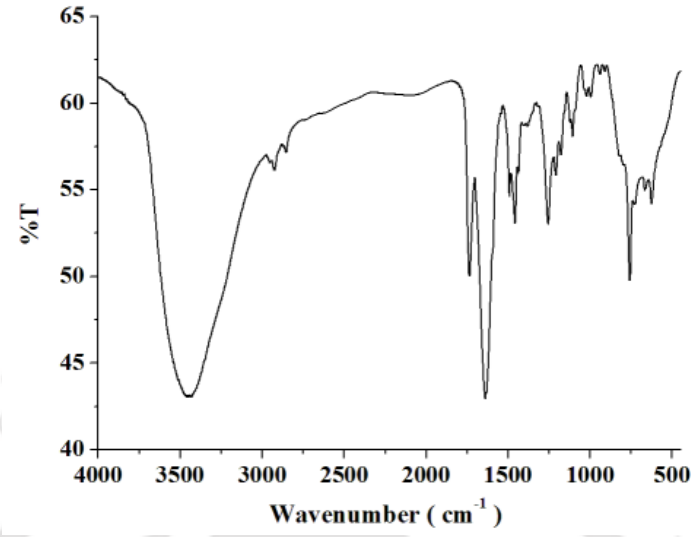

Figure A4.1 FT-IR spectrum of $\mathbf{L_4}$ in KBr.

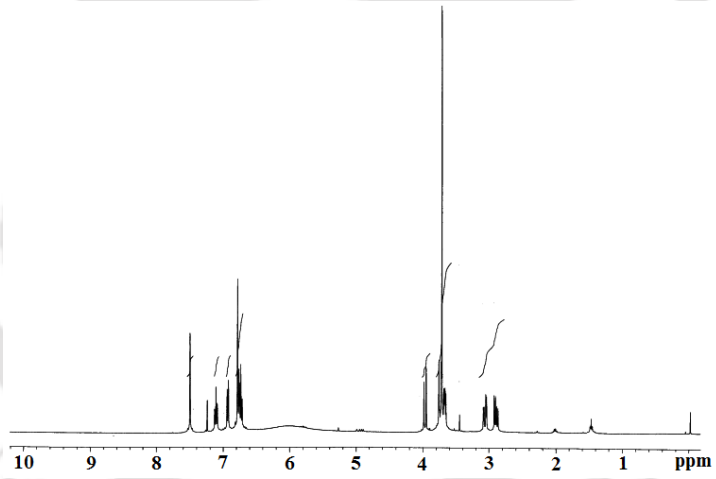

Figure A4.2 ^{1}H-NMR spectrum of $\mathbf{L_4}$ in $CDCl_3$.

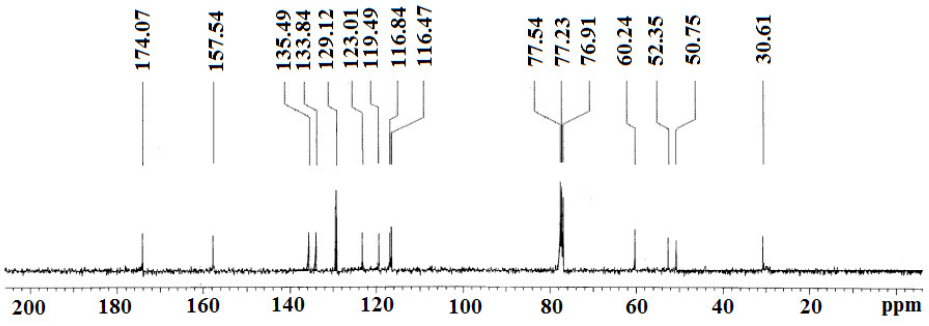

Figure A4.3 ^{13}C-NMR spectrum of $\mathbf{L_4}$ in $CDCl_3$.

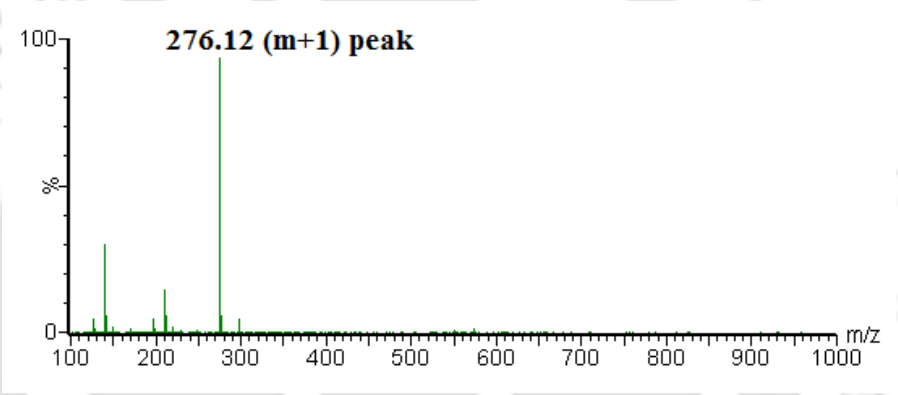

Figure A4.4 ESI-mass spectrum of $\mathbf{L_4}$ in methanol.

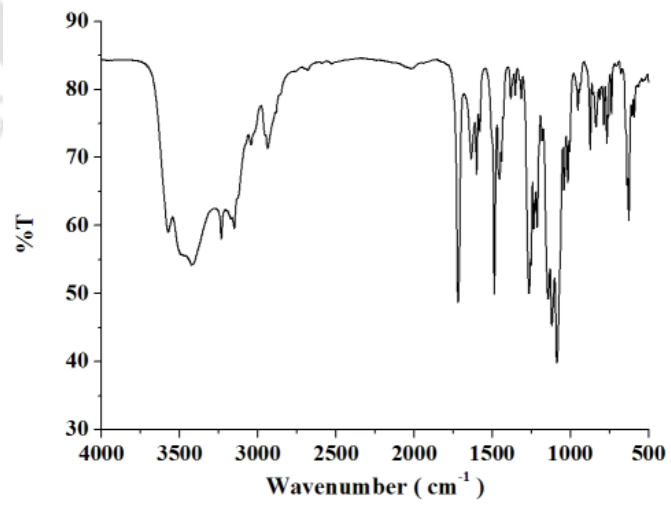

Figure A4.5 FT-IR spectrum of complex **5.1** in KBr.

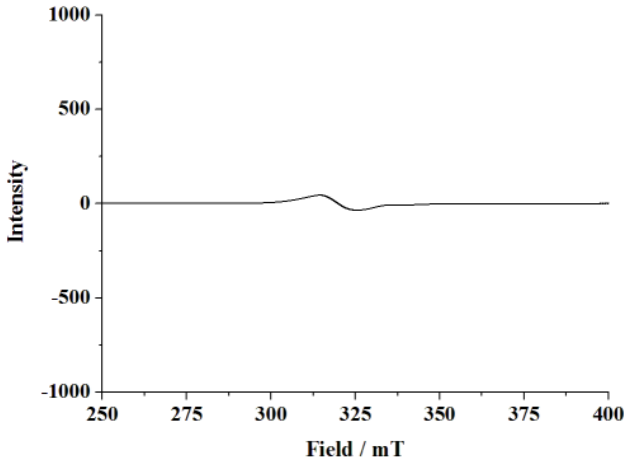

Figure A4.6 X-band EPR spectrum of the complex **5.1** in acetonitrile at room temperature.

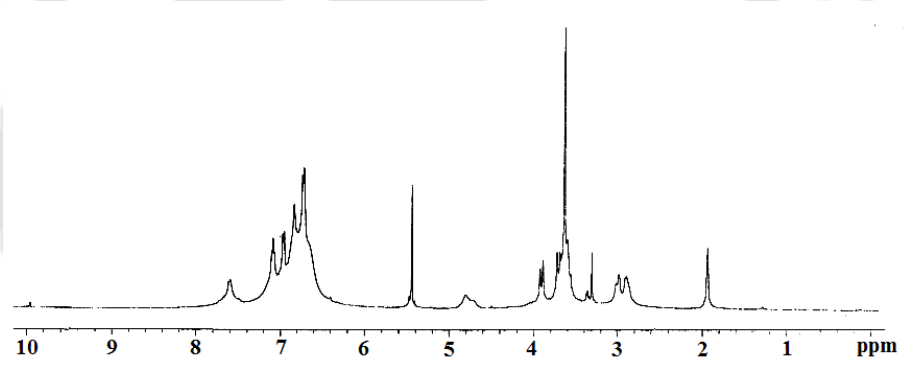

Figure A4.7 ^{1}H-NMR spectrum of complex **5.1** in CD_3CN.

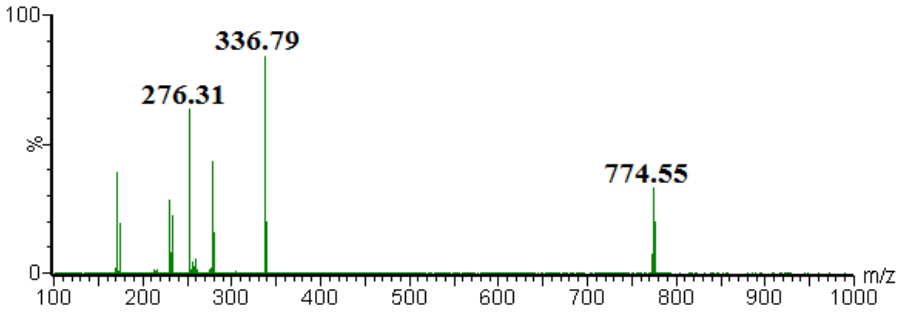

Figure A4.8 ESI-mass spectrum of complex **5.1** in acetonitrile.

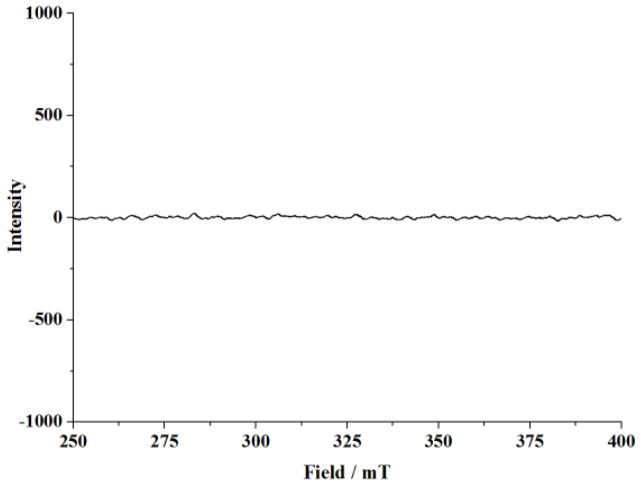

Figure A4.9 X-band EPR spectrum of complex **5.2** in acetonitrile at room temperature.

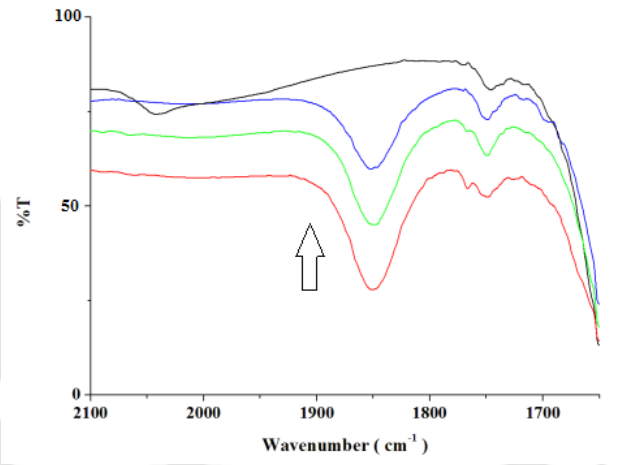

Figure A4.10 FT-IR spectra of complex **5.2** in acetonitrile solution before (red) and after applying vacuum [at 5 minutes (green), 10 minutes (blue) and 15 minutes (black)].

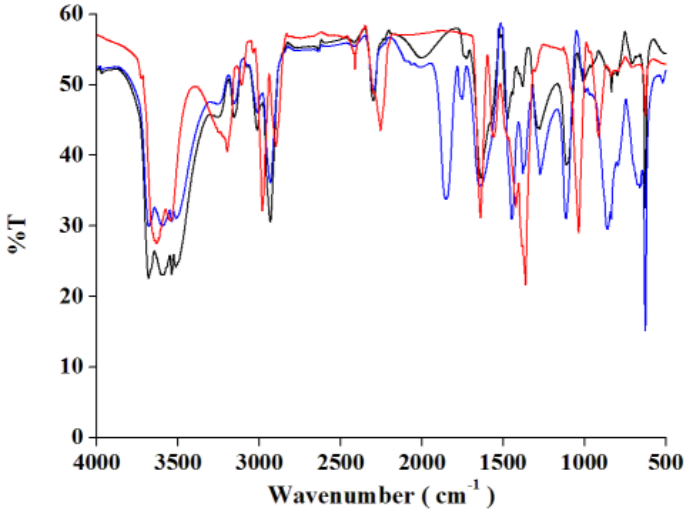

Figure A4.11 FT-IR spectra of complexes **5.1** (black), **5.2** (blue) and after reaction of **5.2** with H_2O_2 in acetonitrile solvent.

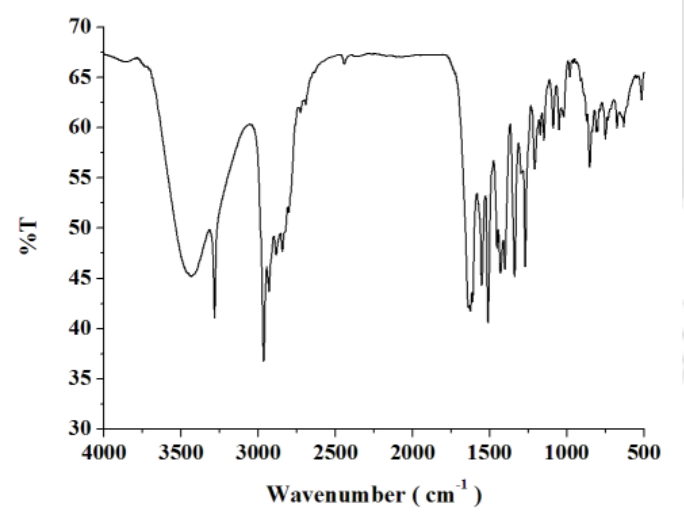

Figure A4.12 FT-IR spectrum of $\mathbf{L_4'}$ in KBr.

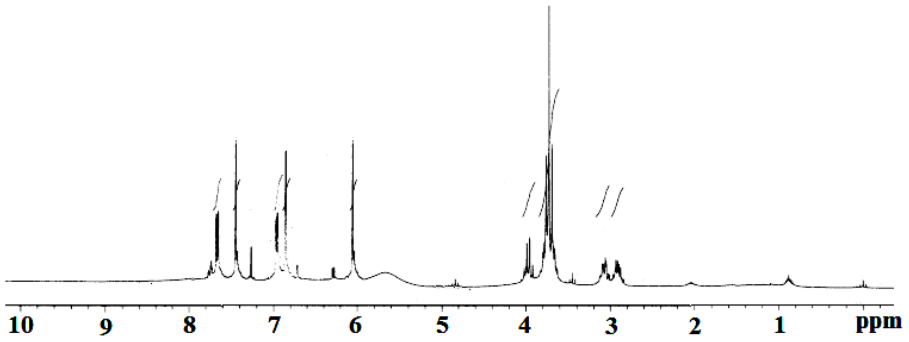

Figure A4.13 ^{1}H-NMR spectrum of $\mathbf{L_4'}$ in $CDCl_3$.

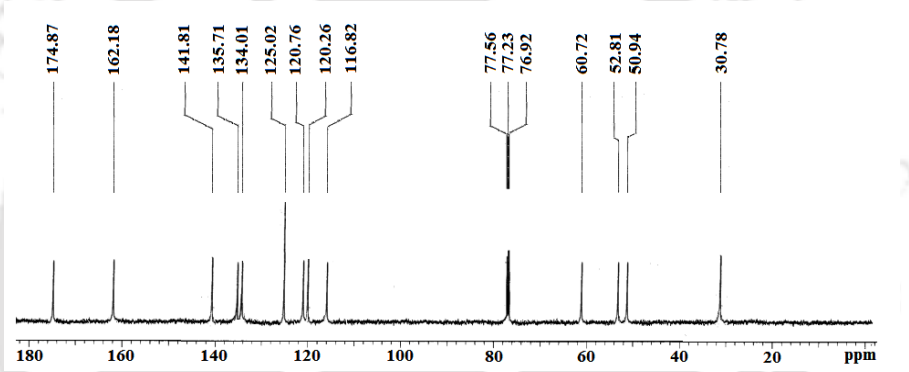

Figure A4.14 ^{13}C-NMR spectrum of $\mathbf{L_4'}$ in $CDCl_3$.

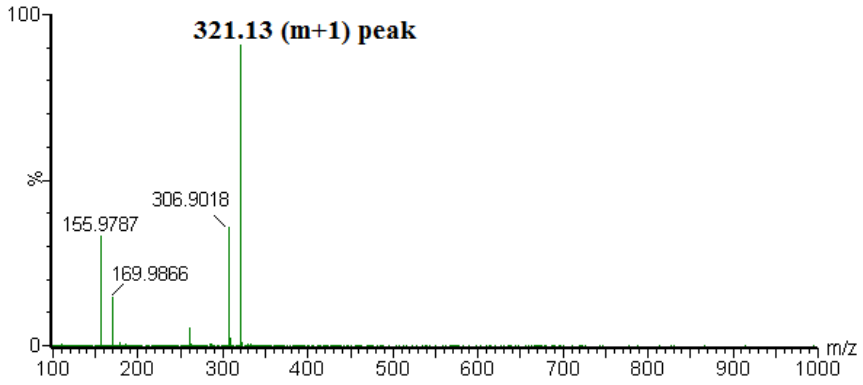

Figure A4.15 ESI-mass spectrum of $\mathbf{L_4'}$ in methanol.

List of publications

1. **Nitric oxide reactivity of Cu(II) complexes of tetra- and pentadentate ligands: structural influence in deciding the reduction pathway**

   Kumar, P.; Kalita, A.; Mondal, B. *Dalton Trans.* **2013**, DOI:10.1039/C3DT32580F.

2. **Copper(II) complexes as turn on fluorescent sensors for nitric oxide**

   Kumar, P.; Kalita, A.; Mondal, B. *Dalton Trans*. **2012**, *41*, 10543.

3. **Reaction of a copper(II)–nitrosyl complex with hydrogen peroxide: putative formation of a copper(I)–peroxynitrite intermediate**

   Kalita, A.; Kumar, P.; Mondal, B. *Chem. Commun*. **2012**, *48*, 4636.

4. **First example of a Cu(I)–(η^2-O,O)nitrite complex derived from Cu(II)–nitrosyl**

   Kalita, A.; Kumar, P.; Deka, R. C.; Mondal, B. *Chem. Commun*. **2012**, *48*, 1251.

5. **Role of ligand to control the mechanism of nitric oxide reduction of copper(II) complexes and ligand nitrosation**

   Kalita, A.; Kumar, P.; Deka, R. C.; Mondal, B. *Inorg. Chem.* **2011**, *50*, 11868.

6. **Fluorescence-based detection of nitric oxide in methanol and aqueous media using copper(II) complex**

   Mondal, B.; Kumar, P.; Ghosh, P.; Kalita, A. *Chem. Commun.* **2011**, *47*, 2964.

7. **Reduction of copper(II) complexes of tridentate ligands by nitric oxide and fluorescent detection of NO in methanol and water media**

   Kumar, P.; Kalita, A.; Mondal, B. *Dalton Trans*. **2011**, *40*, 8656.

8. **An asymmetric dinuclear copper(II) complex with phenoxo and acetate bridge: synthesis, structure and magnetic studies**

   Dutta, G.; Debnath, R. K.; Kalita, A.; Kumar, P.; Sarma, M.; Shankar, R. B.; Mondal, B. *Polyhedron* **2011**, *30*, 293.

9. **Reduction of copper(II) complexes of tripodal ligands by nitric oxide and trinitrosation of the ligands**

   Sarma, M.; Kalita, A.; Kumar, P.; Singh, A.; Mondal, B. *J. Am. Chem. Soc*. **2010**, *132*, 7846.